2011

DISTAL RADIOULNAR JOINT BIOMECHANICS AND FOREARM MUSCLE ACTIVITY

Joseph Scott Bader
University of Kentucky, jsbader@gmail.com

ABSTRACT OF DISSERTATION

Joseph Scott Bader

The Graduate School

University of Kentucky

2011

DISTAL RADIOULNAR JOINT BIOMECHANICS AND FOREARM MUSCLE ACTIVITY

_____

ABSTRACT OF DISSERTATION

_____

A dissertation submitted in partial fulfillment of the
requirements for the degree of Doctor of Philosophy in
the Graduate School at the
University of Kentucky.
By

Joseph Scott Bader

Lexington, Kentucky

Director: Dr. David Pienkowski, Associate Professor of Biomedical Engineering

Lexington, Kentucky

2011

ABSTRACT OF DISSERTATION

DISTAL RADIOULNAR JOINT BIOMECHANICS AND FOREARM MUSCLE ACTIVITY

Optimal management of fractures, post-traumatic arthritis and instability of the distal radioulnar joint (DRUJ) requires an understanding of the forces existing across this joint as a function of the activities of daily living. However, such knowledge is currently incomplete. The goal of this research was to quantify the loads that occur at the DRUJ during forearm rotation and to determine the effect that individual muscles have on those loads.

Human and cadaver studies were used to analyze the shear (A-P), transverse (M-L) and resultant forces at the DRUJ and to determine the role that 15 individual muscles had on those forces. Data for scaling the muscles forces came from EMG analysis measuring muscle activity at nine positions of forearm rotation in volunteers during isometric pronation and supination. Muscle orientations were determined from the marked muscle origin and insertion locations of nine cadaveric arms at various stages of forearm rotation. The roles that individual muscles played in DRUJ loading were analyzed by removing the muscle of interest from the analysis and comparing the results.

The EMG portion of this study found that the pronator quadratus, pronator teres, brachioradialis, flexor carpi radialis and palmaris longus contribute significantly to forearm pronation. The supinator, biceps brachii, and abductor pollicis longus were found to contribute significantly to supination.

The results of the DRUJ analysis affirm that large transverse forces pass from the radius to the ulnar head at all positions of forearm rotation during pronation and supination (57.5N-181.4N). Shear forces exist at the DRUJ that act to pull the radius away from the ulna in the AP direction and are large enough to merit consideration when examining potential treatment options (7.9N-99.5N).

Individual muscle analysis found that the extensor carpi radialis brevis, extensor pollicis longus, extensor carpi ulnaris, extensor indicis and palmaris longus had minimal effect on DRUJ loading. Other than the primary forearm rotators (pronator quadratus, pronator teres, supinator, biceps brachii), the muscles that exhibited the largest

influence on DRUJ loading were the abductor pollicis longus, brachialis, brachioradialis, extensor carpi ulnaris, flexor carpi radialis, and flexor carpi ulnaris.

KEYWORDS: distal radioulnar joint, electromyography, isometric muscle contraction, joint reaction forces, forearm biomechanics

Joseph S Bader
Student's Signature

9/7/2011
Date

DISTAL RADIOULNAR JOINT BIOMECHANICS AND FOREARM MUSCLE ACTIVITY

By

Joseph Scott Bader

David Pienkowski
Director of Dissertation

Abhijit Patwardhan
Director of Graduate Studies

9/7/2011
Date

RULES FOR THE USE OF DISSERTATIONS

Unpublished dissertations submitted for the Doctor's degree and deposited in the University of Kentucky Library are as a rule open for inspection, but are to be used only with due regard to the rights of the authors. Bibliographical references may be noted, but quotations or summaries of parts may be published only with the permission of the author, and with the usual scholarly acknowledgments.

Extensive copying or publication of the dissertation in whole or in part also requires the consent of the Dean of the Graduate School of the University of Kentucky.

A library that borrows this dissertation for use by its patrons is expected to secure the signature of each user.

Name	Date

DISSERTATION

Joseph Scott Bader

The Graduate School

University of Kentucky

2011

DISTAL RADIOULNAR JOINT BIOMECHANICS AND FOREARM MUSCLE ACTIVITY

DISSERTATION

A dissertation submitted in partial fulfillment of the
requirements for the degree of Doctor of Philosophy in
the Graduate School at the
University of Kentucky

By

Joseph Scott Bader

Lexington, Kentucky
Director: Dr. David Pienkowski, Associate Professor of Biomedical Engineering
Lexington, Kentucky
2011

For my parents, whose support and patience through MANY years of
Graduate school, through good times and bad, have helped me to accomplish my goals
in academia as well as my goals in life.

ACKNOWLEDGEMENTS

I would like to acknowledge the support and patience of my PhD advisor Dr. David Pienkowski throughout my time at the University of Kentucky. I would like to acknowledge Dr. Michael Boland for serving as the advisor for all clinical related matters, for finding ways to keep the project funded and for teaching me how truly amazing and complex the forearm is. I would like to thank Dr. Timothy Uhl for his biomechanics and research expertise as well as letting me use his extensive array of biomechanics research tools. I would like to thank Dr. Arthur Nitz for his EMG expertise and for patiently dealing with me as I developed the project and collected data on 44 subjects for which he had to be present. I would like to acknowledge Dr. Robert Shapiro for his help in the early stages of this project as well as for being the outside examiner. I would like to thank Dr. David Puleo and Dr. Keith Rouch for their guidance and patience as members of my dissertation committee. I would also like to thank the orthopedic residents that assisted in this project: Dr. Joseph Stone, Dr. Yanni Pappou and Dr. Robert Royalty as well as the medical students that assisted over the years. Lastly, I would like to thank the faculty, staff and students of the Center for Biomedical Engineering, Department of Orthopedics, Department of Kinesiology and Health Promotion as well as the College of Health Sciences Division of Physical Therapy for their support throughout my years at the University of Kentucky.

TABLE OF CONTENTS

LIST OF TABLES

LIST OF FIGURES

CHAPTER 1: BACKGROUND

1.1 The Distal Radioulnar Joint

1.1.1 Anatomy and Function

The forearm consists of two long bones, the radius and ulna. The radius and ulna rotate about each other to create forearm rotation. The radius and ulna meet at the elbow and wrist, creating the proximal radioulnar joint (PRUJ) and the distal radioulnar joint (DRUJ), respectively (Fig. 1.1). The DRUJ is considered to be a synovial pivot joint where the shallow sigmoid notch of the ulnar aspect of the distal radius articulates on the circular head of the ulna (163). In the neutral forearm position, the radio-carpal unit rests on top of the ulna seat with gravity pulling the head and its load toward the ground (111, 154). During pronation and supination, the radius rotates about the ulna and has a reported rotational range between 150° and 190° (3, 46, 110, 154). The average rotation angle of the radius at maximum pronation is 66.1° and at maximum supination is 75° (142). In addition to the rotational motion, there is also a translational motion present in the DRUJ (97). The ulnar head translates palmarly with supination about the ulna and dorsally with pronation (5, 151, 152). The ulna also rotates about its center of gravity between a range of 3° and 6° during forearm rotation (142). As the forearm rotates from supination to pronation the ulnar head shifts distally within the sigmoid notch (55, 152). The relative translation of the radius and ulna can change as much as 2mm during forearm rotation (112). The axis of rotation of the forearm is typically considered to be the longitudinal axis formed from a straight line connecting the radial head at the elbow and the fovea of the distal ulna at the wrist (186). However, others report that the center of rotation changes with different forearm arcs (110).

The distal ulna has an articular surface covering approximately two thirds of its circumference (50). Articular cartilage covers a 90° to 135° arc of the ulnar head, while the arc of the sigmoid notch of the radius is only 47° to 80° (2). The structural presence

and health of the articular surface of the ulnar seat are critical in providing a painless mechanical fulcrum for all radioulnar load bearing activity (111). The concave radius of curvature of the radial sigmoid notch is approximately 50% larger than the ulnar head with which it articulates (2, 3, 5, 191). Joint surface contact ranges from 60% in neutral position to <10% at full pronation and supination (81). The incongruity of the articular surfaces creates a geometrically nonconstrained articulation at the DRUJ (111), thus making it susceptible to translational dorsal and palmer instability.

Instability is defined as an abnormal path of articular contact occurring during or at the end of the arc of motion attempted (26). Because of the small surface contact area at the DRUJ, osseous anatomy provides minimal stability. Therefore, a variety of soft tissue structures (Figs. 1.2 and 1.3) is thought to contribute to DRUJ stability. There is controversy as to which components provide overall DRUJ stability and how much they provide (1-4, 26, 39, 50, 54, 71, 81, 82, 104, 107, 108, 111, 120, 136, 183, 191, 194, 201, 205, 210). Soft tissue stabilization of the DRUJ is obtained through extrinsic and intrinsic structures (111). Extrinsic stabilizers reside outside of the joint capsule and intrinsic structures within the joint capsule (111). Extrinsic factors that are thought to contribute include muscles such as the pronator quadratus as well as the flexor and extensor carpi ulnaris (81, 94, 100, 104, 108, 111, 164, 183). The interosseous membrane (IOM), which connects the radius and ulna, is also thought to play an extrinsic role in DRUJ stabilization (23, 60, 83, 92, 107, 108, 111, 130, 136, 157, 159, 183, 201, 204, 205, 207). However, the rotational stability provided by these extrinsic stabilizers is considered to be of minor consequence compared to that of the intrinsic stabilizers (111). The intrinsic stabilizers collectively blend together to form the triangular fibrocartilage complex (TFCC) (81, 107, 111, 126, 136, 145, 153). The TFCC is thought to include the triangular fibrocartilage disc, the dorsal and palmar radioulnar ligaments, the meniscus homolog and the sheath of the extensor carpi ulnaris (50). The role of individual components of the TFCC to DRUJ stability such as the radioulnar ligaments (3, 4, 26, 51, 81, 86, 108, 111, 175, 183, 189, 205) as well as the contribution of the joint capsule itself (111, 113, 201, 205, 206) have also been investigated.

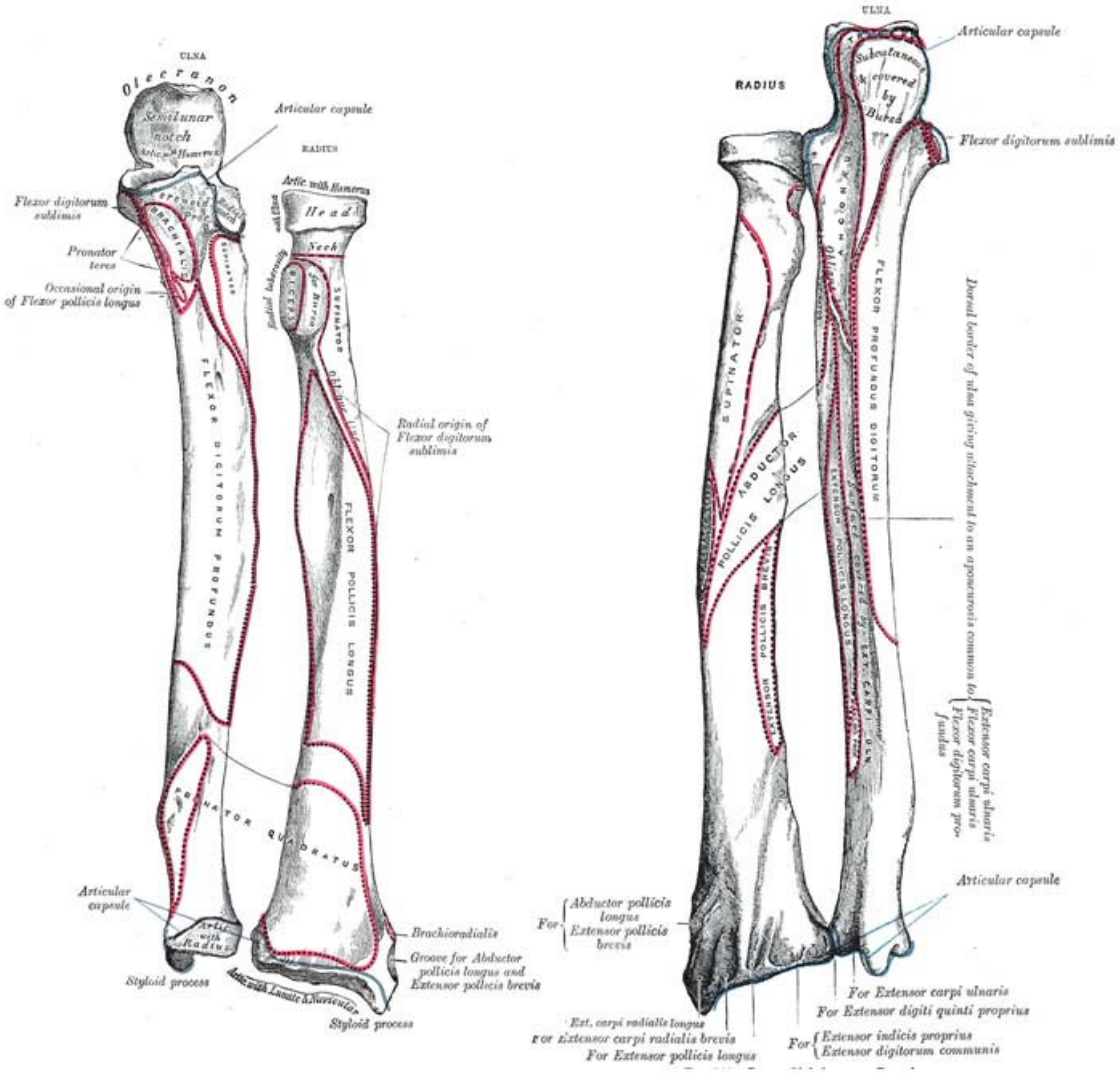

Figure 1.1. Osseous Anatomy of the Forearm

The figure on the left shows the osseous anatomy of the anterior forearm, and the figure on the right shows the osseous anatomy of the posterior forearm.

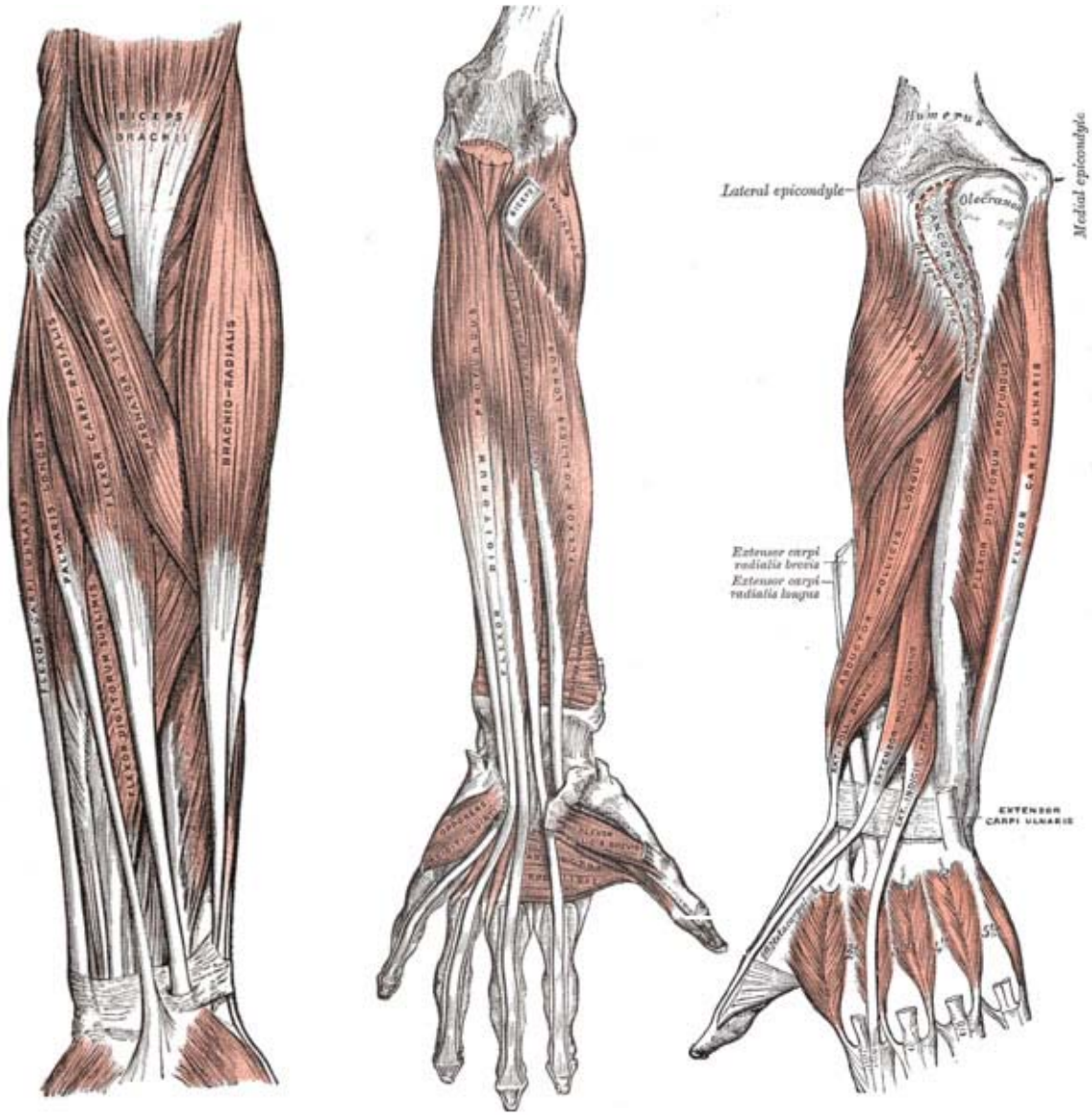

Figure 1.2. Muscular Anatomy of the Forearm

The figure on the left shows the superficial muscles of the forearm. The figure in the middle shows the deep muscles of the anterior forearm. The figure on the right shows the deep muscles of the posterior forearm.

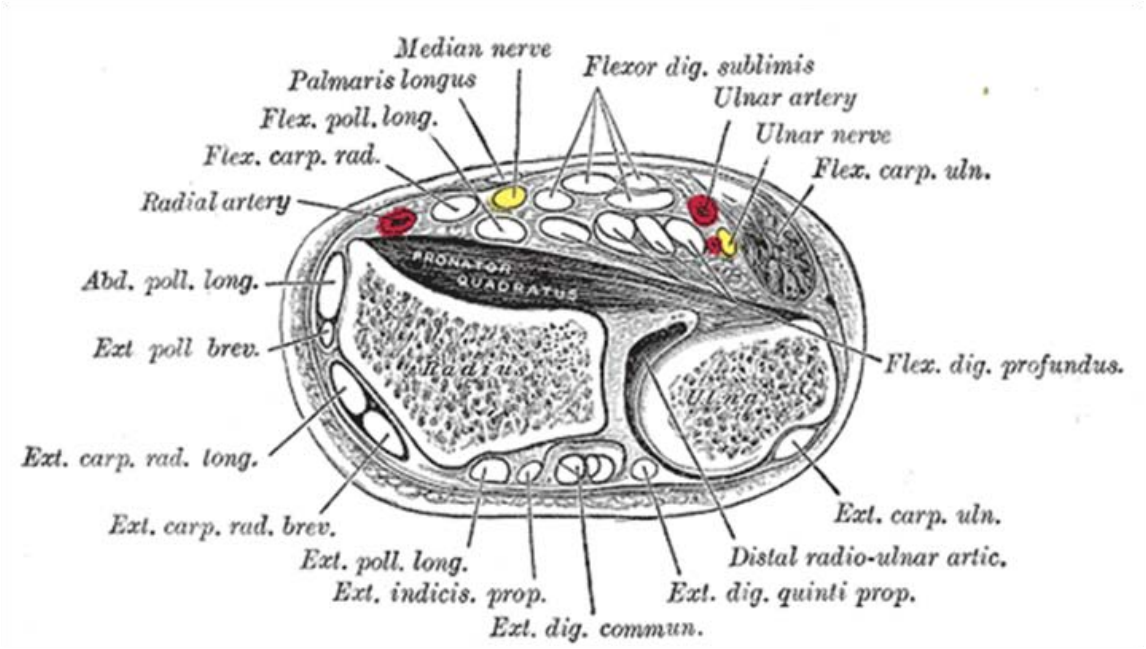

Figure 1.3. Cross-sectional Anatomy of the Forearm

1.1.2 Dysfunction of the DRUJ

Trauma, degenerative diseases, and pathoanatomy of the distal forearm can result in dysfunctional DRUJ biomechanics. Conditions such as arthritis, osteoarthritis, ulnocarpal impingement syndrome, chronic instability, malunion, and posttraumatic disorders (50) can cause DRUJ dysfunction that must be addressed. The primary conditions resulting from these causes are triangular fibrocartilage wear and perforation, ulnar variation with DRUJ incongruity, ulnar styloid nonunion and general joint instability. Acute injury to the DRUJ is most frequently a result of a fall on the outstretched hand, forced hyperpronation or forced hypersupination. Instability typically follows because osseous damage, ligamentous damage or both occur (81). Fracture and instability of the distal radioulnar joint commonly result in osteoarthritis.

1.1.2.1 DRUJ Dysfunction Incidence and Cost

Distal radial fractures account for approximately 10-15% of all fractures (30, 123) and approximately 72% of all forearm fractures (6). Approximately 23-67 of every 10,000 people will experience a distal radius fracture each year (52). The aging baby

boomer population and increasing incidence of osteoporosis-related bone loss suggest that this incidence will increase by more than 38% by 2020 (122). A study of Medicare costs associated with distal forearm fracture treatment from diagnosis through six month follow-up found the average medical costs to be $7788 per incident (109). According to the US Census Bureau, the 2010 United States population was 308,745,538. Therefore, based on forearm fracture incidence data (52), the medical treatment alone costs Americans between $5.5 billion and $16.1 billion annually. By 2020, these costs will be between $7.6 billion and $22.2 billion because of the aging baby boomer population.

1.1.2.2 DRUJ Fractures

In a review of forearm injuries, two or more sites of injury are routine and the DRUJ is affected in 60% of cases (73). There are different types of fractures that occur at the distal forearm. Distal radius fractures are sometimes called Colles' fractures because they were first described by Colles in 1814 (41). A Colles' fracture is characterized by volar tilt, radial inclination and shortening of the distal radius (163). 97% of Colles' fractures result in some permanent disability. The impairment in passive forearm motion is noted more frequently in supination (37%) than in pronation (28%) (12). The complication rate of Colles' fractures has been noted to approach 23% (43). A diaphyseal fracture occurring at the junction of the mid and distal thirds of the radius is called a Galeazzi (162), Piedmont (93) or Darrach-Hughston-Milch (199) fracture and is associated with dislocation of the DRUJ (163). Such a fracture is thought to result in hyperpronation under axial load (132, 136, 199). A Smith's fracture is characterized by dorsal tilt, radial inclination and shortening of the distal radius (163). Essex-Lopresti fracture dislocations are uncommon and involve a radial head fracture associated with acute disruption of the DRUJ joint secondary to proximal migration of the radial shaft. A fall on the outstretched hand producing a longitudinal compression force is the most common mechanism of injury (163).

1.1.2.3 DRUJ Disease

Joint diseases, specifically rheumatoid arthritis and osteoarthritis, exert significant adverse effects on the DRUJ. The DRUJ is prone to joint disease because of its inherent instability. The problem stems from the tendency of the sigmoid notch and ulnar head to heal in an incongruent fashion. Because only approximately 20% of DRUJ stability is attributed to articular contact (183), synovial-lined ligamentous stabilizers are needed for stabilization, making it vulnerable to rheumatoid disease (54, 74, 158). Of the people that have rheumatoid arthritis, as many as 95% exhibit symptoms in one of the wrist's three major articulations (74, 185). The highest incidence occurs in the DRUJ (119). Rheumatoid arthritis in the DRUJ can be debilitating because it can lead to dorsal dislocation of the ulnar head resulting in pain, decreased forearm rotation, and rupture of the extensor tendons. Patients with all forms of arthritis of the DRUJ may have limited forearm rotation, pain with active motion, and limited grip strength (146).

1.1.3 Surgical Treatment of DRUJ Dysfunction

Some current surgical techniques used to alleviate DRUJ dysfunction include interosseous wiring (150), ulnar shortening (173), and various forms of ulnar head or shaft resection with or without interposition (14, 25, 32, 47, 70, 102, 164, 165, 168, 208, 209). Resection procedures produce at best fair results (21, 62, 67, 75, 208) and have been associated with significant complications which include radioulnar impingement and distal ulna instability (95). Ulnar impingement is caused by a shortened ulna impinging on the distal radius and causing a painful, disabling pseudorarthrosis (19). Recent biomechanical studies have shown that even with a longitudinally directed force, some pressure goes across the radioulnar articulation (157) and that maintaining the distal ulna is biomechanically preferable to resection (167).

1.1.3.1 DRUJ Prostheses

There is an increasing number of prosthesis options available for treatment of DRUJ dysfunction. Most of these either fall under the ulnar head replacement category

(25, 57, 63, 89, 90, 114, 170, 174, 184, 196, 214) or the total joint arthroplasty category (150, 161, 171, 172, 176). Total ulnar head replacements are used in cases of DRUJ posttraumatic osteoarthritis and in cases of ulnar disability after resection of the distal ulna (176). The primary total ulnar head replacements on the market are the Swanson silicone ulna head (184), the Herbert-Martin ceramic head prosthesis (89, 90), and the Avanta metal head prosthesis (179). Partial ulnar head replacements (63, 114) are used in cases of DRUJ incongruency (176). The long term success of partial and total ulnar head replacements have had mixed results (14, 25, 32, 57, 62, 67, 70, 75, 76, 131, 133, 165-167, 170, 179, 180, 196, 202, 214). Some of the complications that can occur with ulnar head prostheses include recurrent instability, fracture of the implant, continued pain, loss of motion, as well as the progressive erosion of the prosthesis head on the sigmoid notch (176, 179).

Complete DRUJ replacement may be indicated if there is a lack of soft tissue stabilizers to stabilize an ulna head prosthesis (176). Development of total DRUJ prostheses is progressing as biomechanical knowledge of the DRUJ is improving. Total prostheses currently on the market include the Alkmaar prosthesis (161), the Aptis DRUJ prosthesis (117, 171, 172), and the Schuurman prosthesis (176). The latter two are made specifically for the DRUJ. The Alkmaar prosthesis is part of a modular wrist system and is fixed with screws and bony ingrowth (176). At twenty-month follow-up, twenty-two of thirty-two patients implanted with the Alkmar device reported increased wrist movement, increased grip strength, and reduced pain (161). The Aptis prosthesis consists of four parts and is fixed by means of five screws and bony integration (171, 176). Aptis has received reports of improved grip strength and range of motion in thirty-one patients with an average follow-up of 5.9 years (117). The Schuurman prosthesis consists of two components and uses a hydroxyapatite coating (176). There were three development iterations of the Schuurman device. The first had no failures in four patients, the second failed in all five patients, and the third failed in two out of ten patients. Of the twelve that succeeded, there was a significant improvement in grip strength and range of pronation.

1.1.3.2 DRUJ Analysis and Reduction of Treatment Complications

Suboptimal methods of treating distal radius injuries or diseases, manifested through instability, joint incongruency, and ulnocarpal abutment (66) are the most common cause of residual wrist disability and loss of productivity or independence. Understanding the forces that the ulnar head is exposed to at the distal radioulnar joint is essential for determining efficacy of current treatment options. This information is also vital for the development of new treatment options which would maintain anatomical function as well as the load bearing capability of the DRUJ. Because of the growing development of prosthetic joint replacements at the DRUJ, obtaining a clear understanding of DRUJ biomechanics has never been more important.

1.2 Problem Statement and Purpose

1.2.1 Problem Statement

Instability and dysfunction at the DRUJ are significant problems both in terms of frequency and the impact on quality of life. A variety of treatment methods producing at best fair results exists for the treatment of these issues. Treatment methods are improving, but as new methods are developed, it becomes increasingly important to obtain a clearer understanding of DRUJ biomechanics. Loads at the DRUJ are of particular concern when developing new improved treatment options that would maintain anatomical function and load bearing capability, such as total DRUJ replacements. Currently, such knowledge is incomplete, and further study is required to fully quantify the loads seen at the DRUJ as well as the role that individual muscles play in creating those loads.

1.2.2 Purpose

The ultimate goal of this research is to improve treatment outcomes related to DRUJ dysfunction. The present research helps to achieve this goal by the following specific aims:

1. To determine the muscle activity and force exerted during forearm rotation from muscles thought to influence DRUJ loading and cause forearm rotation
2. To create a mathematical model of forearm muscles to quantify the loads occurring at the DRUJ during forearm rotation
3. To examine the individual contribution of each muscle on the total calculation of DRUJ loads

1.2.3 Research Plan

The rationale for determining forces at the DRUJ has already been discussed in the preceding sections of this chapter. Previous attempts and methods used to analyze forearm and DRUJ loading are discussed for the rest of Chapter 1.

Electromyographic data were collected for fifteen muscles thought to impact DRUJ loads at various stages of forearm rotation during pronation and supination. The data were then examined to see which muscles may have an impact on DRUJ loading based solely on their electrical activity. The EMG study is described in Chapter 2.

The EMG activity of the fifteen muscles was used to scale published physiological cross-sectional area data and muscle tension fraction data that represented the maximum force generating capacity of each muscle. The resulting scaled muscle forces represented muscle exertion during forearm pronation and supination. The muscle forces were then paired with muscle orientation data collected from cadaveric forearms at various stages of forearm rotation. Once the magnitude and direction of the muscle forces were determined, a mathematical model of loading at the DRUJ based on the muscle forces was created. This model allowed for the calculations of transverse (medial-lateral), shear (anterior-posterior), and resultant forces at the DRUJ. The resultant forces are the resultant of the shear and transverse forces (forces in the

transverse plane of the DRUJ). The development and results of the muscle loading model are described in Chapter 3.

Once the mathematical model of DRUJ forces had been created, the roles of the individual muscles in DRUJ loading were analyzed. This analysis was done by removing each muscle from the model, one at a time, to examine the effect that the muscle of interest had. The results of this analysis can be seen in Chapter 4.

Chapter 5 gives an overview of the results found in Chapters 2-4 in addition to study limitations, clinical implications of the results, and possible future studies.

1.3 Electromyography

1.3.1 EMG Background

For a muscle to produce a force, the muscle fibers must be activated by an electrical impulse from a motoneuron in the central nervous system. Once the impulse reaches the muscle fibers, a series of events occurs resulting in the generation of an action potential in the muscle fiber. The analysis of these action potentials is called electromyography (EMG), and it can be used to determine the muscular force based on the amplitude of the EMG signal (101). If a quantitative relationship between the EMG signal and force is required, the contraction of interest must be isometric (48). The general approach for estimating muscle activation is to normalize EMG data obtained during functional isometric tests to EMG data from a maximal contraction (116, 118).

EMG signals can be collected from surface electrodes or indwelling electrodes which are placed directly within the muscle. Surface electrodes are placed on the skin and are good for measuring large muscles close to the skin surface. However, surface electrodes may be inadequate for detailed studies of muscle activation (197), muscles far from the skin surface, and small muscles. This inadequacy is due to the size of the electrodes and the possibility of receiving signal noise from other muscles. An alternative to the surface electrode is the indwelling electrode. This type of EMG involves using needles to place two fine wires into the belly of the muscle of interest

which act as leads to directly monitor the electrical activity. The primary drawbacks of fine wire EMG involve the invasive nature of electrode placement. This results in more human subject regulation, limits on the allowable number of electrodes that can be inserted at one time as well as the physical discomfort associated with the electrode placement. It is important to remember that both types of EMG are tools used to give an overview of muscle function. The measured action potentials come from the section of the muscle where the electrode is placed, and the observed signal does not necessarily represent the action of the muscle as a whole. Electromyography and electrophysiology are time-tested methods of muscle research and encompass an entire field of study. Therefore, numerous publications exist regarding EMG activity of various upper extremity muscles while performing a large variety of tasks. However, there is not a comprehensive set of indwelling EMG data that contains each of the forearm muscles thought to affect forearm rotation and DRUJ loading throughout the range of forearm rotation during isometric supination and pronation. Understanding of muscle activity during isometric exertion is a key step needed to determine muscle forces and the role those forces play in DRUJ loading. A review of literature involving the motion of interest, forearm pronation and supination, is provided in section 1.3.2.

1.3.2 Forearm Rotation EMG Literature Review

Basmajian and Latif (16) used indwelling electrodes in twenty subjects at the short and long head of the biceps brachii (BB), brachialis (BRA), and the brachioradialis (BRAR). They examined muscle activity during forearm pronation and supination both with and without resistance and with the elbow flexed at 90° and 135°. They found minimal muscle activity during forearm supination with the elbow extended. However, they found that when the elbow was flexed and supination was resisted, there was marked activity in both heads of the biceps and some activity of the brachialis and brachioradialis. During pronation with the elbow fully extended, no activity was seen without resistance. When resisted, potentials of marked amplitude were observed for the BRAR and slight activity for the BB and BRA.

Basmajian and Travill (17) used indwelling electrodes in eight subjects to investigate the EMG activity of the pronator quadratus (PQ) and the pronator teres (PT). The activities studied were pronation and supination performed both slowly and quickly. They found that during pronation activities that the pronator quadratus was much more active than the pronator teres, and during supination, the activity of both muscles was negligible.

De Sousa et al. (49) examined the BRAR in ten subjects during free pronation and supination both with and without an added load of 360 gm. They found that free pronation and supination of the forearm resulted in no action potentials of the BRAR. Loaded pronation and supination also exhibited no muscle activity.

Moore used indwelling electrodes to examine the role of the short and long heads of the BB and the BRAR in eighteen subjects during pronation and supination (135). The subjects were asked to hold their position at maximum pronation and supination. She found that none of the subjects exhibited muscle activation in the same manner. During the hold in the fully pronated position, most subjects exhibited a decrease in action potential for the BB. During the hold in the fully supinated position, a marked increase was exhibited in at least two of the three muscles investigated.

Taniguchi et al. (187) used surface EMG to examine reaction times of the BB during simultaneous forearm flexion and supination in sixteen subjects. The elbow flexion angles examined were 45° and 110° while the forearm rotation angles were 90° of pronation and 45° of supination. They found that during supination the reaction times were significantly faster with the forearm at 90° of pronation than at 45° of supination.

Hebert et al. (88) used surface EMG to examine the cocontraction of the BB, BRAR, triceps brachii (TB) and anconeus (AN) during a combination of pronation, supination and flexion exercises in six subjects. The subjects were asked to flex the forearm from 0 to 100% maximum voluntary contraction (MVC), do the same thing with the addition of a 20% MVC pronation effort followed by a similar coordinated contraction with a 20% MVC supination effort. This was done with the elbow in the

semi-prone position with the elbow flexed at 50°, 90° and 130°. They found that the BB is more active in supination than in pronation. No significant difference from forearm rotation was observed for the BRAR, TB and AN.

Van Zuylen et al. (197) examined the behavior of the supinator (SUP), pronator teres (PT), TB, BRA, BRAR and BB using fine wire electrodes in eight subjects. The forearm was held at the neutral position with elbow flexion ranging between 40° and 180°. The subject was asked to pronate or supinate to a specified torque level while maintaining a specified elbow flexion torque. They found that the contribution of individual muscles to forearm torque seemed to be independent of the amount of torque exerted. They also found that elbow flexion angle significantly affected the activation of the BB and SUP during supination. The activation of the SUP increased whereas the activation of the BB decreased, indicating that the more biomechanically effective muscle received more activation. The PT and PQ exhibit a similar relationship as the BB and SUP. As the arm extends, the PT becomes biomechanically less effective while the PQ remains unaffected.

Jamison and Caldwell (98) used surface EMG to examine the activity of the BRAR, TB, and BB. Twenty subjects were asked to maintain maximum elbow flexion force while simultaneously maintaining one of seven specified torque levels during either pronation or supination. The elbow was flexed at 90° and the forearm was midway between fully supine and fully prone. They found that the flexion and supination task of the BB tended to increase EMG activity while the flexion and pronation task acted to diminish it. The trends of the BRAR were opposite those of the BB. In a similar study, Caldwell et al. (35) used surface EMG to examine the activity of the BB and BRAR in fourteen subjects. EMG data were collected during maximum flexion with supination torque at 0 Nm, supination with flexion torque at 0 Nm, flexion torque with maximum supination torque as well as supination torque with maximum flexion torque. They found that the combined tasks exhibited greater EMG amplitude than any of the individual tasks.

Bechtel and Caldwell (18) also analyzed muscle activity during dual tasks of flexion and supination. They used surface electrodes on the BB, BRAR and TB of ten subjects who were asked to exert maximum forearm flexion, maximally supinate the arm and then exert a combination of maximum flexion and 50% supination. All tests were done between 30° and 110° of elbow flexion in 20° increments. They concluded that the BB exhibits greater EMG activity as the arm extends. They also found that the BB and BRAR exhibit a reciprocal co-activation relationship during dual activation tasks.

Naito et al. used indwelling electrodes to examine the activity of the BB, BRA and BRAR during pronation and supination, slow and fast movement, with and without load, for a single subject (141) and for nine subjects (140). During pronation and supination exercises, the elbow was either at 30°, 60° or 90° of flexion. They found that during slow forearm rotation, the BB exhibited more activity during supination than during pronation while the BRAR exhibited the opposite. An increase in the BB activity was often accompanied by a decrease in the activity of the BRA and BRAR.

Mukhopadhyay et al. (137) used surface EMG to measure BB and PT activity in twenty-seven subjects. They performed 20% maximum pronation torque with the forearm 60% prone, neutral and 60% supine. All of these tests were done with elbow flexion angles of 45°, 90° and 135° and upper arm angles of 45° of flexion, N and 45° of extension. They found few combinations of arm articulations that exhibited significant change in muscle activity. The PT exhibited a significant increase from neutral to the pronated position. A significant difference in BB activity was only observed during changes in elbow flexion and upper arm position and not the position of forearm rotation.

Staudenmann et al. (181) used a combination of surface and indwelling electrodes to analyze the BB, BRA, BRAR and TB. Ten subjects were asked to isometrically pronate and supinate their arms while simultaneously exerting a forearm flexion force. All experiments were done with the forearm in the neutral position and the elbow flexed at 90°. They found no correlation between pronation and supination torques and the time to failure of a sustained elbow flexor contraction. Subjects that

exhibited a high correlation between EMG amplitudes also demonstrated a high correlation between EMG amplitude and changes in forearm rotation torque.

Boland et al. (24) used fine wire EMG to measure the BRAR activity of ten subjects. Forearm rotation tasks were conducted with the elbow at 90° of flexion and included supination to neutral and back as well as pronation to neutral and back. These tests were done under four different loading conditions (0N, 9N, 18N, and 27N). The tasks were divided into concentric supination and eccentric pronation as well as concentric pronation and eccentric supination. Concentric pronation and eccentric supination activity were significantly greater than the concentric supination and eccentric pronation activity with 18N and 27N loads.

O'Sullivan and Gallwey (147) investigated EMG activity of multiple muscles during isometric pronation and supination at different positions of forearm rotation. They used surface EMG to measure the activity of the PT, PQ, BB, BRAR, deltoid (DT) and extensor carpi radialis brevis (ECRB) during maximum torque exertions in twenty-four subjects. Maximum torque was measured with the elbow flexed at 0°, 45°, 90° and 135° while the forearm exerted isometric rotational effort at 75% prone, neutral and 75% supine positions. Subjects generated maximum strength for three seconds and then held the maximum for one to two more seconds. They found that during supination torque, the forearm rotation angle significantly affected the activity of the activity of the BB, BRAR and ECRB. During pronation torque, forearm rotation angle significantly affected activity of the PT, BRAR, DT and ECRB.

Gordon et al. (80) used indwelling electrodes to determine the activity of the SUP, BB, PQ and PT during isometric pronation and supination. They used fourteen subjects, maintained the elbow at 90° of flexion and asked the subjects to maximally pronate or supinate with the forearm in full supination, mid-supination, neutral, mid-pronation and full pronation. They found that the BB and SUP were highly active during supination and that the PQ and PT were highly active during pronation. They also determined that the SUP is the primary muscle involved in supination and the PT is the dominant muscle involved in pronation.

1.4 Muscle Modeling Parameters

1.4.1 Introduction to Muscle Modeling Parameters

The sarcomere is the basic unit of muscle contraction (27). The characteristics that influence the mechanical force producing properties of muscle are known as muscle architecture (33). Muscle architecture is defined as the arrangement of muscle fibers relative to the axis of force generation (61). Muscle groups are highly specialized with regard to architecture and, therefore, function (125). The variables that distinguish one muscle from another relate to the number of sarcomeres in a series and the number of sarcomeres in parallel. Fibers of fusiform muscle run parallel to a line joining the muscle origin and insertion (33). Pennate muscles have fibers oriented at an angle to the tendon and produce force both parallel and perpindicular to the tendon. This means that the force transmitted in the direction of the tendon (33) is represented by:

$$F_T = F_F \cos\Theta_P \qquad \text{Equation 1.1}$$

F_T represents the force in the direction of the muscle tendon, F_F represents the force of the muscle fiber and Θ_P represents the angle of pennation of the muscle fiber.

A pennate muscle has shorter fibers than a fusiform muscle of equal volume. Therefore, it can produce more force than a similar fusiform muscle (33). A muscle's anatomic cross sectional area (ACSA) indicates the number of fibers in parallel and can thus be used as an indicator of the muscles maximum force capacity (33). Because not all fibers run in parallel and to account for the fact that not all fibers run the entire length of a muscle belly (Fig. 1.4), the term physiological cross-sectional area (PCSA) was introduced. PCSA is calculated by dividing muscle volume by the mean fiber length (33). The physiological cross-sectional area of muscle fibers is proportional to the maximum tension they can produce (27, 28, 96, 160, 217). Several studies have examined PCSA and other modeling parameters of upper extremity muscles (7, 18, 27, 28, 34, 96, 116,

124, 125, 139, 198, 216). Many of these calculated the PCSA differently from one another. When PCSA is used for the determination of relative muscle contributions, the exact calculation procedure for PCSA is of lesser importance than the use of a consistent data set (44).

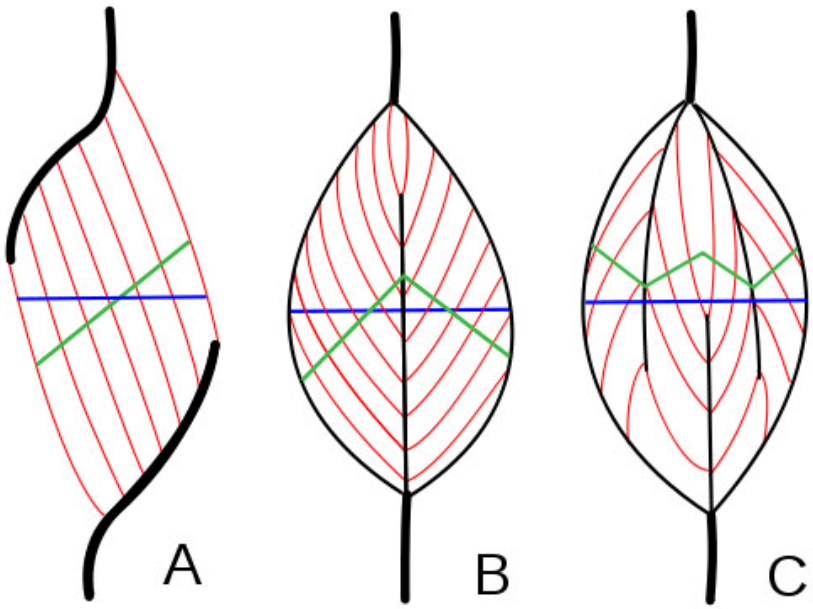

Figure 1.4. Muscle PCSA and ACSA

This figure demonstrates different pennate muscle fiber arrangements. Anatomic cross sectional area (APCA) is illustrated with blue lines and physiological cross sectional area (PCSA) is demonstrated with green lines. This figure is reproduced with permission of the original author, Uwe Gille. The terms of the licensing agreement can be viewed at http://creativecommons.org/licenses/by-sa/3.0/deed.en.

1.4.2 Muscle Parameters Used

Of all the upper extremity muscle PCSA studies examined, the study by Brand et al. (27) investigated the largest number of muscles of interest (thirteen muscles) for the purposes of this dissertation. Because of the importance of maintaining a consistent set of muscle architecture data (44), the data from Brand study were used for every muscle

of interest except for the BB and the BRA. They reported their findings not as PCSA, but as a percentage of the single contraction tension capability of all muscles below the elbow combined, which they termed "tension fraction". Their study used fifteen hands to determine the mean and standard deviation of multiple muscle modeling parameters. Mass and fiber length measurements from the last five of these hands were used to calculate tension fraction. The mass of each muscle of interest was converted to volume by a conversion factor of 1.02 gm/cm^3 and then divided by the mean muscle fiber length. This gave the PCSA of that muscle. They reported that the average combined PCSA of all the forearm muscles was 141 cm^2 and the PCSA of each muscle was expressed as a percentage (tension fraction) of that figure.

Because Brand's group focused on the role of muscles below the elbow, architectural characteristics of the BB or the BRA were not reported (27). Architectural parameters for the BB and BRA published by Murray et al. (139) were used instead. In their study, ten upper extremities were analyzed that had been fixed in formalin. Upon removal of a particular muscle, the length of the distance from the origin to the insertion was measured as well as the pennation angle, fascicle length and sarcomere length. Because it was hard to measure individual fiber lengths, fascicle lengths were used instead. They calculated the optimum fascicle length (lo) by normalizing the measured fascicle lengths (lf) to a sarcomere length (ls) of 2.8 µm which is considered to be the optimum sarcomere length in human muscle (203) to get the equation:

$$lo = lf \frac{2.8}{ls} \qquad \text{Equation 1.2}$$

They then calculated the PCSA of each muscle by dividing the muscle volume by the optimum fascicle length (lo). To get the muscle volume from the muscle mass measurements, a conversation factor of 1.06 gm/cm^3 was used. The reported values for the PCSA of the BB was a combination of the PCSA of the long head of the biceps (2.5 cm^2) and the short head of the biceps (2.1 cm^2) to get a PCSA of 4.6 cm^2.

To get the theoretical force produced by a muscle, the PCSA must be multiplied by a constant representing the amount of work that a muscle can do per unit area. There is a great variety in the actual reported values of this constant. Zajac (217) reports that muscles with high PCSA's have the capacity to generate high forces ranging from 2.55-3.57 kg/cm^2 (217). Holzbaur created a model of the upper extremity and used 4.59 kg/cm^2 for muscles of the forearm and hand (91, 96, 124, 125) and 14.29 kg/cm^2 for muscles of the elbow (9, 91, 139) and shoulder (115). The figure of 3.6 kg/cm^2 was first used by Recklinghausen in 1920 and was used by Brand in his muscle analysis (27, 28). Because this value is in the approximate middle of the ranges (excluding the 14.29 kg/cm^2 value) and because Brand's data were the primary source for the muscle modeling parameters used here, 3.6 kg/cm^2 was used as the muscle force constant in this dissertation.

1.5 Forearm Loading Overview

Forces in the DRUJ occur along three primary axes. Axial forces are transmitted at the distal ends of the radial and ulnar head along the long axis of the forearm. Shear forces occur in the anterior/posterior direction relative to the radius. Transverse forces occur in the medial/lateral direction relative to the radius. The relative muscle-to muscle strength in forearms is fairly constant. It is not the strength that matters but balance.

Axial forces have been determined in a variety of ways because the assumption can be made that force is transmitted along the entire length of the radius and ulna. Shaaban et al. (177, 178) used strain gauges to measure axial load. Gauges were placed on the dorsal and volar surfaces of the distal third of the radius and ulna. Load transmission during pronation-supination was reported for axially loaded and unloaded states for a variety of pathological and surgical conditions. Shaaban's data were limited because only force, but no acceleration, data were provided. Load cells have also been used to quantify axial loading in the distal forearm. Werner (211) quantified axial force

changes in the radius/ulna in response to wrist deviation, ulnar length changes and removal of the triangular fibrocartilage. This study involved mounting the load cell across an excised portion of the bone in the distal half of the arm. A similar load cell configuration has been used by others to quantify: the effect of excising the interosseous membrane (23), varying wrist and forearm position (5), and distal ulna replacement and hemi-resection arthroplasty (192). Other load cell mounting configurations have also been employed (128, 129, 153, 154, 156, 157).

Because of the small contact area between the radius and ulna, in situ measurements of transverse and shear forces are much more difficult, and few attempts have been made. The only known means of obtaining transverse and shear force data in the normal DRUJ that have been attempted utilize either pressure sensitive film or thin film pressure sensitive transducers (95, 144, 178, 200, 212). Despite the spatial resolution of these techniques, they do not provide reliable transverse or shear force data. The only report of both transverse and shear forces in the DRUJ is found from data based on an instrumented prosthetic ulnar head placed in cadavers mounted in a joint simulator (78, 79).

In addition to cadaver studies, a number of finite element analysis (FEA) models have been developed to look at various characteristics of the wrist and distal forearm. Some of the models that have been developed for the forearm examine stress distribution of a ceramic lunate (149), stress transfer at the radio-carpal joint (10, 11), stress distribution in malunited Colles' fracture (134), carpal load transmission to the wrist (37), load transfer of the distal radius (193), and load transfer of the wrist to the radius and ulna during gripping (69). None of these studies has specifically examined the DRUJ, and none has simulated the effect that muscles might play on joint mechanics.

Mathematical modeling of the DRUJ (8, 65, 194, 210) and mechanical joint simulators (72, 78, 79, 87, 99, 213) have been used to quantify forces in the distal forearm, design new implants, and evaluate therapeutic procedures. These, however, have incorporated only a few forearm muscles (8, 65, 72, 78, 87, 99, 194, 210, 213),

making the accuracy of the results from these methods unclear. A forearm model that more realistically represents the anatomy may lead to an improved analysis of the DRUJ and enable improved understanding of forearm biomechanics.

None of the experimental or computational methods mentioned provides three dimensional forces experienced by the normal DRUJ during pronation-supination. In addition, none of the theoretical finite element models has been used to calculate the force between the radius and the ulna, only force transmission from the wrist. Furthermore, none of these models has considered the effect of more than four muscles on DRUJ resultant forces. A model based on in-vivo data that would include muscle forces during pronation-supination would provide previously unavailable insights into the DRUJ joint reaction forces and distal forearm biomechanics, thereby leading to improved treatment options and outcomes.

CHAPTER 2: DETERMINATION OF FOREARM MUSCLE ACTIVITY DURING FOREARM PRONATION AND SUPINATION

NOTE: This chapter was written as a stand-alone manuscript submitted to the Journal of Hand Surgery in May of 2011.

2.1 Introduction

Compared to the hip or knee, little is known about the biomechanics of the forearm, yet injuries and diseases of this extremity are of increasing importance as baby boomers age, incur fractures, and develop subsequent disability. Distal radius fractures are one of the most common upper-extremity injuries, comprising approximately 15% of all fractures (30). Suboptimal treatments for distal radius fractures have been associated with significant complications, e.g. radioulnar impingement and distal ulna joint instability (95). Improved treatments for distal radius fractures, especially those involving the distal radioulnar joint, require an understanding of the forces to which the distal radius and ulnar head are exposed at the distal radioulnar joint (DRUJ).

Mathematical modeling of the DRUJ (8, 65, 194, 210) and mechanical joint simulators (72, 78, 87, 213) have been used to quantify forces in the distal forearm, design new implants, and evaluate therapeutic procedures. Most of these methods, however, have incorporated only a few forearm muscles (8, 65, 72, 78, 87, 194, 210, 213), and, thus, the accuracy of the resulting models and long-term implant performance have been questioned. Forearm models that more realistically represent the anatomy may lead to an improved model of the DRUJ and enable better understanding of forearm biomechanics.

Electromyography (EMG) is useful for understanding how forearm muscle activity is associated with forearms biomechanics, but to date few publications exist that provide comprehensive quantitative upper extremity EMG data. EMG data, in

conjunction with anatomic landmarks, are essential because these data enable quantification of unknown muscle forces. It is widely accepted that the biceps brachii, supinator, pronator quadratus and pronator teres muscles are predominantly responsible for forearm pronation and supination (15, 85, 148, 215), but the role of other forearm muscles is unclear. The purpose of the present study was to quantify the role of each of the fifteen individual muscles thought to contribute to forearm pronation and supination.

2.2 Material and Methods

2.2.1 Study Design

This was a prospective Institutional Review Board approved laboratory study of forearm pronation and supination motion and accompanying muscle activity in normal adults. All of the muscles acting across the elbow contribute some portion of forearm pronation-supination torque or varus-valgus torque (31) and, thus, could be considered in an analysis of forearm biomechanics (197). The present design examines muscles that were either thought to predominate in forearm rotation, cross the central axis of the forearm, or have a potential role in DRUJ loading. The muscles analyzed include the abductor pollicis longus (APL), biceps brachii (BB), brachialis (BRA), brachioradialis (BRAR) , extensor carpi radialis brevis (ECRB), extensor carpi radialis longus (ECRL), extensor carpi ulnaris (ECU), extensor indicis (EI), extensor pollicis longus (EPL), flexor carpi radialis (FCR), flexor carpi ulnaris (FCU), palmaris longus (PL), pronator quadratus (PQ), pronator teres (PT), and the supinator (SUP).

2.2.2 Subject Inclusion and Exclusion Criteria

Young healthy adult volunteers were examined by a physician to ensure that no forearm or wrist pathology existed. Subjects were excluded from consideration if they had prior forearm/wrist/elbow surgery, injury or arthritis involving the elbow or wrist, neurologic disorders, or aversion to needles. Since fifteen forearm muscles were

studied by invasive techniques, this study was divided into four sub-studies. The right arm of eleven healthy subjects was used for each of these four studies. Some subjects volunteered for more than one of the four sub-studies (Table 2.1).

Table 2.1. EMG Study Subject Data

Muscles and subjects examined in the four separate EMG test sub-groups

Test Group	Muscles Examined	Subjects	Males	Females	Mean Age(SD)	Reused Subjects
1	APL, ECU, FCU	11	7	4	26.3 (2.5)	0
2	BB, ECRB, FCR, EPL	11	8	3	25.6 (3.2)	6
3	ECRL, EIP, PT, SUP	11	6	5	26.5 (2.6)	9
4	BRA, PQ, BRAR, PL	11	6	5	26.4 (3.1)	9

2.2.3 EMG Experimental Protocol

The muscles of interest were isolated by using published guidelines (155). Two sterile, bipolar, Teflon-insulated 50µm fine-wire electrodes (California Fine Wire Co., Grover Beach, CA) with 3-5 mm exposed tips were inserted 1 cm apart in each muscle of interest by using a two-needle sterile insertion technique (105). The 27-gauge needles were immediately removed leaving the indwelling fine wire electrodes imbedded. A grounding surface electrode was placed on the acromion of the right shoulder.

A five second baseline test was collected while the subjects relaxed their arm in the horizontal position. To scale the muscle activity among subjects, maximum EMG activity of the muscle of interest was determined by using published maximum voluntary isometric contraction exercises (MVIC) (106). Each MVIC was performed three times for five seconds with a two minute rest interval between trials. An abduction pillow was placed under each arm to standardize the procedure during dynamometer testing and to allow the subject to comfortably rest between trials. To obtain the maximum torque values (18, 31), each subject was asked to stand upright, hold the handle of a dynamometer (BTE Technologies, Hanover, MD) in a neutral forearm position with the elbow at 90° of flexion (Fig. 2.1). The height of the dynamometer was adjusted so that the subject's forearm was horizontal throughout the

tests. The foot position of each subject was marked so that this position could be replicated throughout all trials.

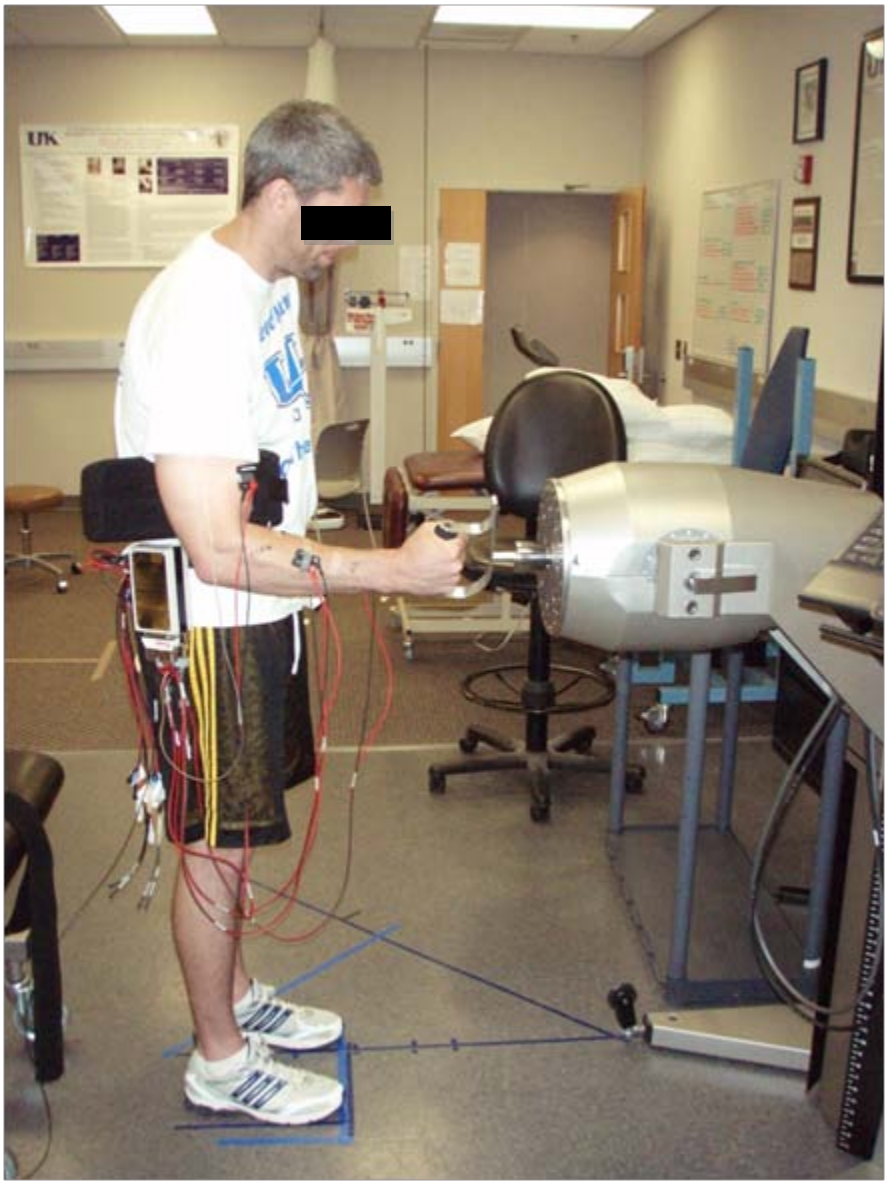

Figure 2.1. Testing Apparatus

Testing procedure showing subject holding the handle of an isokinetic dynamometer with an abduction pillow under the instrumented (fine wire EMG electrodes) arm.

The handle of the dynamometer was randomly placed in one of nine positions of forearm rotation: 1) maximum pronation, 2) 75° of pronation, 3) 50° of pronation, 4) 25°

of pronation, 5) neutral, 6) 25° of supination, 7) 50° of supination, 8) 75° of supination, and 9) maximum supination. Each subject was asked to grip the dynamometer handle at the specified position and pronate the forearm with as much force as comfortably possible for five seconds. Gripping was combined with pronation and supination because it was considered representative of daily functional motions. After five seconds, a tone from the dynamometer signaled the end of the trial. Each subject had a two minute rest interval prior to the next effort to reduce fatigue effects (22, 188). This procedure was followed for a total of three repetitions, and then the same procedure (five seconds of effort and two minutes of rest) was repeated with the subject exerting a supination effort. For the maximum pronation and maximum supination positions, the angle of rotation was measured and recorded by using a magnetic protractor. This series of dynamometer tasks resulted in a total of 54 pronation-supination trials per subject. The value chosen to represent the maximum signal of a given muscle was the largest root-mean-square value recorded for that muscle from an individual subject throughout the MVIC tests or dynamometer tests. The effects of muscle fatigue and order bias were reduced by employing a Latin Squares test sequence design for the specific angles used for each subject.

2.2.4 Data Processing

EMG data were collected at 2,000 Hz by using a portable Myopac amplifier (Run Technologies, Mission Viejo, CA) and stored on a personal computer for post-processing. The EMG data were full wave rectified and then filtered by using a low-pass cutoff threshold of 5 Hz and a 2^{nd}-order Butterworth filter. All raw EMG signals were digitally band pass–filtered between 10 and 1,000 Hz and smoothed with a root-mean-square algorithm that had a time constant of 20 milliseconds. The processed average value of the appropriate baseline test was subtracted from all processed EMG data. The largest root-mean-square amplitude observed during all individual muscle testing for each subject was used to represent 100% muscle exertion. The peak values for each of the three trials for a specific direction and arm position were averaged and normalized to

the maximum activity recorded for an individual muscle and subject. The normalized data for a specific muscle, forearm direction, and angle were then averaged across all eleven subjects. All data were processed with Datapac 5 software (Run Technologies, Mission Viejo, CA) and Matlab 7.0.1 (The Mathworks, Natick, MA).

2.2.5 Data Analysis

A repeated measures ANOVA was used to compare normalized EMG data obtained from each muscle as a function of forearm rotation angle and direction. Individual differences were determined by post-hoc analyses employing the Newman-Keuls test.

To determine if a muscle primarily contributed to forearm pronation or forearm supination, it had to meet two of the three following criteria:

1.) The average muscle activity must be among the three most active muscles observed during any position or direction.
2.) A statistically significant difference must exist between overall pronation activity and overall supination activity for a specific muscle.
3.) A significant difference must exist between pronation activity and supination activity of that muscle at one or more of the nine tested positions.

If a muscle did not meet two of these three criteria, then it was considered not to affect forearm rotation in either direction. It should be noted that just because a muscle was considered to have no affect on forearm rotation does not mean that the muscle does not contribute to the biomechanics of the forearm.

2.3 Results

The muscles that exhibited the highest activity levels during pronation were the PQ, PL, PT, and FCR (Table 2.2). The muscles that exhibited the highest activity levels

during supination were the BB, ECU, SUP, and APL (Table 2.2). The muscles which exhibited significantly higher activity levels during pronation compared to supination at the same position were the BRAR, FCR, PL, PQ, and PT (Fig. 2.2). The PQ and PT were significantly greater while pronating in each of the nine tested positions. The biceps brachii was the only muscle that exhibited significantly higher activity levels during supination compared to pronation at the same position; this difference was significant at each of the nine tested positions.

When comparing overall pronation to overall supination activity, the muscles which had a greater pronation activity were the BRA, BRAR, ECRL, FCR, PL, PQ, and PT (Table 2.3). The muscles which had greater supination activity were the APL, BB, and SUP (Table 2.3).

Table 2.2. EMG Activity Ranking of 15 Forearm Muscles

The EMG activity of each of the muscles examined is listed from most active to least active at each position of forearm forearm rotation during both pronating and supinating efforts. Muscle abbreviations are noted in the methods section.

	Pronating									Supinating								
	MaxP	**75P**	**50P**	**25P**	**N**	**25S**	**50S**	**75S**	**MaxS**	**MaxP**	**75P**	**50P**	**25P**	**N**	**25S**	**50S**	**75S**	**MaxS**
1	PQ	PQ	PQ	PQ	PQ	PL	PL	PL	PL	ECU	ECU	ECU	ECU	SUP	APL	BB	BB	BB
2	PT	PT	PT	PT	PL	PT	PT	PQ	FCR	SUP	SUP	BB	SUP	ECU	SUP	APL	APL	SUP
3	EIP	ECU	FCR	ECU	ECU	PQ	PQ	FCR	ECU	BB	APL	SUP	BB	BB	BB	SUP	SUP	APL
4	ECU	EIP	ECU	PL	PT	FCR	ECU	ECU	PQ	APL	BB	APL	APL	APL	ECU	EIP	EPL	ECU
5	SUP	SUP	ECRB	FCR	FCR	ECU	FCR	PT	PT	ECRB	ECRB	FCR	ECRB	EPL	EPL	EPL	EIP	EPL
6	ECRL	EPL	EPL	EIP	ECRB	SUP	SUP	SUP	SUP	ECRL	PL	ECRB	EPL	EIP	ECRB	ECU	ECU	EIP
7	EPL	ECRL	PL	SUP	SUP	BRAR	BRAR	BRAR	BRAR	FCU	FCR	EIP	EIP	ECRL	ECRL	ECRB	FCR	FCR
8	PL	ECRB	EIP	ECRL	ECRL	EIP	APL	ECRB	FCU	BRAR	ECRL	PL	FCR	ECRB	EIP	PQ	ECRL	ECRL
9	APL	APL	APL	ECRB	EIP	ECRL	BRA	BRA	APL	EPL	BRAR	ECRL	ECRL	PQ	FCR	ECRL	FCU	FCU
10	ECRB	PL	ECRL	EPL	EPL	APL	EIP	APL	ECRB	PL	EIP	EPL	PL	FCR	FCU	PL	ECRB	PL
11	BRA	FCR	SUP	APL	APL	FCU	ECRL	FCU	ECRL	EIP	EPL	BRAR	FCU	BRAR	PL	FCU	PL	ECRB
12	BRAR	BRAR	BRAR	BRAR	BRAR	ECRB	ECRB	EIP	EIP	FCR	FCU	FCU	BRAR	FCU	PQ	BRA	BRA	PT
13	FCR	BRA	BRA	BRA	BRA	BRA	FCU	ECRL	BRA	PQ	PQ	PQ	PQ	PL	BRAR	FCR	PQ	BRA
14	FCU	FCU	FCU	FCU	FCU	EPL	EPL	EPL	EPL	BRA	BRA	BRA	BRA	BRA	PT	PT	PT	PQ
15	BB	BB	BB	BB	BB	BB	BB	BB	BB	PT	PT	PT	PT	PT	BRA	BRAR	BRAR	BRAR

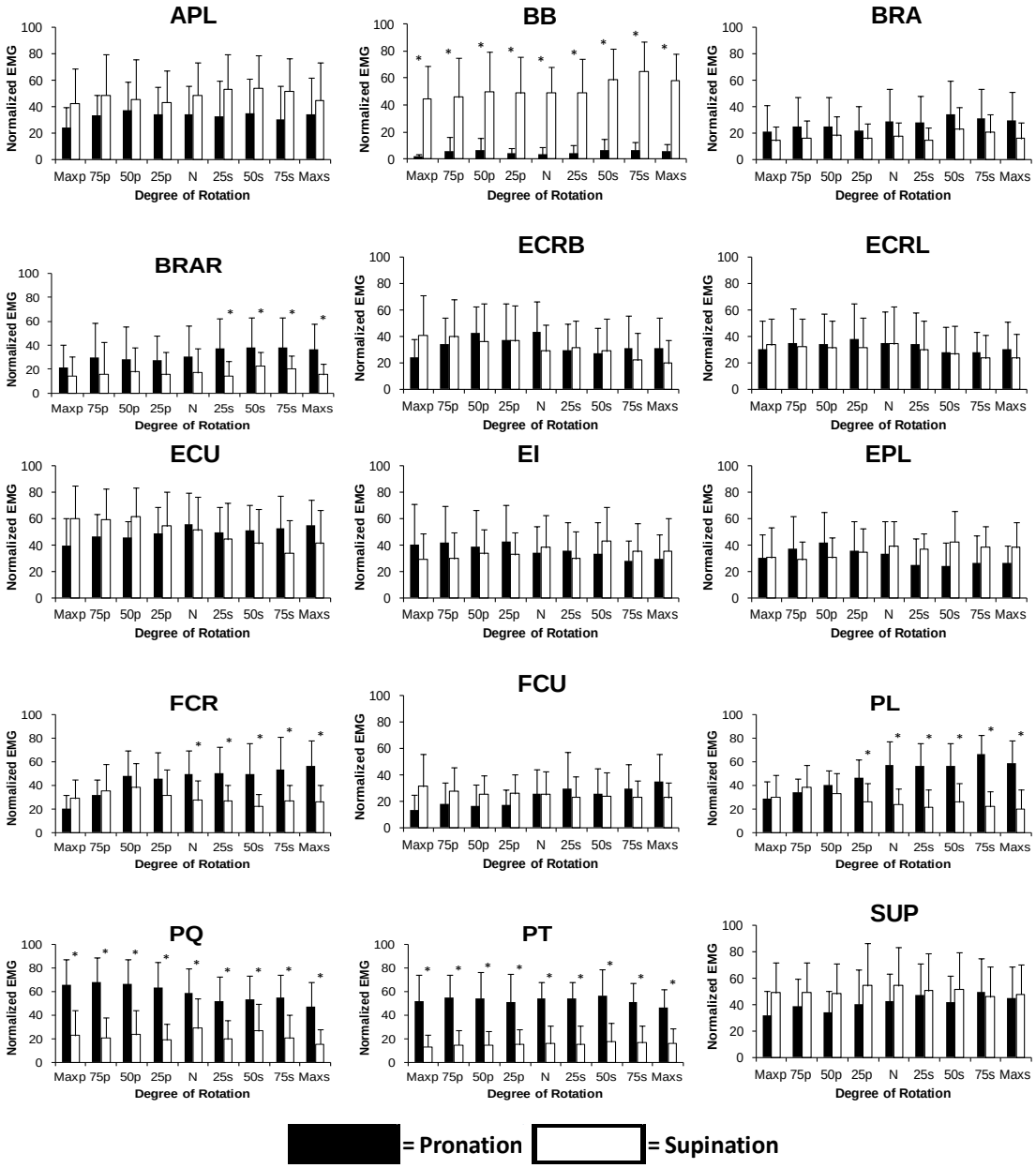

Figure 2.2. Forearm Muscle EMG Activity

Mean (± SD) normalized muscle activity for each of fifteen muscles at nine positions in eleven subjects during maximum voluntary isometric pronation and supination. * indicates a significant difference ($P<0.05$) in muscle activity between pronation and supination at the same angle. Larger versions of these plots are included in Appendix D.

Table 2.3. Muscles with Overall Significant Differences

Muscles which exhibited a significant difference between the overall rotation effort exerted in pronation (P) and supination (S) are shown.

	p value	Dominant Direction
APL	<0.001	S
BB	<0.001	S
BRA	<0.001	P
BRAR	0.048	P
ECRB	0.622	
ECRL	0.023	P
ECU	0.957	
EIP	0.524	
EPL	0.218	
FCR	0.01	P
FCU	0.57	
PL	0.006	P
PQ	<0.001	P
PT	<0.001	P
SUP	0.004	S

2.4 Discussion

It has been widely accepted that the primary pronators of the forearm are the pronator teres and pronator quadratus while the primary supinators are the biceps brachii and supinator (15, 85, 148, 215). The new information contributed by the present study is that additional muscles contributing to forearm pronation are the BRAR, FCR, and PL. Similarly, the APL contributes to forearm supination. The BRA, ECRB, ECRL, ECU, EIP, EPL, and the FCU muscles were presently found to have neither an overall pronating nor supinating effect on forearm biomechanics. It is important to note that lack of classification as a pronator or supinator does not mean that these muscles have no role in forearm biomechanics.

This study agrees with previous findings that the PT and PQ act as primary forearm pronators while the BB and SUP act as primary forearm supinators (15, 85, 148, 215). Three (PT, PQ, and BB) of these four muscles exhibited all three of the criteria used to positively categorize a pronator or a supinator. The SUP met only two of the three criteria. There were no significant differences between EMG activations during pronation and supination at each position tested for the SUP muscle (Fig. 2.2). Because the dominant role that these muscles play in forearm rotation has been well established (15, 85, 148, 215), the following discussion will be focused on how pronation and supination are assisted by other forearm muscles identified in this study.

The FCR, whose primary role is flexion and radial deviation of the wrist (28, 53, 190), is one of two muscles, other than the primary pronators, that met all three pronator criteria. During pronation the FCR was the second most active muscle at the maximal supination position. The other muscle that met all three criteria was the PL; it generates torque in the pronation direction while the forearm is supinated as well as in the supination direction while the forearm is pronated (143). While pronating in the present study, the PL was the most active muscle in all supinated positions.

The pronating effect of both the FCR and the PL can be explained by their moment arms. The linear direction of the FCR and PL across the forearm is similar to that of the PT. The origin of these three muscles is near the medial epicondyle of the humerus, and all three insert into the lateral side of the forearm when in an anatomically neutral position.

The present data, in agreement with the results of others (24, 98, 140, 141), find that the BRAR is more active as a pronator than as a supinator. Most agree that the BRAR acts as a forearm flexor (24, 53, 190), but the other roles of this muscle are unclear. Basmajian claims that it is a pronator of the supine forearm and supinator of the prone forearm in resisted movements only (15). Others assert that it acts as both a pronator and a supinator (28, 36, 85, 147). Gielen et al. note that during pronation, the BRAR motor units receive no input (68). Still others claim that this muscle produces no signal during pronation or supination (49, 197). The present findings also agree with the

results of a number of other groups which note a reciprocal relationship between the BB and other flexors of the forearm, including the BRA and BRAR (31, 35, 40, 68, 84, 88, 98, 197).

Although the present data showed that the APL was one of the two most active supinators, these data need to be interpreted with caution because this study collected data during a gripping exercise. Gripping the handle while supinating would have activated the APL because the thumb was trying to extend; this did not occur during pronation. It is worth noting that the APL is active throughout pronosupination, and, thus, preventing or minimizing pronation and supination may be an important additional consideration when prescribing rest for first compartment tendonitis of the wrist. Muscles can also be activated even if their mechanical action does not contribute directly to the external forearm torque, and motor units in muscles are not necessarily activated if their mechanical action contributes to a prescribed torque (197).

2.4.1 Study Limitations

Pure forearm rotation in the absence of gripping (80), may better represent true pronation and supination, but rarely is this forearm motion performed with an unloaded hand. Although muscular isometric force capacity is directly related to the number of motor units activated (36), because motor unit and muscle activation are not homogeneous across all subjects, the published MVIC exercises used (106) may not actually provide a true maximum signal. This is the rationale for normalizing the EMG data by the largest value observed instead of just the MVIC exercises. It should also be noted that muscles are not activated homogeneously (197) and that the particular motor units being measured by the indwelling electrodes may not be representative of the activity of the muscle as a whole. Because other studies have found that elbow position affects torque (59, 68, 147, 215), the present findings may be limited to horizontal forearms with elbows flexed at a right angle.

2.4.2 Study Conclusions

In conclusion, the brachioradialis, flexor carpi radialis, palmaris longus, and abductor pollicis longus contribute significantly to forearm pronation and supination along with the previously recognized major contributions of the pronator quadratus/pronator teres and the supinator/biceps brachii. Biomechanical models of forearm pronation – supination should include these eight muscles to obtain greater accuracy from models of forearm motion and upper extremity biomechanical calculations. Improved forearm biomechanical models will enable advances in fracture treatment, trauma-induced muscle dysfunction, or joint replacement.

CHAPTER 3: DETERMINATION OF JOINT REACTION FORCES AT THE DISTAL RADIOULNAR JOINT

NOTE: This chapter was written as a stand-alone manuscript to be submitted to the Journal of Hand Surgery at a later date.

3.1 Introduction

Fracture and instability of the distal radioulnar joint commonly result in osteoarthritis. The problem stems from the tendency of the sigmoid notch and ulnar head to heal in an incongruent fashion. Current surgical techniques used to alleviate this problem include ulnar head replacement (131, 196), total joint arthroplasty (150, 172), ulnar shortening (173), and some form of ulnar head or shaft resection with or without interposition (14, 25, 32, 47, 70, 102, 164, 165, 168, 208, 209). Resection procedures produce at best fair results (21, 62, 67, 75, 208) and have been associated with significant complications which include radioulnar impingement and distal ulna instability (95). Recent biomechanical studies have shown that even with a longitudinally directed force, some pressure goes across the radioulnar articulation (157) and that maintaining the distal ulna is biomechanically preferable to resection (167). Improved understanding of the forces occurring at the ulnar head and sigmoid notch could facilitate future efforts aimed at improving treatment and clinical outcomes.

Forces at the DRUJ occur along three primary axes. Axial forces are transmitted at the distal ends of the radial and ulnar head along the length of the forearm. Shear forces occur in the anterior/posterior direction relative to the radius. Transverse forces occur in the medial/lateral direction relative to the radius. Axial forces have been determined in a variety of ways because the assumption can be made that force is transmitted along the entire length of the radius and ulna. Some investigations have utilized strain gauges to measure axial load (177, 178) while other studies have used

load cells to quantify axial loading in the distal forearm (5, 23, 128, 129, 153, 154, 156, 157, 192, 211). Because of the small contact area between the radius and ulna, in situ measurements of transverse and shear forces are much more difficult to obtain, and few attempts have been made. The only known means of obtaining compressive or shear force data in the normal DRUJ that have been attempted utilize either pressure sensitive film or thin film pressure sensitive transducers (95, 178, 200, 212). Despite the spatial resolution of these techniques, they do not provide reliable compressive or shear force data. The only report of both compressive and shear forces in the DRUJ is found from data based on an instrumented prosthetic ulnar head placed in cadavers mounted in a joint simulator (77). Forces occurring in multiple planes at the DRUJ, thus, remain unclear. The purpose of this study was to determine the forces at the DRUJ to enable future efforts to optimize post surgical rehabilitation and to provide new knowledge facilitating future DRUJ implant design.

3.2 Material and Methods

3.2.1 Study Design

This was a theoretical model based on empirically determined muscle vector orientations and subject measured muscle forces. The muscle forces were determined from published tension fraction (27) physiological cross sectional area (PCSA) values (139) which determined the theoretical maximum forces that a particular muscle could exert. These were then scaled down with the EMG data discussed in Chapter 2. The maximum signal observed over the course of all EMG tests for each muscle was used as the normalizing factor and represented the maximum muscle force from the PCSA data. All other EMG data were then expressed as a percentage of this maximum signal. The percentage of the maximum signal that each muscle exhibited for each exercise was then used to scale the maximum force values. These scaled muscle forces were combined with the muscle orientation data collected on nine cadaveric upper

extremities. This procedure allowed a model of each of the nine forearms to be created, and the data from each of these nine models was then averaged and reported.

3.2.2 Cadaveric Specimen Preparation

Nine left fresh cadaveric upper extremities were amputated at mid humerus. All skin and major muscles were excised, with origins and insertions left intact. Muscle origins and insertions were marked by drilling a small hole in the bone at the location of interest and inserting a small aluminum pin (Fig. 3.1). Origins and insertions were marked for the following muscles: radial and ulnar attachments of the abductor pollics longus (APLR and APLU), biceps brachii (BB), brachialis (BRA), brachioradialis (BRAR), extensor carpi radialis brevis (ECRB), extensor carpi radialis longus (ECRL), extensor carpi ulnaris (ECU), extensor indicus (EI), extensor pollicis longus (EPL), flexor carpi radialis (FCR), flexor carpi ulnaris (FCU), pronator quadratus (PQ), humeral and ulnar attachments of the pronator teres (PTH and PTU), and supinator (SUP). Reference points marked were the anterior and posterior aspects of the sigmoid notch of the radius as well as the anterior distal humerus at the coronoid fossa.

Figure 3.1. Example of Cadaver Marker Placement

3.2.3 Data Collection

The humerus of each arm was attached to the end of a support beam using nylon straps, allowing the forearm to hang down at a right angle (Fig. 3.2). In addition the ulna was secured to the fixture so that the only movement occurring was the rotation of the radius about the ulna. A goniometer was used to measure the angle of rotation of the forearm. When collecting data, the angle of rotation, θ, was determined by measuring the angle formed by the marker representing the brachioradialis insertion and the line represented by the humerus as shown in Figure 3.3. Neutral position corresponded to an angle of 0°. Angles in supination were positive, and angles in pronation were negative. The forearms were rotated in 10° increments until both maximum pronation and maximum supination were reached. At each orientation, 3D coordinates were acquired for each marker by touching a stylus used in conjunction with an electromagnetic tracking system (Motion Star, Ascension Technologies, Burlington, VT, USA) using MotionMonitor software (Innovative Sports, Chicago, IL).

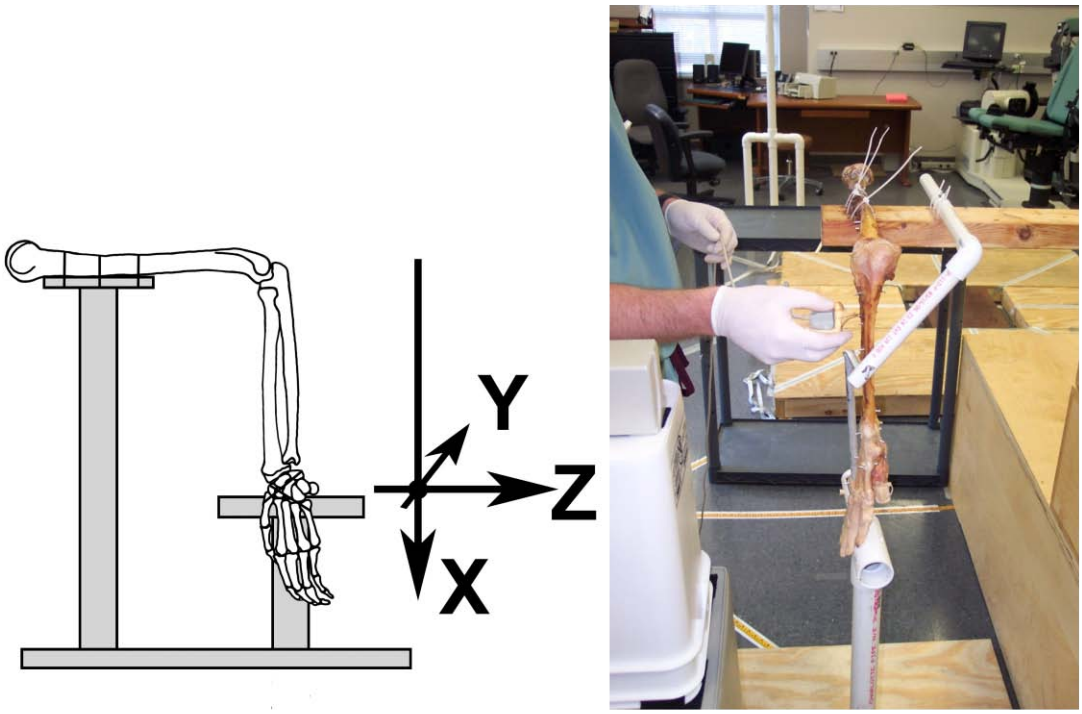

Figure 3.2. Arm Orientation during Muscle Data Collection

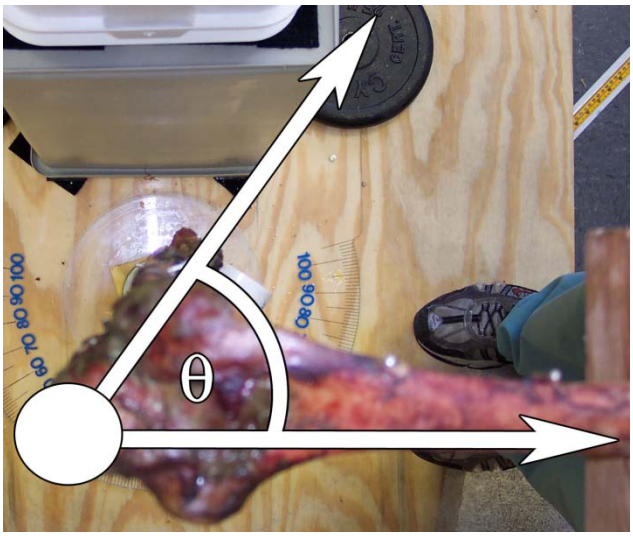

Figure 3.3. Determination of Angle of Forearm Rotation

3.2.4 Coordinate Transformation

Because all data were collected using the same coordinate system, it was necessary to transform the coordinates to an orientation that would be anatomically relevant. For the purposes of this analysis, it was determined that the x-axis would be along the long axis of the radius with the line from the coronoid fossa to the marker on the anterior sigmoid notch of the radius. The y-axis would represent the shear axis in the anterior-posterior direction (parallel to the sigmoid notch) and the z-axis would be perpendicular to the other two, representing the transverse axis as shown in Figure 3.2. A transformation matrix was calculated for each orientation to convert from the global machine coordinates to the local coordinate system of the forearm. The three points used to determine this transformation matrix were the marker representing the coronoid fossa at the elbow, the marker representing the anterior side of the DRUJ at the sigmoid notch, and the marker representing the posterior side of the DRUJ at the sigmoid notch.

Once all of the 3D coordinates had been transformed into the anatomically relevant coordinate system, the actual angle of forearm rotation was calculated. θ was mathematically calculated by determining the angle between the line representing the

z-axis (transverse direction across radius and ulna) and the line of the humerus represented by the marker of the coronoid fossa and the marker representing the biceps brachii on the proximal end of the amputated humerus.

3.2.5 Joint Reaction Force Determination

The joint reaction forces at the DRUJ were determined by summing the moments produced by the muscle forces in both the transverse direction (z-direction) and in the shear direction (y-direction). Maximal muscle forces were calculated by using published tension fraction data provided by Brand et al. (27) for all muscles except the BB and the BRAR. Brand determined the tension fraction percentage of each muscle. He contended that the total PCSA of the arm was 141 cm^2. He also claimed, based on the work of Steindler (182), that the force generating capability of muscle was 3.6 kg/cm^2. Therefore the individual muscle force (N) was determined by:

$$F(N)=(F_{TF})x(PCSA)x(F_M)x(g) \qquad \text{Equation 3.1}$$

Where F_{TF} is the tension fraction of the muscle, PCSA is the total physiological cross sectional area of the arm, F_M is the muscle force generating capability, and g is the gravitational constant (9.81 m/s^2).

Brand did not include data on the biceps brachii and brachialis; therefore, the maximum force capability for these muscles was determined by using published physiological cross section (PCSA) data by Murray et al. (139). Because the PCSA was reported directly for the BB and BRAR, the equation to determine the force was:

$$F(N)= (PCSA)x(F_M)x(g) \qquad \text{Equation 3.2}$$

Maximum muscle forces based on the Brand and Murray data are shown in Table 3.1. The maximum muscle forces were then scaled down to values thought to more accurately reflect those seen in daily activities by using the EMG data presented in

Chapter 2 as a scaling factor. The scaled muscle forces used are shown in Tables 3.2 and 3.3. Once muscle forces and orientations were determined, moments produced by the muscle forces were summed about the elbow. Forces at the DRUJ were determined by dividing the sum of the muscle moments in a particular plane by the distance between the DRUJ and the elbow. Because the scaling EMG data were collected both while the forearm pronated and supinated, the results were calculated both for forearm pronation and forearm supination. For this model, the assumption was made that the only force offsetting the sum of the moments produced by these muscles at each static position was the force occurring at the DRUJ itself. Effects from other soft tissue such as the radioulnar ligaments and the interrosseous membrane were not taken into effect. In addition, because muscle moments were summed about the elbow, any load sharing effect contributed by the proximal radioulnar joint was not taken into consideration.

Table 3.1. Theoretical Maximum Muscle Forces

*Indicates values presented by Murray et al. (139); all other values come from the data presented by Brand et al. (27)

Muscle	PCSA (cm^2)	Force (N)
APL	2.2	77.2
BB	4.6*	162.5
BRA	5.4*	190.7
BRAR	3.4	119.5
ECRB	5.9	209.1
ECRL	4.9	174.3
ECU	6.3	224.1
EI	1.4	49.8
EPL	1.8	64.7
FCR	5.8	204.2
FCU	9.4	333.6
PL	1.7	59.8
PQ	4.2	149.4
PT	3.9	136.9
SUP	10.0	353.5

Table 3.2. EMG Scaled Pronating Forces

Maximum muscle forces are scaled by using EMG data (Chapter 2). The muscles are listed in order of greatest force to least force at each position of forearm rotation. The force (N) is shown in parentheses.

	MaxP	75P	50P	25P	N	25S	50S	75S	MaxS
1	SUP(110.9)	SUP(135.8)	SUP(119.2)	SUP(142.9)	SUP(148.7)	SUP(166.6)	SUP(146.4)	SUP(173.8)	SUP(159.3)
2	PQ(97.7)	ECU(104)	ECU(102.4)	ECU(108.3)	ECU(124.4)	ECU(111.3)	ECU(114.6)	ECU(116.8)	ECU(122.5)
3	ECU(88.4)	PQ(101.8)	PQ(99.1)	PQ(94.5)	FCR(100)	FCR(102.5)	FCR(101.5)	FCR(108.7)	FCU(116.8)
4	PT(70.3)	PT(75.4)	FCR(97.5)	FCR(92.9)	ECRB(89.8)	FCU(97.5)	FCU(85.2)	FCU(97.9)	FCR(114.3)
5	ECRL(53.1)	ECRB(71.4)	ECRB(89.4)	ECRB(77.1)	PQ(87.4)	PQ(76.6)	PQ(79)	PQ(82)	PQ(70.3)
6	ECRB(49.7)	FCR(64)	PT(73.7)	PT(69.5)	FCU(86.3)	PT(74.1)	PT(76.7)	PT(69.7)	ECRB(64.5)
7	FCU(44.5)	ECRL(60.4)	ECRL(59)	ECRL(65.4)	PT(73.5)	ECRB(60.8)	BRA(64.7)	ECRB(65.1)	PT(63.9)
8	FCR(40.8)	FCU(59.6)	FCU(55.1)	FCU(56)	ECRL(60.2)	ECRL(59.4)	ECRB(55.9)	BRA(58.8)	BRA(55.8)
9	BRA(40.4)	BRA(47.6)	BRA(47.2)	BRA(40.7)	BRA(55.1)	BRA(53.5)	ECRL(48.1)	ECRL(48.2)	ECRL(52.2)
10	BRAR(25.3)	BRAR(35.5)	BRAR(34)	BRAR(33)	BRAR(36.3)	BRAR(44.9)	BRAR(45.7)	BRAR(45.3)	BRAR(43.3)
11	EI(20)	APL(25.6)	APL(28.9)	PL(27.5)	PL(33.9)	PL(33.8)	PL(33.7)	PL(39.4)	PL(34.8)
12	EPL(19.6)	EPL(23.8)	EPL(26.9)	APL(26.4)	APL(26)	APL(25.1)	APL(26.6)	APL(23.3)	APL(25.9)
13	APL(18.5)	EI(20.7)	PL(23.9)	EPL(22.7)	EPL(21.4)	EI(17.6)	EI(16.5)	EPL(17.2)	EPL(17.1)
14	PL(17.2)	PL(20.1)	EI(19.4)	EI(21.2)	EI(16.9)	EPL(15.8)	EPL(15.3)	EI(13.7)	EI(14.6)
15	BB(2.8)	BB(9.2)	BB(11.2)	BB(6.6)	BB(5.9)	BB(7.4)	BB(10.6)	BB(10.4)	BB(9.9)

Table 3.3. EMG Scaled Supinating Forces

Maximum muscle forces scaled by using EMG data (Chapter 2). Muscles are listed in order of greatest force to least force at each position of forearm rotation. The force (N) is shown in parentheses.

	MaxP	75P	50P	25P	N	25S	50S	75S	MaxS
1	SUP(171.8)	SUP(173.8)	SUP(169.4)	SUP(190.9)	SUP(192)	SUP(177.5)	SUP(182)	SUP(161.4)	SUP(167.9)
2	ECU(134.5)	ECU(132.1)	ECU(137.1)	ECU(121)	ECU(114.3)	ECU(99.1)	BB(95.2)	BB(105.4)	BB(94.4)
3	FCU(103.9)	FCU(92.1)	FCU(84.4)	FCU(85.2)	FCU(83.3)	BB(80)	ECU(92.2)	FCU(76.8)	ECU(92)
4	ECRB(85)	ECRB(82.7)	BB(81.2)	BB(79.1)	BB(79.5)	FCU(76.5)	FCU(79.6)	ECU(75.5)	FCU(75.2)
5	BB(72.4)	BB(74.2)	FCR(77.4)	ECRB(76.2)	ECRB(60)	ECRB(66)	ECRB(60.1)	FCR(54.3)	FCR(52.5)
6	FCR(58.5)	FCR(72.1)	ECRB(75.3)	FCR(64.3)	ECRL(59.6)	FCR(53.9)	ECRL(46)	ECRB(45.9)	ECRB(41.2)
7	ECRL(58.2)	ECRL(55.9)	ECRL(54.3)	ECRL(54.7)	FCR(55.4)	ECRL(51.5)	FCR(44.7)	ECRL(40.9)	ECRL(40.5)
8	BRAR(36.3)	BRAR(38.2)	APL(35.1)	APL(33.2)	PQ(42.8)	APL(40.8)	BRA(43.4)	APL(39.8)	APL(34.4)
9	PQ(33.6)	APL(37.5)	PQ(34.7)	BRA(29.8)	APL(37.2)	PQ(29)	APL(41.6)	BRA(38.7)	BRA(29.7)
10	APL(32.6)	PQ(31.1)	BRA(34.1)	PQ(27.9)	BRA(32.7)	BRA(27.6)	PQ(39.6)	PQ(30.3)	EPL(24.6)
11	BRA(27.1)	BRA(30.5)	BRAR(32.8)	BRAR(27.7)	BRAR(30.8)	EPL(23.9)	EPL(27.5)	EPL(24.8)	PQ(23.1)
12	EPL(19.6)	PL(22.8)	PL(19.8)	EPL(22.5)	EPL(25)	PT(20.6)	PT(23.7)	PT(22.3)	PT(22.2)
13	PL(17.8)	PT(20)	PT(19.7)	PT(20.2)	PT(21.4)	BRAR(18.3)	EI(21.3)	EI(17.3)	EI(17.6)
14	PT(17.6)	EPL(18.7)	EPL(19.6)	EI(16.2)	EI(18.9)	EI(14.8)	BRAR(18)	BRAR(15.5)	PL(12)
15	EI(14.4)	EI(14.8)	EI(16.6)	PL(15.5)	PL(14.3)	PL(12.7)	PL(15.3)	PL(13.1)	BRAR(10.4)

3.2.6 Data Processing

All data were then interpolated so that the same angles could be compared between specimens. To pair the muscle coordinate data with previously collected EMG data, nine positions of forearm rotation were chosen. The angles included maximum pronation (MaxP), 75° of pronation (75P), 50° of pronation (50P), 25° of pronation (25P), neutral forearm position, 25° of supination (25S), 50° of supination (50S), 75° of supination (75S), and maximum supination (MaxS).

3.2.7 Data Analysis

When comparing forces at each angle, only the magnitude, not the direction of the force, was used. This only affected the analysis in the shear direction because all other comparisons involved positive forces. To determine whether there was a significant difference between DRUJ forces due to force direction, a repeated measures ANOVA was used to compare pronation efforts and supination efforts at the same forearm position. Individual differences were determined by post-hoc analyses employing the Newman-Keuls test.

3.3 Results

Both pronation and supination shear forces exhibit a trend where they are largest (94N and 99.5N respectively) in pronated positions, decrease to their minimum in the positions of mid forearm rotation, and then increase again in the positions of supination (Fig. 3.4). The greatest magnitude average value of the shear force during pronation occurred at 75° of pronation, and the greatest value during supination occurred at MaxP (95N and 99.5N respectively). The average magnitude for shear force was the smallest during pronation at the 50S position, and during supination it was smallest at the 25S position (7.9N and 12.5N respectively). There was no significant difference between shear forces during pronation or supination at any of the nine forearm positions.

Transverse forces during both pronation and supination tended to exhibit a pattern where the greatest transverse force was at neutral, and then the value decreased as the arm either pronated or supinated (Fig. 3.5). The largest average transverse forces occurred at the neutral position during pronation and supination (181.4N and 135.6N respectively). For each of the nine forearm positions, the transverse forces observed during pronation were significantly larger than the forces seen during supination.

Resultant force curves showed that the total force seen at the DRUJ during pronation was greatest from 50P to N and then decreased in both directions of rotation (Fig. 3.6). During supination, the forces stayed relatively constant with a slight tendency to decrease from pronated to supinated positions. The largest average resultant force for pronation and supination exercises were at 25P and N (190.60N and 138.1N) respectively. A significant difference between pronation efforts and supination efforts was at every forearm position with the exception of MaxP.

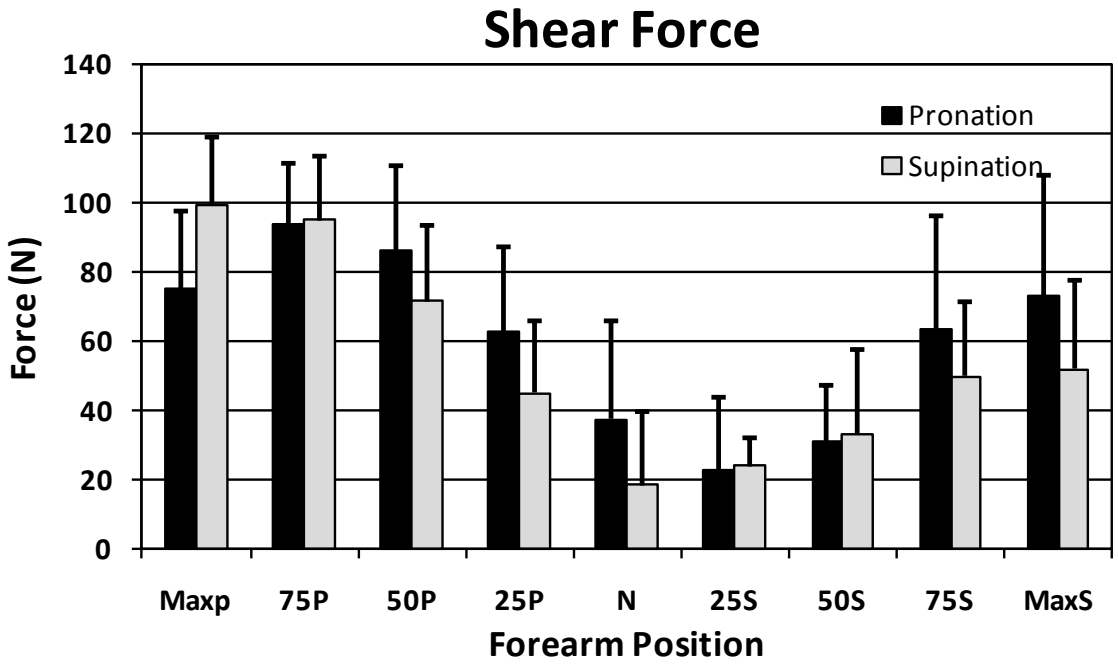

Figure 3.4. Mean Absolute Value Shear Forces at the DRUJ ± SD

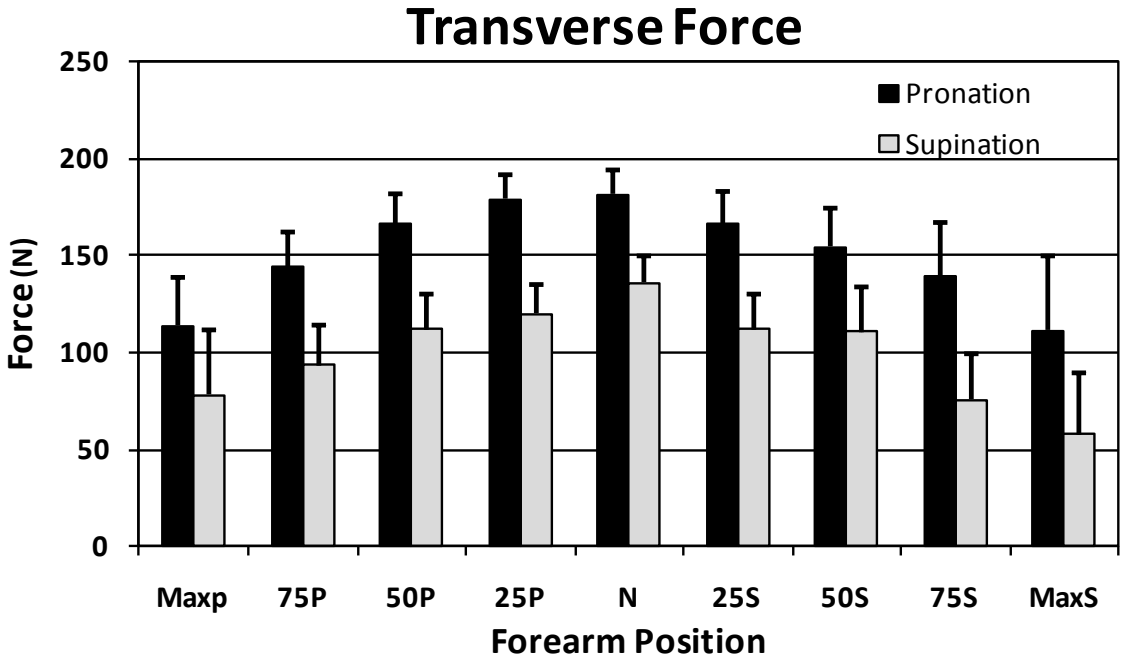

Figure 3.5. Mean Transverse Forces at the DRUJ ± SD

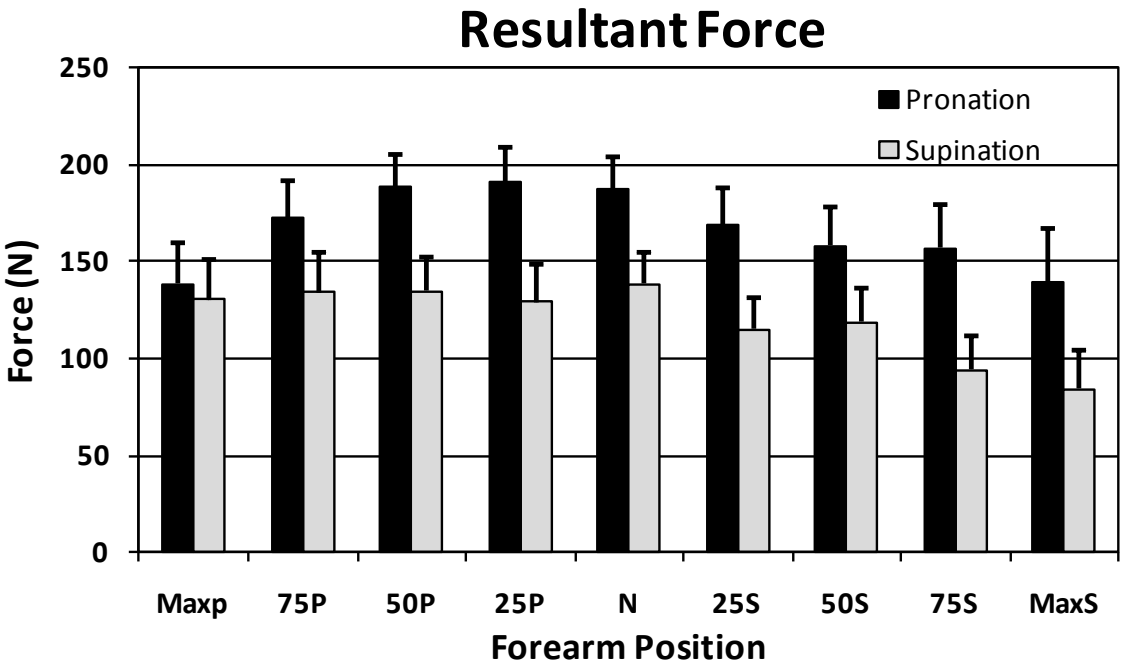

Figure 3.6. Mean Resultant Forces at the DRUJ ± SD

3.4 Discussion

3.4.1 Key Findings

The results of this study affirm that compressive transverse forces pass from the radius to the ulnar head at all points of forearm rotation. In addition to large transverse forces, this study indicates that shear forces exist in the DRUJ. These shear forces act to pull the radius away from the ulna in the AP direction and are large enough to be taken into consideration when examining potential treatment options. These shear forces are greatest in pronation and least between neutral and 25° of supination.

3.4.2 Comparison to Previous Findings

Only two previous studies have examined forces in either the transverse or shear direction of the DRUJ. Both of these studies relied on empirical data obtained from force transducers while the present study is an analytical model based on theory. The first study utilized pressure sensitive film (172) while varying axial loads were applied to the forearm. The results found that transverse loads across the DRUJ increase from pronation to supination while the present study found the opposite. Differences in force trends may be because the forces in the present study are based solely on estimated muscle force data while the film study did not take muscle loading into consideration. The second study utilized an instrumented ulnar head placed within cadaveric specimens in a joint simulator (67). DRUJ loads for the simulator study were only reported at 40̊ of prona tion, 40̊ of supination and neutral. ML, AP, and IS axis bending moments were reported in 20̊ increments. Differences in the results between the simulator study and the current study may come from the fact that muscle forces for 18 different sets of muscle origins and insertions were used in the current study while the simulator only utilized the forces from four muscles.

3.4.3 Clinical Relevance

To maintain the biomechanical function of the forearm, maintaining the natural anatomy and function of the distal ulna is vital. Compressive and longitudinal force transmission across the ulna can be demonstrated by the trabecular lines radiating perpendicular to the two articular facets of the ulnar head (13). In clinical practice, the need for maintaining ulnar head anatomy can be seen from the mixed results (67) associated with procedures involving distal ulna resection such as the Darrach (47) or Sauve-Kapandji (165, 168). The need for maintaining anatomy is further demonstrated by the loads at the DRUJ that are reported here. The need for treatment methods maintaining ulnar anatomy has lead to procedures that attempt to restore the ulnar head. Early results of these prosthetic replacements seem favorable (214).

The results of this study indicate that instability splints should be placed around 25° of supination to minimize shear. Loading after distal ulna procedures should begin in significant pronation and supination to minimize the compressive transverse forces seen at neutral. These data also suggest that plate fixation of the distal ulna should be in more than one plane. In addition, arthroplasty and fracture system designs need to address these forces. Resection of the ulna head should be avoided.

3.4.4 Study Limitations and Potential Improvements

Anatomy that was previously not taken into account, such as the radioulnar ligaments and the interosseous membrane, could be incorporated. To get the most accurate data possible, in-vivo MRI data could be collected and digitally reconstructed. This would involve asking a subject to scan their arm at various stages of pronation-supination and then analyzing the positions of the muscle origins and insertions. A combination of in-vivo MRI data and the muscle force data reported here could also be used as the basis of a finite element model which can investigate DRUJ loading on a more localized scale. For this project, data were only collected with the elbow flexed at 90°. However, analyzing EMG and cadaveric data at other positions of elbow flexion would provide additional information regarding the loads acting at the DRUJ. Straight-

line orientations from the muscle origin to the muscle insertion were utilized in this model, while factors such as muscle rapping were not taken into account. Incorporating this kind of data would improve the accuracy of the orientation of muscle forces used. In addition, this model was a collection of static models used to obtain an overall picture of the DRUJ loading behavior. A dynamic model utilizing cadaver data collected from a camera motion capture system while rotating the arm, as well as collecting dynamic EMG data, would be helpful in the advancement of DRUJ biomechanical knowledge.

3.4.5 Conclusions

Compressive transverse forces (ranging from 57.5N - 181.4N) are transmitted from the radius to the ulnar head at all points of forearm rotation, therefore, indicating a need for maintaining the ulnar anatomy. Because these transverse forces are greatest at neutral (181.4N for pronation and 135.6N for supination), loading after distal ulna procedures should occur at the maximally pronated or maximally supinated position. Shear forces are least around 25° of supination (13.7N for pronation and 12N for supination), making that the orientation to place stability splints. Forces at the DRUJ occur in more than one plane. This should be considered when fixing fractured distal ulnae and designing implants pertaining to the DRUJ.

CHAPTER 4: THE ROLE OF INDIVIDUAL MUSCLES IN DRUJ LOADING AND FOREARM ROTATION

NOTE: This chapter was written as a stand-alone manuscript to be submitted to the Journal of Hand Surgery at a later date.

4.1 Introduction

While understanding the forces at the DRUJ is important, understanding the role that individual muscles play contributing to those forces as well as the muscle behavior during forearm rotation is also important. Clarifying the role that a particular muscles plays in DRUJ loading can help to determine which tendons can be transferred to different locations, which muscles are vital in maintaining proper function of the DRUJ and which muscles could be removed all together to allow for better outcomes when treating for DRUJ pathologies. Muscle data collected over the course of this project including activity, length and contribution to DRUJ loading can all be combined to create a more in-depth view of the behavior of each muscle. The purpose of this study was to determine the role that each of these muscles played, if any, in DRUJ and forearm biomechanics.

4.2 Material and Methods

All data obtained over the course of this project were examined for each muscle. The electromyographic (EMG) data are the same as reported in Chapter 2, and the muscle length was determined from the electromagnetic tracking data discussed in Chapter 3. The length data are reported as a percent of the maximum length seen during forearm rotation for each subject and then averaged so that the length data can be comparable across subjects (Appendix D).

To determine the role that an individual muscle played in DRUJ loading, the muscle was simply removed from the model reported in Chapter 3. A comparison of the original model and the model with the muscle of interest removed is shown graphically in Appendix D. Statistically, all muscles were compared to the intact model using repeated measures ANOVA and individual differences were determined through post-hoc analyses employing the Newman-Keuls test.

Positions at which the muscles were analyzed include maximum pronation (MaxP), 75° of pronation (75P), 50° of pronation (50P), 25° of pronation (25P), neutral (N), 25° of supination (25S), 50° of supination (50S), 75° of supination (75P), and maximum supination (MaxP). The muscles analyzed include the abductor pollicis longus (APL), biceps brachii (BB), brachialis (BRA), brachioradialis (BRAR) , extensor carpi radialis brevis (ECRB), extensor carpi radialis longus (ECRL), extensor carpi ulnaris (ECU), extensor indicis (EI), extensor pollicis longus (EPL), flexor carpi radialis (FCR), flexor carpi ulnaris (FCU), palmaris longus (PL), pronator quadratus (PQ), pronator teres (PT), and the supinator (SUP).

4.3 Results

4.3.1 Overall Data

The overall trends of all the muscles are shown in Appendices A and B. Table 4.1 is shown as an example of the tables in Appendix A. The tables represent the percent change caused when a muscle is removed to shear force, transverse force and resultant force both while pronating and while supinating. Graphical representation of combined muscle contribution for the shear and transverse forces can be seen in Appendix B. Figure 4.1 is shown as an example. Because resultant forces are quantitative and do not represent a direction, they do not add up to 100% and are not included in Appendix B. Some of the key findings taken from the tables in Appendix A are shown in Table 4.2. Information regarding individual muscles extracted from the tables in Appendix A are in Appendix C. Figures regarding each individual muscle including muscle length, EMG

activity, and its effect on DRUJ forces can be seen in Appendix D. Additional information about muscle length and muscle location is shown in Table 4.3.

Table 4.1. Muscle Contributions to DRUJ Shear Forces During Forearm Pronation

This table is shown as an example of the tables presented in Appendix A. Muscles which contributed to loading of the joint are black while muscles which acted to unload the joint are in red. The number is the % change that removal of the muscle caused in the intact model. Muscles are listed in order from the largest contributer of loading to the smallest contributer of loading (or unloading). Cells which are shaded indicate a significant difference between the intact model forces and the forces observed when the muscle is removed.

	MaxP	75P	50P	25P	Neutral	25S	50S	75S	MaxS
1	SUP(28)	SUP(24.3)	FCR(23.8)	FCR(30.2)	FCR(48.2)	PT(107.1)	SUP(243.5)	SUP(55.5)	SUP(52)
2	ECU(19.6)	PT(16.2)	PT(20.4)	PT(26.7)	PT(42.9)	FCR(85.6)	APL(146.2)	PQ(22.8)	PQ(27.6)
3	EI(13.6)	ECU(15)	SUP(15.39)	FCU(17.6)	FCU(42)	FCU(73.7)	ECU(122.1)	APL(18.3)	APL(16.8)
4	PT(13.2)	FCR(13.2)	FCU(12.64)	SUP(9.9)	PL(12.9)	ECRL(28.7)	EPL(46.6)	ECU(10)	FCU(11.3)
5	ECRB(12.4)	ECRB(12.1)	ECRB(10.5)	EI(9.2)	EI(5.9)	PL(22.8)	ECRB(35.6)	EPL(8.4)	FCR(11.2)
6	FCR(9.4)	FCU(11.4)	ECU(9.22)	PL(6.7)	ECRL(5)	BRAR(22.4)	EI(22.2)	FCR(8.3)	EPL(6.7)
7	FCU(9.3)	EI(10.7)	EI(8.84)	ECRB(5.5)	BB(0.1)	BRA(20.5)	PQ(-10.7)	FCU(8.1)	PT(5)
8	EPL(7.3)	EPL(6.4)	EPL(5.02)	ECU(3.9)	ECRB(-0.9)	BB(4)	PL(-12.1)	ECRB(3.6)	PL(3.8)
9	APL(6.6)	APL(6.3)	PL(4.02)	EPL(1.8)	BRA(-1.8)	EI(-2.9)	BB(-18)	EI(3.4)	EI(2.4)
10	PL(2.2)	PL(2.6)	APL(3.23)	PQ(1.5)	BRAR(-2.9)	PQ(-4.6)	FCU(-21)	PL(3)	ECU(2.1)
11	ECRL(1.6)	ECRL(0.9)	PQ(1.67)	ECRL(0.9)	EPL(-4.6)	ECRB(-17.1)	FCR(-46.9)	PT(-2)	ECRB(-0.5)
12	BB(-0.6)	BB(-1.5)	ECRL(0.13)	BB(-0.7)	ECU(-7.5)	EPL(-20.9)	ECRL(-60)	BB(-2.7)	BB(-2.5)
13	BRAR(-6.2)	PQ(-3.1)	BB(-1.57)	APL(-2.5)	PQ(-9.3)	ECU(-54.4)	BRAR(-87.9)	ECRL(-8.7)	ECRL(-10.6)
14	BRA(-7.9)	BRAR(-7)	BRA(-6.5)	BRA(-4.7)	SUP(-12)	APL(-68.9)	BRA(-90.5)	BRA(-13.8)	BRA(-12.5)
15	PQ(-8.4)	BRA(-7.4)	BRAR(-6.8)	BRAR(-6)	APL(-17.9)	SUP(-96.3)	PT(-169.1)	BRAR(-14)	BRAR(-12.9)

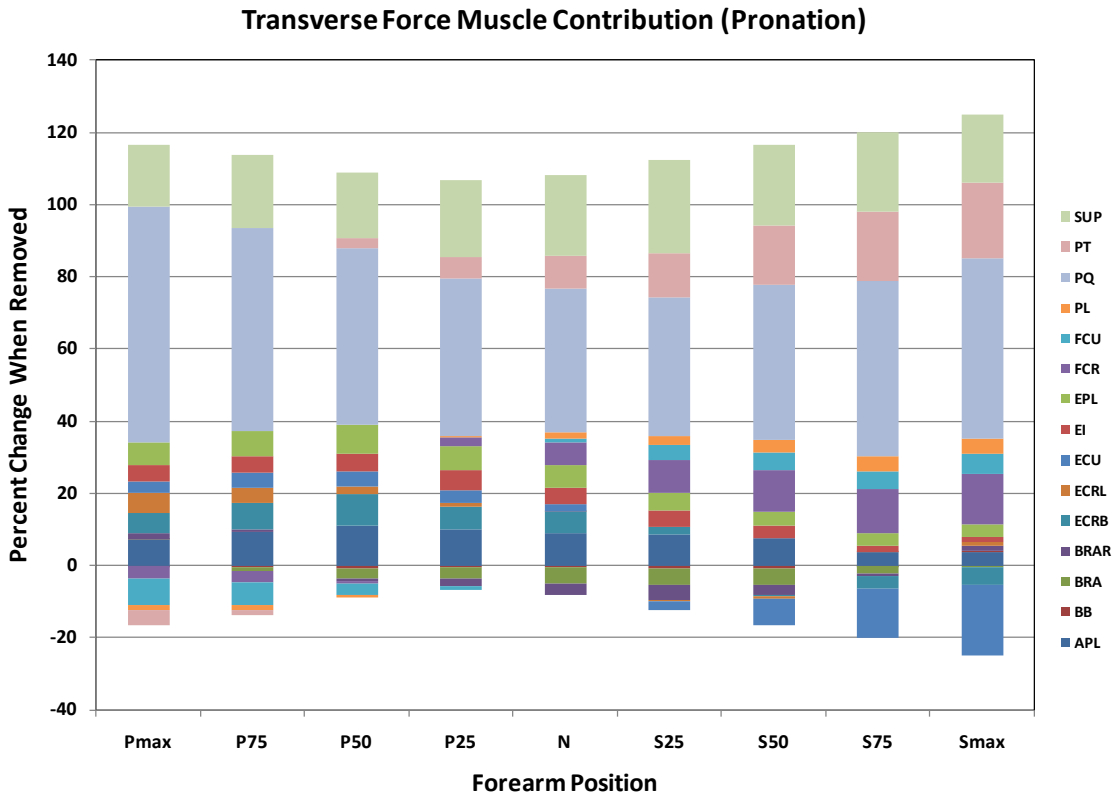

Figure 4.1. Muscle Effect on Transverse Forces During Pronation

This figure shows the percent change that each muscle contributes to transverse DRUJ forces during pronation when the muscle is removed. The positive and negative sides of the bars combine to equal 100% of the force observed at that particular position.

Table 4.2. Muscle Trends and Characteristic

Table 4.2 shows characteristics of each muscle that were extracted from Appendices A and C. The first six categories pertain to the number of situations where the muscle had a significant effect on the in-tact forces overall, during pronation, supination, shear forces, transverse forces and resultant forces. The "Max." and "Min." categories refer to the number of times that a muscle had the largest positive or largest negative effect on the in-tact forces. The "Max % Δ" category refers to absolute value of the largest percent difference that the muscle made. "Mean % Δ" is an average of the absolute values of the change when the difference was statistically significant. The top five muscles for each category are shaded.

	# Times significant						Max.	Min.	Max %Δ	Mean % Δ
	Total	Pron.	Sup.	Shear	Trans.	Res.				
APL	46	22	24	13	15	18	2	3	146.2	22.9
BB	22	0	22	8	5	9	0	18	44.9	16.3
BRA	19	16	3	6	4	9	0	10	90.5	10.3
BRAR	13	10	3	8	2	3	0	4	12.9	12.9
ECRB	26	12	14	6	9	11	0	0	16	9.7
ECRL	1	0	1	1	0	0	0	0	11.2	11.2
ECU	34	16	18	10	10	14	0	8	122.1	17.2
EI	31	16	15	7	10	14	0	0	13.6	7
EPL	36	17	19	5	13	18	0	0	23	8.3
FCR	36	19	17	12	9	15	3	0	85.6	15.2
FCU	31	17	14	13	9	9	2	6	114.8	18.8
PL	4	4	0	0	1	3	0	0	4	3.4
PQ	40	20	20	4	18	18	18	1	65.1	31.3
PT	32	21	11	9	10	13	1	1	169.1	17.4
SUP	53	26	27	17	18	18	29	1	243.5	39.6

4.3.2 Muscle Ranking

To rank the contribution that the fifteen muscles provided to DRUJ loading, a new metric was developed. The goal of this metric was to determine the fewest muscles required to get 75% of the total force exhibited in the shear or transverse directions. This was done both for the muscles which loaded the DRUJ and for the

muscles that exhibited force in the opposing direction. The muscle forces in a particular direction were ranked in order from greatest to least magnitude for positive forces and negative forces. The force provided by an individual muscle was added to the previous muscle until 75% of the positive and negative force exhibited by all the muscles was reached. This analysis was done for transverse and shear forces during pronation and supination at each of the nine positions for a total of thirty-six plots which can be seen in Appendix E. An example of one of the plots used in this analysis is shown in Figure 4.2. These plots were then used to rank the contribution of the muscles (Table 4.3).

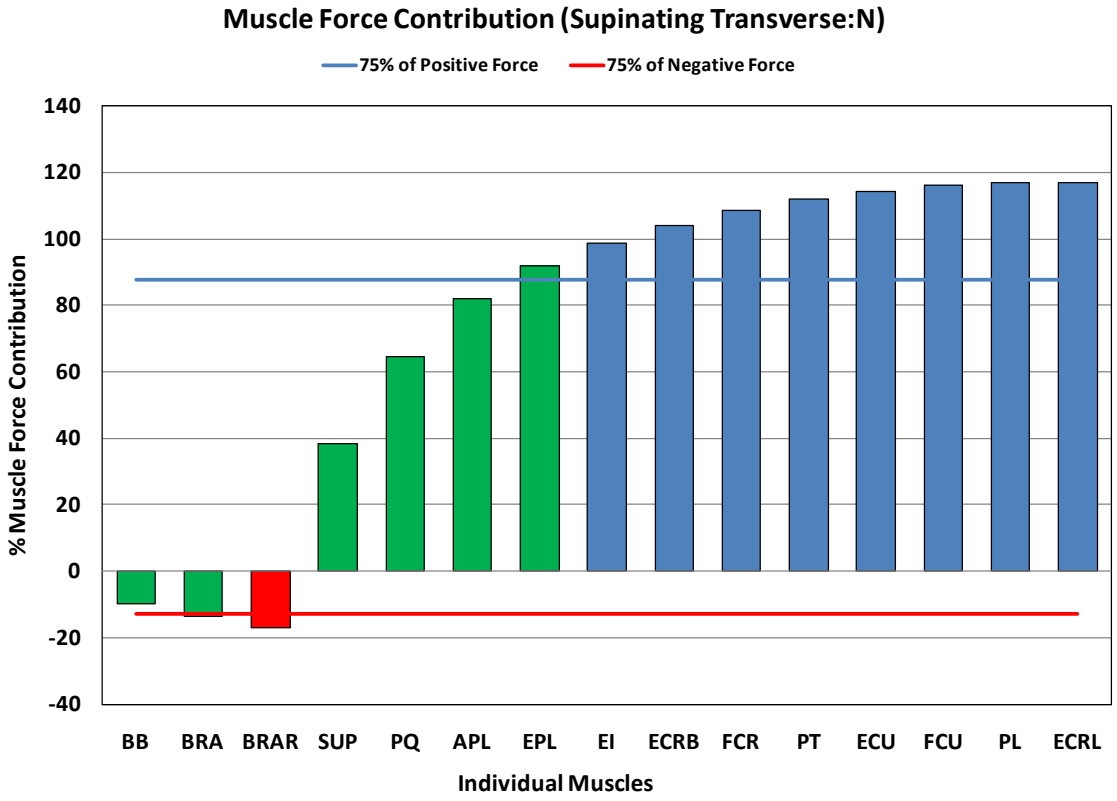

Figure 4.2. Mean Transverse Force Contributions during Supination at N

The muscles providing a negative force are on the left side of the plot while the positive forces are on the right side of the plot. The positive and negative forces are seperately ranked from the largest magnitude to smallest magnitude. The force provided by each muscle is added to the sum of the muscle forces in the bar before it. The horizontal blue line indicates 75% of the combined positive force of all muscles while the horizontal red

line indicates 75% of the combined negative force of all the muscles. The total positive force is usually greater than 100% because the positive and negative forces combine to make the overall 100% force. Therefore the lines do not occur at 75% of the total force, but 75% of the total positive and total negative force. Green bars indicate that the muscle contributes to reaching the 75% mark. Red and blue bars indicate that a muscle provides negative force and positive force, respectively but do not contribute to reaching 75% of the force. To rank the muscles, the total number of times that a muscle contributed to reaching 75% of the force (green bars) as well as in individual sub-categories were counted (Table 4.3) .

Table 4.3. Overall Muscle Contribution Rankings

This table shows the total number of times a muscle was counted as a contributor to DRUJ loading (0-36) as well as the amount it contributed to sub-categories. The top four muscles in each category are highlighted as well as their positions in the overall muscle contribution column.

Total Force		**Pronating Force**		**Supinating Force**		**Shear Force**		**Transverse Force**	
Muscle	***Frequency***	***Muscle***	***Frequency***	***Muscle***	***Frequency***	***Muscle***	***Frequency***	***Muscle***	***Frequency***
SUP	36	SUP	18	SUP	18	SUP	18	SUP	18
APL	24	PT	14	BB	15	ECU	13	PQ	18
PQ	24	PQ	13	APL	14	FCR	12	APL	14
FCR	22	FCR	12	PQ	11	FCU	12	FCR	10
ECU	21	BRA	12	FCR	10	PT	11	BRA	10
BRA	20	BRAR	12	ECU	10	BRAR	11	PT	9
PT	20	ECU	11	FCU	9	APL	10	ECU	8
FCU	18	APL	10	BRA	8	BRA	10	BB	7
BRAR	17	FCU	9	ECRB	7	BB	8	FCU	6
BB	15	ECRB	5	PT	6	ECRL	7	BRAR	6
ECRB	12	ECRL	4	EPL	6	PQ	6	ECRB	6
EPL	8	EPL	2	BRAR	5	ECRB	6	EPL	6
ECRL	7	EI	2	ECRL	3	EI	3	ECRL	0
EI	3	BB	0	EI	1	EPL	2	EI	0
PL	0	PL	0	PL	0	PL	0	PL	0

Table 4.4. Individual Muscle Properties

When referring to the origins "(R)" indicates the radial origin, "(U)" indicates the ulnar origin and "(H)" indicates the humeral origin.

Muscle	Site of Origin	Site of Insertion	Longest Position	Shortest Position	Shortest % of Maximum
APL	Posterier radius/ulna near the interosseous membrane	Base of the 1st metacarpal	25P (R) MaxP(U)	50S (R) 50S (U)	94.5% (R) 95.1% (U)
BB	Supralglenoid tubercle (long) and coracoid (short) of the shoulder	Bicipital tuberosity and lacertus fibrosus	MaxP	MaxS	92.3%
BRA	Anterior Humerus	Ulnar tuberosity	75S	50P	95.3%
BRAR	Lateral supracondylar ridge	Distal lateral radius	MaxP	N	93.7%
ECRB	Lateral epicondyle ridge	Base of the 3rd metacarpal	N	MaxP	97.8%
ECRL	Lateral supracondylar ridge	Base of the 2nd metacarpal	MaxS	N	97.8%
ECU	Lateral epicondyle	Base of the 5th metacarpal	N	MaxP	97.7%
EI	Posterior ulna near the interosseous membrane	Sagittal bands, central slip and distal phalanx of index finger	N	MaxP	96.4%
EPL	Posterior ulna near the interosseous membrane	Base of thumb and distal phalanx	25P	MaxP	96.0%
FCR	Medial epicondyle of humerus	Base of the 2nd and 3rd metacarpal	50P	50S	98.2%
FCU	Medial epicondyle of humerus and posterior ulna	Pisiform, hook of the hamate and the 5th metacarpal	25P	75S	96.6%
PL	Medial epicondyle of humerus	Flexor retinaculum/palmar aponeurosis	75P	25S	97.7%
PQ	Ulnar border of the distal ulna	Anterior aspects of the distal radius	MaxS	MaxP	56.5%
PT	Medial epicondyle of the humerus and coronoid of the ulna	Lateral mid-radius	75P(H) MaxS(U)	MaxS(H) 75P(U)	92.3% (H) 92%(U)
SUP	Posterior medial Ulna	Proximal lateral radius	N	75S	81.8%

4.4 Discussion

4.4.1 Overview

The biomechanics of the forearm are complex. Very few muscles contribute to DRUJ loading and forearm rotation under all circumstances. Factors such as the position of forearm rotation, direction of forearm force, degree of elbow flexion, and whether the actions studied were static or dynamic all affect the role that individual muscles play in forearm biomechanics. This study examined fifteen muscles during isometric pronation and supination activities at pronated and supinated positions with the elbow

flexed at 90°. Many conclusions can be drawn from these data which are shown in Appendices A-E. In the following sections, the role of the individual muscles will be discussed based on the data provided in this chapter and the appendices, followed by a general discussion.

4.4.2 Abductor Pollicis Longus

Of the eight muscles that control the thumb, only the APL and APB directly connect to the thumb (29). The APL is divided into distinct divisions and each division has a separate function (29), thus making the APL a complex muscle to analyze. Most literature suggests that the primary movement of the APL is abduction and extension of the thumb (42, 53, 190). The present study agrees with this and also shows that the APL is more active as the forearm supinates. Note that this does not necessarily mean that the APL is a forearm supinator. This assertion is because the present data were collected during a gripping exercise. The act of gripping the handle may have activated the APL because the thumb was trying to extend during forearm supination but not during pronation. Of the eight muscles that control the thumb, only the APL and APB are directly connected to the actual digit (29).

Overall, the APL was one of the dominant players of forearm biomechanics and ranked among the top five muscles in nine of the ten categories chosen. The APL generated more force in pronation and supination than every muscle except the SUP. It also had the most significant contribution to generating the resultant DRUJ force (along with the EPL, PQ and SUP). The APL was the second most influential muscle in overall DRUJ loading, the third most influential muscle during supination, and the third most influential muscle regarding transverse force.

4.4.3 Biceps Brachii

The role of the BB is to flex and supinate the forearm (53, 190, 197). The present study confirms this as the BB was one of the most active muscles while supinating and was least active of the fifteen muscles during pronation. Most BB EMG studies confirm

that the muscle is much more active while supinating than pronating (15, 40, 80, 85, 88, 98, 147). However, Taniguchi et al. (187) claim that the BB does not act as a supinator while the forearm is in a supinated position. It was most active in mid-full supinated positions; however, the differences were not significant which is similar to the findings of Gordon et al. (80). O'Sullivan et al. found that the supinating signals were greatest at N and 75S (147). There is a decline in activity level as the forearm approaches full pronation which agrees with the observations in other studies (16, 38, 80, 103, 135, 141). This decline may be because of the length-tension relationship which indicates that when a muscle is longer (the BB in pronation), less activity is required to achieve a given torque (31, 40, 80). All movements of forceful supination against resistance require the cooperation of the biceps in varying degrees with the supinator (15, 16).

The BB is considered one of primary rotators of the forearm along with the PT, PQ and SUP. The BB was in the top five in only two of the ten chosen categories. However, it exhibited the largest unloading force on the DRUJ in eighteen instances. It also had the third most instances of significant difference between the in-tact model and the BB-removed model during supination. The BB is the tenth most influential muscle regarding overall DRUJ loads and the second most influential muscle regarding supinating force.

4.4.4 Brachialis

It is widely accepted that the BRA is considered a flexor of the forearm (53, 190) at all positions because its line of action does not change as the forearm rotates (15). However, some researchers have noted that it may play a minor role in forearm pronation-supination as well (16, 36, 85, 147). The BRA was among the seven least active muscles during pronation at all positions and among the four least active during supination. There was not a significant difference between pronation and supination activity at any position of forearm rotation. The BRA exhibited the greatest activity during pronation and supination at 50S. Overall, the BRA is more active as the forearm pronates which agrees with other published findings (140, 141).

The BRA is among the top five in only one of the ten chosen categories. It exhibited the largest amount of unloading influence on various DRUJ forces in ten instances. The BB is the only muscle with more influence in this aspect. The BRA is the sixth most influential muscle in overall DRUJ loading, the fourth most influential regarding pronating force and the fourth most influential regarding transverse force.

4.4.5 Brachioradialis

There is a great deal of variety in the literature when determining the role of the BRAR. Most references agree that the BRAR acts as a forearm flexor (53, 190), but the other roles of the muscle are disputed. Basmajian claims that it is a pronator of the supine forearm and supinator of the prone forearm in resisted movements only (15). Other studies agree that it acts as both a pronator and a supinator (28, 36, 85, 147) Gielen et al. state that during pronation, the BRAR motor units receive no input (68). Yet, others claim that the muscle produces no signal during pronation or supination (49, 197). The EMG data in the present study suggest that the BRAR is more active as a pronator than a supinator. Several other studies have also found that the BRAR is more active as a pronator than as a supinator (24, 98, 140, 141).

Overall, the BRAR was among the top five muscles in only one category of the ten chosen categories. It was the largest unloader of the DRUJ in four different instances. The BRAR was the ninth most influential DRUJ load contributor overall and it had the fourth largest effect on pronating force.

4.4.6 Extensor Carpi Radialis Brevis

The primary role of the ECRB is wrist extension and radial deviation (28, 53, 190). The ECRB was in the bottom half of active muscles during pronation except at 50P. During supination it was in the bottom half at all positions and least active at 50S, 75S and MaxS. There was not a significant difference between pronating and supinating ECRB activity at any position of forearm rotation. The ECRB exhibited the greatest activity during pronation at N and during supination at MaxP.

The ECRB was one of only three muscles that was not among the top five in any of the ten chosen categories. However, it did exhibit significant influence on loads at the DRUJ in twenty-six instances. Overall, the ECRB was the fourth least influential muscle on DRUJ loading and was not among the four most influential muscles in any sub-category.

4.4.7 Extensor Carpi Radialis Longus

The primary purpose of the ECRL is to extend and abduct the wrist (28, 53, 190). There was not a significant difference between pronation and supination ECRL activity at any position of forearm rotation. The ECRL exhibited the greatest activity during pronation at 25P and during supination at neutral. Fujii et al. (58) suggest that forearm supination from the prone position should be added to one of the actions of the ECRL. The data from the current study agree with this because the supination activity is greater in pronated positions than in supinated positions, even though these differences are not statistically significant.

The ECRL was among the least influential muscles on DRUJ loading of any of the muscles that were studied. The ECRL was not among the top five muscles of any of the ten chosen categories and only exhibited significant influence on DRUJ loads in one of the fifty-four instances studied. The ECRL was the third least influential muscle on DRUJ loading and was not among the four most influential muscles in any sub-category.

4.4.8 Extensor Carpi Ulnaris

The primary role of the ECU is flexion and ulnar deviation of the wrist (28, 53, 190). However, Garcia et al. (64) report slight to marked action potentials in subjects while pronation is performed against resistance. There was not a significant difference between pronation and supination ECU activity at any position of forearm rotation. The ECU may also help to initiate pronation and supination at the extremes of forearm rotation. The ECU exhibited the greatest pronation activity at MaxS and during supination at MaxP. Haugstvedt et al. (85) and Nathan (143) report that the ECU and

FCU generate a potential pronating torque with the forearm in maximum supination and to a lesser extent, a potential supination torque while the forearm is in maximal pronation. The present study seems to agree with their findings. These findings also agree with the assertion from Haugstvedt et al. (85), that the ECU and FCU may be responsible for initiating pronation from the maximally supinated position.

The ECU was ranked among the top five muscles in five of the ten categories chosen. It was the largest unloader of DRUJ forces in eight instances. The ECU was the fifth most influential DRUJ loader overall and was the second most influential muscle regarding shear forces.

4.4.9 Extensor Indicis

The primary purpose of the EI is to extend the index finger (28, 53, 190). However, a study by Nathan (143) showed that the EI has the potential to generate pronation torque in supinated positions. There was not a significant difference between pronation and supination EI activity at any position of forearm rotation. The EI exhibited the greatest activity during pronation at 25P and during supination at 50S.

The EI was among the top five muscles in only one of the ten chosen categories. It was among the top transverse force loaders and exhibited significant loading in thirty-one instances. Overall, the EI was the second least influential muscle in DRUJ loading.

4.4.10 Extensor Pollicis Longus

The primary role of the EPL is extension and adduction of the thumb (15, 42, 190). It produces extension of the IP, MCP joints (28, 53, 127) and also has an adduction moment at the TM joint (121). It also assists the abductor muscles in repositioning or spreading the thumb out widely so that it can grasp large objects (15) as well as adduct and extend the CMC joint (28). There was not a significant difference between pronation and supination EPL activity at any position of forearm rotation. The EIP exhibited the greatest activity during pronation at 50P and during supination at 50S.

The EPL significantly increased shear forces only at the extremes of forearm rotation while it increased the transverse forces at supinated and mid-rotation positions. The EPL was a significant resultant force loader of the DRUJ at every position of forearm rotation both while pronating and while supinating. It was also among the top five muscles in five of the ten chosen categories. The EPL was one of the four muscles that significantly affected resultant forces in eighteen instances. It was also among the top influences in total loading, loading during pronation, loading during supination and loading of transverse force. However, overall, the EPL was the fourth least influential DRUJ loader.

4.4.11 Flexor Carpi Radialis

The primary role of the FCR is flexion and radial deviation of the wrist (28, 53, 190). FCR activity was significantly greater in pronation than supination at N, 25S, 50S and MaxS. The FCR exhibited the greatest activity during pronation at MaxS and during supination at 50P.

The FCR was among the top five muscles in five of the ten chosen categories. It was the largest loader of the DRUJ in three instances and had one of the larger influences in overall DRUJ loads, pronating, shear and resultant loads. Overall, the FCR was the fourth most influential muscle in DRUJ loading, the fourth most influential muscle during pronation, the third most influential muscle regarding shear forces and the fourth most influential muscle regarding transverse forces.

4.4.12 Flexor Carpi Ulnaris

The primary role of the FCU is flexion and ulnar deviation of the wrist (28, 53, 190). However Garcia et al. (64) report slight to marked action potentials in subjects while pronation is performed against resistance. There was not a significant difference between pronation and supination FCU activity at any position of forearm rotation. The FCU exhibited the greatest pronation activity at MaxS and supination activity at MaxP.

The FCU was ranked among the top five muscles in six of the ten categories chosen. It had one of top percentages of change in DRUJ loading as an overall average as well as in a single instance. It was among the most influential muscles regarding pronating and shear loads. It exhibited the largest loading effect on the DRUJ in two instances and unloading effect in six. The FCU was the eighth most influential muscle in overall DRUJ loading and the fourth most influential muscle in shear loading.

4.4.13 Palmaris Longus

The primary role of the PL is wrist flexion and neutral deviation (28, 53, 190). Nathan reports that the PL generates torque in the pronation direction while the forearm is in supinated positions and in the supination direction while the forearm is in pronated positions (143). PL pronation activity was significantly larger than supinating activity all positions from 25P-MaxS. The PL exhibited the greatest pronation activity at 75S and the greatest supination activity at 75P. Overall, PL activity is significantly greater during forearm pronation than in supination.

The PL was among the least influential muscles on DRUJ loading. It was not among the top five muscles in any of the ten chosen categories and exhibited significant influence on the DRUJ in only four of the fifty-four possible instances. Overall, the PL is the single least influential muscle in DRUJ loading and was not found among the muscles accounting for 75% of the load in any sub-category.

4.4.14 Pronator Quadratus

The primary action of the PQ is to pronate the forearm (28, 53, 190). The PQ exhibited significantly greater activity during pronation than during supination at each of the forearm positions. During pronation, the PQ exhibited the greatest activity at 75P and during supination at Neutral. Overall, the PQ is more active as the forearm pronates which agrees with the findings of other studies (80, 147). A number of studies say that the PQ is a pronator only, and there is little to no activity in the early stages of

pronation (15, 49). The current study shows that while pronating activity was smallest at full supination, it was not significantly less than other positions.

The PQ was among the most influential muscles on DRUJ loading that was studied. It was among the top five most influential muscles in seven of the ten categories chosen. The PQ was the third most influential muscle overall, the third most influential muscle during pronation, the fourth most influential muscle during supination and the second most influential muscle regarding transverse force.

4.4.15 Pronator Teres

The primary actions of the PT are to pronate (53) and flex (190, 197) the forearm. The PT exhibited significantly greater activity during pronation than during supination at each of the forearm positions. The PT exhibited the greatest activity during both pronation and supination at 50S. Overall, the PT is more active as the forearm pronates which is consistent with other studies (80). During pronation, the PQ is significantly more active than the PT. Based on muscle activity alone, Basmajian et al. (15) and Haugstvedt et al. (85) suggest that the PQ is the more dominant agonist during forearm pronation and that the PT is called in as a reinforcing muscle to the PQ during resisted torques. The Gordon study (80) also shows that the PQ activity level is higher than that of the PT; however, they claim that the PT is the primary agonist when other factors are considered such as moment arm and PCSA. Haugstvedt et al. (85) claim that the PQ and PT do not generate torque in the maximally supinated positions and that the potential of the ECU and FCU may be responsible for initiation pronation from that position. However, the current study shows that both muscles exhibit activity at full supination.

While the PT is considered to be one of the primary rotators of the forearm, the only category of the ten chosen in which it was among the top five muscles was the largest single percent change in DRUJ loading. However, it was the largest loader and unloader once and significantly affected DRUJ loading in thirty-two instances. Overall,

the PT was the seventh most influential muscle in DRUJ loading and had the second largest effect on pronating force.

4.4.16 Supinator

The primary action of the SUP is to supinate the forearm (53, 190); however, there were no significant differences in SUP activity between directions at the same forearm position. During forearm pronation, the SUP exhibited the greatest activity at 75S and during supination at Neutral. Overall, the SUP is more active as the forearm supinates than as it pronates. Two studies (15, 68) found that the SUP is not active during pronation at all. Conversely, the present study found that SUP supination activity was larger than the pronation activity at all tested positions; however, these differences were not significant and agree with the results found in other studies (80). The largest SUP activity occurs around midrange of forearm rotation which is different than the results from Gordon et al. (80) who found that activity was higher in full supination compared to neutral-full pronation. However, Gordon did find that the activity level in full pronation was greater compared to full supination which is consistent with the findings of the present study. Other EMG studies have found that the overall activity level of the SUP was greater than that of the biceps, indicating that the SUP was the primary agonist during supination (15, 85). Based on EMG data alone, this study has found that that the ECU and BB are more active in pronated and supinated positions respectively than the SUP. This finding somewhat agrees with the Gordon study which claims that even though their EMG results indicated more activity for the SUP compared to the BB, the BB is the more influential agonist when anatomic factors such moment arms and PCSA are taken into account.

The SUP was the most influential muscle on DRUJ loads observed in this study. It was highlighted in nine of the ten chosen categories. It has the largest average percent force change as well as the largest single instance of change. It is also the single most influential muscle in each of those nine categories. The SUP was the most influential muscle on DRUJ loading overall and in each of the four ranked sub-categories.

4.4.17 General Discussion

It has been widely accepted that the primary pronators of the forearm are the pronator teres and pronator quadratus while the primary supinators are the biceps brachii and supinator (15, 85, 148, 215). However, their role in loading of the DRUJ as well as the other muscles examined is not clearly understood. The SUP played a significant role in loading the DRUJ during supination and pronation for shear, transverse and resultant forces and was the largest loading muscle at every forearm position for supinating shear and transverse forces. The BB acted as a significant unloader of the supinating DRUJ for shear, transverse and resultant forces. It was the largest unloader of the resultant forces during supination at every position of forearm rotation. During pronation it acted to unload the DRUJ, but the effect was not significant for any kind of force at any position and was ranked as only the tenth most influential DRUJ loader. The PQ was the largest transverse and resultant force loader during pronation at all forearm positions and had a significant effect on shear forces at 2 positions. The PQ was also a significant loader of transverse and resultant forces during supination; however, it played no significant role in supinating shear forces. The PQ was the largest unloader of pronating shear forces at MaxP, even though the effect was not considered significant. Overall, the PQ was the third most influential muscle regarding DRUJ loading and was among the four most influential muscles forces during pronation, during supination and transverse force. The PT was a significant loader during shear pronation at pronated positions and neutral, while during supination, it was significant at only two positions. During pronation, shear forces were significantly affected at supinated positions, neutral and 25P while during supination, they were affected at all supinated positions. It was a significant resultant loader at all positions except MaxP during pronation, and during supination, it was significant at neutral and supinated positions. The PT was the only primary forearm rotator that was not the largest loader or largest unloader of the DRUJ at any point. Overall, the PT was the seventh most

influential muscle on DRUJ and was only among the top four muscles affecting pronating force.

This study demonstrated that muscles other than the primary four pronators and supinators of the forearm had an effect on loads at the DRUJ. Muscles that exhibited the greatest loading effect at any instance included the APL, FCR, FCU in addition to the PQ and SUP. Muscles that exhibited the greatest unloading effect included the APL, BRA, BRAR, ECU, and FCU in addition to all four of the primary forearm rotators. The top four most influential muscles in pronating force are the SUP, PT, PQ, FCR, BRA, and BRAR (FCR, BRA and BRAR tied for fourth most influential). The most influential muscles in supinating force were the SUP, BB, APL and PQ. The most influential shear force muscles were the SUP, ECU, FCR and FCU. The most influential transverse force muscles were the SUP, PQ, APL, FCR, and BRA (FCR and BRA tied for fourth most influential). All of these muscles make up the ten overall most influential muscles of the fifteen studied.

Even though all muscles were found to significantly affect DRUJ forces in at least one instance, some proved to have an overall minimal effect. The three muscles that were not among the top five in any of the chosen categories included the ECRB, ECRL, and the PL. Overall, the ECRB, EPL, ECRL, EI, and PL were the five least influential muscles and were not seen among the top four muscles in any sub-category.

4.4.18 Study Conclusions

The role that individual muscles play during forearm rotation and the relationship they have to loads at the DRUJ are complex. Classically, the PT, PQ, SUP, and BB are considered the primary rotators and contributors to DRUJ loading. The present findings support the claim that these are influential muscles. All of the muscles studied here demonstrated that they significantly affect the DRUJ in some way. The muscles that exhibited the largest loading or unloading role at any single instance included the APL, BB, BRA, BRAR, ECU, FCU, PQ, PT, and SUP. The muscles that were among the four most influential in any sub-category included the SUP, APL, PQ, FCR, ECU, BRA, PT, FCU, BRAR, and BB (the ten most influential muscles overall). The

accuracy of future analytical and experimental models of the DRUJ as well as the forearm can be improved. Incorporating these ten muscles will help to improve that accuracy.

CHAPTER 5: OVERALL DISCUSSION AND CONCLUSIONS

5.1 Key Findings

The EMG portion of this study found that the BRAR, FCR, PL, and APL contribute significantly to forearm pronation and supination along with the previously recognized major contributions of the PQ, PT, SUP, and BB. The results of the in-tact DRUJ mathematical model affirm that compressive forces pass from the radius to the ulnar head at all points of forearm rotation. In addition to large compressive forces, this study indicates that shear forces exist in the DRUJ. These shear forces act to pull the radius away from the ulna in the AP direction and are large enough to be taken into consideration when examining potential treatment options. These shear forces are greatest in pronation and least between N and 25° of supination. The individual muscle analysis portion of this study found that of the fifteen muscles analyzed, ten had a major effect on forearm and DRUJ biomechanics. Other than the classic primary forearm rotators (PQ, PT, SUP, BB), the top ten most influential muscles included the APL, FCR, ECU, BRA, FCU, and BRAR.

5.2 Discussion

5.2.1 EMG Study

Prior to this research, a comprehensive set of indwelling EMG data that contained each of the forearm muscles thought to affect forearm rotation and DRUJ loading throughout the range of forearm rotation during isometric supination and pronation did not exist. The previous study that was closest to what was needed for this research examined the PQ, PT, SUP, and BB at five positions of forearm rotation (80). Understanding muscle activity during isometric exertion is a key step needed to

determine muscle forces and the role those forces play in DRUJ loading. Expanding the knowledge base about muscle activity to fifteen muscles and to nine forearm positions was a key contribution to the understanding of forearm biomechanics.

The EMG analysis found that BB activity was significantly greater during supination than during pronation at each of the nine positions examined. The BRAR activity was significantly greater during pronation at 25S, 50S, 75S, and MaxS. Pronating FCR activity was significantly greater than supinating activity at N, 25S, 50S, 75S, and MaxS. Pronating PL activity was significantly greater than supinating activity at 25P, N, 25S, 50S, 75S, and MaxS. Both PQ and PT activity were significantly greater during pronation than in supination each of the nine positions. The APL, BB, and SUP were found to have overall significantly greater muscle activity during supination while the BRA, BRAR, ECRL, FCR, PL, PQ, and PT exhibited significantly greater overall pronation activity. Muscles that were among the top three most active during pronation at any position included the PQ, PT, EIP, ECU, FCR, and PL. During supination, the top three most active muscles at all positions included the ECU, SUP, BB, and APL. The new information contributed by the EMG study found that other than the PQ, PT, BB, and SUP, that the BRAR, FCR, and PL made a significant contribution to pronation while the APL made a significant contribution to supination. Based on EMG analysis alone, this study determined that the BRA, ECRB, ECRL, ECU, EIP, EPL, or FCU had neither an overall pronating effect nor supinating effect.

5.2.2 In-tact DRUJ Loading Model

The in-tact model portion of this study found that shear forces at the DRUJ range between 18.6N and 99.5N, are lowest at neutral and 25S and increase as the forearm pronates and supinates. The transverse forces range between 57.5N and 181.4N. These compressive forces are greatest at mid-rotation and decrease as the arm rotates in either direction both while pronating or supinating. The pronating transverse forces were significantly greater than the supinating transverse force. Resultant forces ranged between 84.5N and 190.6N and were greatest between 50P and N. The pronation

resultant forces were significantly greater than the supination resultant forces at every position except MaxP.

Only two previous studies have examined forces in either the transverse or shear direction of the DRUJ. Both of these studies relied on empirical data obtained from force transducers while the present study is an analytical model based on theory. The first study utilized pressure sensitive film (172) while varying axial loads were applied to the forearm. The results found that transverse loads across the DRUJ increase from pronation to supination while the present study found the opposite. Differences in force trends may be because the forces in the present study are based solely on estimated muscle force data while the film study did not take muscle loading into consideration. The second study utilized an instrumented ulnar head placed within cadaveric specimens in a joint simulator (67). DRUJ loads for the simulator study were only reported at 40˚ of pronation, 40˚ of supination and neutral. ML, AP, and IS axis bending moments were reported in 20˚ increments. Differences in the results between the simulator study and the current study may come from the fact that muscle forces for eighteen different sets of muscle origins and insertions were used in the current study while the simulator only utilized the forces from four muscles.

5.2.3 Individual Muscle Roles

This study demonstrated that muscles other than the primary four rotators of the forearm had a significant impact on loads seen at the DRUJ. The most influential muscles regarding force during pronation included the SUP, PT, PQ, FCR, BRA, and BRAR. During supination, the muscles with the most influence included the SUP, BB, APL, and PQ. Shear forces were influenced the most by the SUP, ECU, FCR, and FCU. The muscles with the largest effect on transverse force included the SUP, PQ, APL, FCR, and BRA. All of these muscles account for the ten most influential muscles in DRUJ loading. The muscles that were not among the top four contributors in any sub-category and were the least influential overall included the PL, EI, ECRL, EPL, and ECRB.

5.2.4 Overall Discussion

When looking at the overall muscle effect on the DRUJ model, the major contributors based on EMG data were the PQ, PT, BB, SUP, BRAR, FCR, PL, and APL. Based on removing the muscles from the in-tact model, the major contributors were the SUP, APL, PQ, FCR, ECU, BRA, PT, FCU, BRAR, and BB. The PL is the only muscle to be found significant in the EMG portion of the study but not in the muscle analysis portion. The EMG activity showed it to be an active pronator. However, the force generating capability of the PL was the second smallest of all the muscles next to the EI. The BRA, ECU, and the FCU were all listed as major DRUJ loaders based on the model analysis, but not on the EMG analysis. The BRA only met one of the three criteria to be classified as a contributor to forearm rotation based on EMG activity. However, the BRA had the sixth largest force generating potential which made it a significant DRUJ unloader. The ECU had the third largest force generating capacity while the FCU had the second largest. This allowed for a significant contribution to DRUJ forces from both even though the EMG muscle activity was not regarded as significant.

5.3 Limitations

5.3.1 EMG Study

When using EMG to analyze muscle function, a number of limitations must be taken into consideration. This study used a gripping exercise to measure muscle effects during pronation and supination. Pure forearm rotation in the absence of gripping (80), may better represent true pronation and supination, but rarely is this forearm motion performed with an unloaded hand. Although muscular isometric force capacity is directly related to the number of motor units activated (36), motor unit and muscle activation is not homogeneous across all subjects (135) . In addition, it has been found that that the combination of multiple functional tasks may induce a larger activation than what is seen in an individual motion (35). This would indicate that the published maximum voluntary isometric exercises (106) used to obtain a maximum activity level

may not have actually provided a true maximum signal. This phenomenon was observed in the EMG data collected for the APL. The primary function of the APL is abduction and extension of the thumb (42, 53, 190). Gripping the handle while supinating would have activated the APL because the thumb was trying to extend; this did not occur during pronation. As a result, using MVIC as the maximum scaling factor gave APL data that were greater than 100% during supination. This is the rationale for normalizing the EMG data by the largest value observed instead of just the MVIC exercises. It should also be noted that muscles are not activated homogeneously (197) and that the particular motor units being measured by the indwelling electrodes may not be representative of the activity of the muscle as a whole. Because other studies have found that elbow position affects torque (59, 68, 147, 215), the present findings may be limited to horizontal forearms with elbows flexed at a right angle. This study used eleven subjects per muscle. Because each individual recruits and activates the muscles differently, there is a large standard deviation in the data collected between subjects, and is typical for EMG studies.

Generally, the muscle with the greatest mechanical advantage receives the largest input (195). The mechanical advantage of muscles that pronate and supinate the forearm change greatly as the external axis of rotation changes (38). When the elbow is flexed, pronation and supination occur because of the muscles acting on the radio-ulnar joints, and when it is extended, the rotator muscles of the scapulo-humeral joints are called into action (45). Therefore an angle of 90° of elbow flexion was chosen because flexion tends to use the forearm pronators and supinators more than elbow extension and the torque values are supposedly higher in flexion. Hence, the data reported here are only relevant when the forearm is flexed at 90° and not when the forearm is extended.

5.3.2 DRUJ Force Model and Muscle Analysis

A number of limitations should be taken into consideration for the analytical portion of this research as well. This analysis of DRUJ forces only incorporated muscle

loading. Loads from other soft tissue structures such as the radioulnar ligaments and the interosseous membrane were not taken into consideration. Straight-line orientations from the muscle origin to the muscle insertion were utilized in this model while factors such as muscle wrapping were ignored. In addition, because isometric forces were being examined, constant force was assumed for each muscle, and effects, such as stretching, were not taken into consideration. As in the EMG study, the model only examines DRUJ forces with the elbow flexed at 90°. Additionally, this model is comprised of a series of static models over the range of forearm rotation in order to give an idea of the trends at different forearm positions. This model is not a dynamic model, and, therefore, does not take the Newtonian equations into consideration, nor does it consider the change in muscle tension that would be observed by using the Hill muscle model. The PCSA data used for most of the muscles were from a set of 5 different forearms from elderly cadavers. The age of the cadavers can affect the muscle volume for the PCSA calculation as could the small sample size of the forearms used. The EMG data were collected on young healthy subjects, so the pairing of the two sets of data is not ideal. Current technology can be used to find the PCSA in living subjects through the use of MRI or ultrasound (33). The cadaveric muscle orientation data were collected at 10° increments before the EMG protocol had been developed. Due to the amount of time involved in collecting the EMG data for each subject, a decision was made to collect the data at nine forearm positions. Because the two data sets did not match, the cadaver data had to be interpolated and, therefore, did not match the exact coordinates that were collected. The muscle scaling factor of 3.6 kg/cm^2 was used because it was a commonly used number and was roughly around the middle of the range of the other numbers used. The magnitudes from this model are dependent on this scaling factor; however, the resulting trends are not and would not change based on the scaling factor used as long as it was the same for all fifteen muscles. Actual muscle origins and insertions are not single points but cover relatively large amounts of the bone surface area in irregular shapes and thicknesses. Muscle origins and insertions

were chosen as a single point based on visual inspection of the approximate center of the origin and insertion.

5.4 Clinical Implications

In order to maintain the biomechanical function of the forearm, preserving the natural anatomy and function of the distal ulna is vital. Compressive and longitudinal force transmission across the ulna can be demonstrated by the trabecular lines radiating perpendicular to the two articular facets of the ulnar head (13). In clinical practice, the need for maintaining ulnar head anatomy can be seen from the mixed results (67) associated with procedures involving distal ulna resection such as the Darrach (47) or Sauve-Kapandji (165, 168). The need for maintaining anatomy is further demonstrated by the loads at the DRUJ that are reported here. The need for treatment methods that maintain the ulnar anatomy has led to procedures that attempt to restore the ulnar head. Early results of these prosthetic replacements seem favorable (214).

The results of the in-tact loading portion of this research indicate that instability splints should be placed around 25° of supination to minimize shear. Loading after distal ulna procedures should begin in significant pronation and supination to minimize the compressive forces seen at neutral. The data also suggest that plate fixation of the distal ulna should be in more than one plane. In addition, arthroplasty and fracture system designs need to address these forces. Resection of the ulna head should be avoided.

The individual muscle loading portion of this study found that ten of the fifteen muscles examined were needed to make up 75% of the forces seen in the in-tact forearm. Therefore it is important to maintain the function of these ten muscles and to keep them in-tact if possible. Five muscles were found to have minimal influence and, as far as the DRUJ is concerned, could be sacrificed while still maintaining most of the function of the joint.

5.5 Conclusions

Based on the results of this research it can be concluded that:

I. EMG data indicate that the PQ, PT, BRAR, FCR, and PL contribute to forearm pronation.

II. EMG data indicate that the BB, SUP, and APL contribute to forearm supination.

III. DRUJ shear forces are least between mid rotation and early supination and greatest at the two most pronated positions.

IV. DRUJ transverse forces are greatest at mid-rotation and decrease as the arm rotates in either direction.

V. Pronating transverse forces at the DRUJ are significantly greater than supinating transverse forces at all positions of forearm rotation.

VI. DRUJ resultant forces are greatest at neutral and mid-pronation

VII. Pronating resultant forces at the DRUJ are significantly greater than supinating resultant forces at all forearm positions except maximum pronation

VIII. ECRB, EPL, ECRL, EI, and PL had minimal impact on DRUJ loading

IX. Muscles other than the PQ, PT, BB, and SUP significantly affect DRUJ loading during isometric forearm rotation.

5.6 Future Research

Simply changing some of the variables of the current research could yield some potentially useful information regarding forearm biomechanics. EMG and cadaver data could be collected at elbow angles other than 90°. A larger number of subjects could be used. Orientation data could be collected on more cadaveric specimens. Some of the forearm muscles that were not analyzed in this project such as the extensor pollicis brevis or the flexor digitorum sublimis could be investigated. Also, the sites of key soft

tissue structures such as ligaments could be marked and included in the study based on published tension properties (51, 175).

The current study could be improved by a number of factors. More accurate PCSA could be obtained from healthy living subjects using MRI or ultrasound (33). Muscle origin and insertion data could be improved by obtaining MRI scans at different forearm positions and digitally reconstructing the bones using software such as Amira (Mercury Computer Systems/3D Viz group, San Diego, CA). The origins and insertions of each muscle could then be individually reconstructed to find the area of the bone that is the true origin or insertion. An algorithm could then be used to find the geometric center of the actual origin or insertion. This same technique could also be used locate the connection points for other soft tissue structures, such as ligaments and the interosseous membrane. Theoretically, the MRI, EMG and even the PCSA data could all be collected from the same subject and would eliminate the problem of combining datasets that are not ideally matched.

A number of finite element analysis (FEA) models have been developed to look at various characteristics of the wrist and distal forearm (10, 11, 37, 69, 134, 149, 193). Some of the techniques applied in those models could be adapted to a distal forearm model that would yield more insight into how loads are transmitted to the distal radius and ulna. Once the MRI scans have been processed and the muscle origins and insertions have been digitally marked, the groundwork will have been laid for the development of such a model. The 3D model of a particular bone orientation would be converted into a mesh model suitable for FEM analysis. The model would then be imported into a FEA package such as ANSYS (ANSYS Corporation, Pigboat, PA). Material properties of healthy cortical bone could then be applied to all of the surfaces (56, 138). Constraints representing the ligaments could then be modeled using spring elements (37). Spring stiffness would be determined by published wrist ligament (20, 169) and distal radio-ulnar ligament (51, 175) data. Directional forces would be placed into the model representing muscle forces. The magnitude could come from the data presented here and the direction could come from the digitally marked origins and insertions. In

FEM analysis, the muscle origins and insertions would not necessarily have to be a single point. Instead they could be composed of multiple forces at multiple locations representing the true origin or insertion site and direction instead. This particular technique would also prove to be beneficial because, even though the distance from the origin to the insertion is a straight line, the muscle does not necessarily follow that straight line. In vivo muscle orientation data could be used to apply more accurate force directions for the muscles. In developing an accurate FEM model for the normal forearm, there are several other factors which could be included. The triangular fibrocartilage complex (TFCC) plays a significant role in axial loading in the forearm (153). The TFCC could be reconstructed in a manner similar to that of the muscle insertions and placed into the model, or elements with the same mechanical properties could be included. Cartilage at the DRUJ interface may also affect load transfer across the joint. Cartilage could be reconstructed from the MRI scans or it could be modeled by applying its mechanical properties to the articulations between the solid bone interfaces (37). Another factor that could possibly affect load transfer in the arm is the interosseous membrane (23, 83, 129, 157). It could be modeled as a ligament based on its mechanical properties (158) and its effect on forearm load transfer could be quantified. Once a satisfactory model of the normal human forearm has been created, a variety of conditions can be applied to compare the effect on the loads at the DRUJ. Osteoporosis can be simulated by changing the mechanical properties of the cortical bone. Loading can be applied at the wrist to simulate a number of activities. An implant could be added to the model. In the case of an arthroplasty, the bone to tissue interface could be tested and simulated once the radius and ulna were updated to accurately represent cortical and trabecular bone.

Another use for the EMG and muscle data would be as an input for forearm simulators. Mechanical forearm joint simulators (72, 78, 79, 87, 99, 213) have been used to quantify forces in the distal forearm, design new implants, and evaluate therapeutic procedures. These methods, however, have incorporated only a few forearm muscles (72, 78, 87, 99, 213). Adding more actuators to these simulators so

that they could pull on more than four muscle tendons would improve the accuracy of the resulting data.

Other studies that could provide valuable insight would be to develop a model using software such as Opensim (National Center for Simulation in Rehabilitation Research, Stanford, CA). This software allows you to input force values as well as to change the line of action of a muscle to account for muscle wrapping. And finally, a dynamic model could be made. Because EMG data only have a linear relationship during isometric exercises, the force data would have to come from somewhere else. Ideally one could use the Hill muscle model in conjunction with maximum muscle forces. Cadaveric muscle orientation data could be collected by using a marker/camera system with a high resolution to obtain the coordinates of the markers of interest as the forearm is moving. The theoretical actions of the muscles could also be modeled with software utilizing Kane's methods of dynamics.

APPENDIX A: MUSCLE DATA OVERVIEW

Muscles which contributed to loading of the joint are black while muscles which acted to unload the joint are in red. The number in parenthises is the % change that removal of the muscle caused in the intact model. Muscles are listed in order from the largest contributer of loading to the smallest contributer of loading (or unloading). Cells which are shaded indicate a significant difference between the intact model forces and the forces observed when the muscle is removed.

Table A.1. Muscle Contributions to DRUJ Shear Forces During Forearm Pronation

	MaxP	75P	50P	25P	Neutral	25S	50S	75S	MaxS
1	SUP(28)	SUP(24.3)	FCR(23.8)	FCR(30.2)	FCR(48.2)	PT(107.1)	SUP(243.5)	SUP(55.5)	SUP(52)
2	ECU(19.6)	PT(16.2)	PT(20.4)	PT(26.7)	PT(42.9)	FCR(85.6)	APL(146.2)	PQ(22.8)	PQ(27.6)
3	EI(13.6)	ECU(15)	SUP(15.39)	FCU(17.6)	FCU(42)	FCU(73.7)	ECU(122.1)	APL(18.3)	APL(16.8)
4	PT(13.2)	FCR(13.2)	FCU(12.64)	SUP(9.9)	PL(12.9)	ECRL(28.7)	EPL(46.6)	ECU(10)	FCU(11.3)
5	ECRB(12.4)	ECRB(12.1)	ECRB(10.5)	EI(9.2)	EI(5.9)	PL(22.8)	ECRB(35.6)	EPL(8.4)	FCR(11.2)
6	FCR(9.4)	FCU(11.4)	ECU(9.22)	PL(6.7)	ECRL(5)	BRAR(22.4)	EI(22.2)	FCR(8.3)	EPL(6.7)
7	FCU(9.3)	EI(10.7)	EI(8.84)	ECRB(5.5)	BB(0.1)	BRA(20.5)	PQ(-10.7)	FCU(8.1)	PT(5)
8	EPL(7.3)	EPL(6.4)	EPL(5.02)	ECU(3.9)	ECRB(-0.9)	BB(4)	PL(-12.1)	ECRB(3.6)	PL(3.8)
9	APL(6.6)	APL(6.3)	PL(4.02)	EPL(1.8)	BRA(-1.8)	EI(-2.9)	BB(-18)	EI(3.4)	EI(2.4)
10	PL(2.2)	PL(2.6)	APL(3.23)	PQ(1.5)	BRAR(-2.9)	PQ(-4.6)	FCU(-21)	PL(3)	ECU(2.1)
11	ECRL(1.6)	ECRL(0.9)	PQ(1.67)	ECRL(0.9)	EPL(-4.6)	ECRB(-17.1)	FCR(-46.9)	PT(-2)	ECRB(-0.5)
12	BB(-0.6)	BB(-1.5)	ECRL(0.13)	BB(-0.7)	ECU(-7.5)	EPL(-20.9)	ECRL(-60)	BB(-2.7)	BB(-2.5)
13	BRAR(-6.2)	PQ(-3.1)	BB(-1.57)	APL(-2.5)	PQ(-9.3)	ECU(-54.4)	BRAR(-87.9)	ECRL(-8.7)	ECRL(-10.6)
14	BRA(-7.9)	BRAR(-7)	BRA(-6.5)	BRA(-4.7)	SUP(-12)	APL(-68.9)	BRA(-90.5)	BRA(-13.8)	BRA(-12.5)
15	PQ(-8.4)	BRA(-7.4)	BRAR(-6.8)	BRAR(-6)	APL(-17.9)	SUP(-96.3)	PT(-169.1)	BRAR(-14)	BRAR(-12.9)

Table A.2. Muscle Contributions to DRUJ Transverse Forces During Forearm Pronation

	MaxP	75P	50P	25P	Neutral	25S	50S	75S	MaxS
1	PQ(65.1)	PQ(56.2)	PQ(48.8)	PQ(43.5)	PQ(39.9)	PQ(38.3)	PQ(43)	PQ(48.3)	PQ(50.1)
2	SUP(17.2)	SUP(20)	SUP(18)	SUP(21.6)	SUP(22.3)	SUP(25.8)	SUP(22.2)	SUP(21.8)	PT(20.8)
3	APL(7.2)	APL(9.4)	APL(11)	APL(9.9)	PT(9.1)	PT(12.3)	PT(16.4)	PT(19.4)	SUP(19)
4	EPL(6.3)	ECRB(7.4)	ECRB(8.8)	EPL(6.8)	APL(9)	FCR(9.3)	FCR(11.4)	FCR(12.3)	FCR(14)
5	ECRB(5.8)	EPL(7.1)	EPL(8.1)	ECRB(6.5)	EPL(6.4)	APL(8.6)	APL(7.5)	FCU(5)	FCU(5.3)
6	ECRL(5.4)	EI(4.6)	EI(4.8)	PT(5.8)	FCR(6.1)	EPL(4.7)	FCU(5)	PL(4.2)	PL(4.1)
7	EI(4.5)	ECU(4.3)	ECU(4.3)	EI(5.5)	ECRB(5.9)	EI(4.5)	EPL(4.1)	APL(3.8)	APL(3.9)
8	ECU(3.3)	ECRL(4)	PT(2.9)	ECU(3.5)	EI(4.6)	FCU(4)	PL(3.5)	EPL(3.2)	EPL(3.5)
9	BRAR(1.7)	BRAR(0.7)	ECRL(2.1)	FCR(2.6)	ECU(1.9)	PL(2.6)	EI(3.4)	EI(1.8)	EI(1.7)
10	BRA(0)	BB(-0.4)	PL(-0.5)	ECRL(0.9)	PL(1.5)	ECRB(2.2)	ECRB(-0.3)	ECRL(0)	BRAR(1.3)
11	BB(0)	BRA(-1.2)	FCR(-0.7)	PL(0.4)	FCU(1.3)	ECRL(-0.6)	ECRL(-0.5)	BB(-0.2)	ECRL(1)
12	PL(-1.6)	PL(-1.2)	BB(-0.8)	BB(-0.6)	ECRL(0.1)	BB(-0.7)	BB(-0.7)	BRAR(-0.7)	BB(0.1)
13	FCR(-3.6)	PT(-1.4)	BRAR(-1)	FCU(-1.1)	BB(-0.5)	ECU(-2.3)	BRAR(-2.9)	BRA(-2.1)	BRA(-0.6)
14	PT(-4)	FCR(-3.1)	BRA(-2.7)	BRAR(-2.1)	BRAR(-3.1)	BRAR(-4)	BRA(-4.7)	ECRB(-3.3)	ECRB(-4.8)
15	FCU(-7.2)	FCU(-6.4)	FCU(-3.2)	BRA(-3.1)	BRA(-4.6)	BRA(-4.7)	ECU(-7.3)	ECU(-13.6)	ECU(-19.5)

Table A.3. Muscle Contributions to DRUJ Resultant Forces During Forearm Pronation

	MaxP	75P	50P	25P	Neutral	25S	50S	75S	MaxS
1	PQ(32.3)	PQ(32.1)	PQ(35.4)	PQ(37.3)	PQ(36.9)	PQ(37.3)	PQ(41.3)	PQ(41.7)	PQ(38.3)
2	SUP(20.3)	SUP(21.3)	SUP(17.45)	SUP(20.2)	SUP(20.7)	SUP(24.1)	SUP(21.7)	SUP(25.6)	SUP(25.2)
3	ECU(8)	ECRB(8.8)	APL(9.21)	APL(8.4)	PT(10.1)	PT(12.3)	PT(14.8)	PT(14.7)	PT(15.4)
4	ECRB(7.7)	APL(8.4)	ECRB(9.14)	PT(7.9)	APL(7.9)	FCR(9.7)	FCR(11.3)	FCR(11.8)	FCR(13.6)
5	EI(7.3)	ECU(7.4)	EPL(7.42)	ECRB(6.4)	FCR(7.4)	APL(7.9)	APL(7.8)	APL(6.1)	FCU(7.8)
6	APL(7)	EPL(6.8)	PT(6.37)	EPL(6.2)	EPL(6)	EI(4.6)	FCU(5.1)	FCU(5.8)	APL(7.4)
7	EPL(6.6)	EI(6.4)	EI(5.65)	EI(5.9)	ECRB(5.7)	EPL(4.5)	EPL(4.2)	EPL(4.2)	EPL(4.5)
8	ECRL(4.2)	PT(3.6)	ECU(5.44)	FCR(5.2)	EI(4.6)	FCU(4.4)	EI(3.6)	PL(4)	PL(3.9)
9	PT(0.9)	ECRL(3)	FCR(4.06)	ECU(3.6)	FCU(2.6)	PL(2.7)	PL(3.4)	EI(2.3)	EI(2.3)
10	FCR(0.3)	FCR(1.6)	ECRL(1.71)	PL(1)	PL(1.9)	ECRB(2.1)	ECRB(0.1)	BB(-0.7)	BB(-0.6)
11	BB(-0.2)	PL(-0.1)	PL(0.44)	ECRL(0.9)	ECU(1.7)	ECRL(-0.4)	ECRL(-0.6)	ECRL(-1.4)	ECRL(-1.9)
12	PL(-0.5)	BB(-0.7)	FCU(0.03)	FCU(0.8)	ECRL(0.3)	BB(-0.7)	BB(-0.8)	ECRB(-1.8)	ECRB(-2.7)
13	BRAR(-0.8)	FCU(-1.3)	BB(-0.96)	BB(-0.6)	BB(-0.5)	ECU(-2.5)	BRAR(-3.2)	BRAR(-3.1)	BRAR(-2.9)
14	FCU(-2.3)	BRAR(-1.7)	BRAR(-2.19)	BRAR(-2.5)	BRAR(-3)	BRAR(-3.9)	BRA(-4.9)	BRA(-4.2)	BRA(-3.9)
15	BRA(-2.4)	BRA(-3.1)	BRA(-3.44)	BRA(-3.2)	BRA(-4.5)	BRA(-4.5)	ECU(-6.6)	ECU(-9.1)	ECU(-12)

Table A.4. Muscle Contributions to DRUJ Shear Forces During Forearm Supination

	MaxP	75P	50P	25P	Neutral	25S	50S	75S	MaxS
1	SUP(32.6)	SUP(30.8)	SUP(26.2)	FCU(37)	FCU(114.8)	APL(128)	SUP(83.6)	SUP(65.7)	SUP(74.1)
2	ECU(22.5)	ECU(18.9)	FCU(23.3)	FCR(29)	FCR(75.6)	SUP(117.1)	APL(63.2)	APL(39.8)	APL(30.2)
3	FCU(16.4)	FCU(17.4)	FCR(22.7)	SUP(18.4)	PT(35.4)	ECU(55.2)	ECU(27.2)	EPL(15.5)	EPL(13.1)
4	ECRB(16)	FCR(14.8)	ECU(14.8)	PT(10.8)	EI(18.8)	EPL(36)	EPL(23)	PQ(10.7)	PQ(12.3)
5	FCR(10.1)	ECRB(13.8)	ECRB(10.6)	EI(9.8)	PL(15.4)	ECRB(21.1)	ECRB(10.6)	ECU(8.3)	FCU(9.8)
6	APL(8.8)	APL(9.1)	EI(9.1)	ECRB(7.5)	ECRL(14)	EI(2.8)	EI(7.9)	FCU(8.1)	FCR(7)
7	EI(7.4)	EI(7.6)	PT(6.6)	ECU(6.1)	BB(2.1)	PQ(2)	PQ(-1.5)	EI(5.4)	EI(4)
8	EPL(5.5)	EPL(5)	APL(4.7)	PL(5.3)	ECRB(-1.7)	PL(-9.8)	PL(-1.5)	FCR(5.3)	PT(2.3)
9	PT(2.5)	PT(4.3)	EPL(4.4)	EPL(2.4)	BRA(-3)	BRAR(-10.4)	FCU(-5.4)	ECRB(3.2)	ECU(2.2)
10	PL(1.7)	PL(2.9)	PL(4)	ECRL(1.1)	BRAR(-7.1)	BRA(-12.1)	FCR(-5.7)	PL(1.3)	PL(1.8)
11	ECRL(1.3)	ECRL(0.8)	PQ(0.7)	PQ(0.6)	PQ(-13)	ECRL(-28.4)	BRAR(-9.6)	PT(-0.8)	ECRB(-0.5)
12	PQ(-2.2)	PQ(-0.9)	ECRL(0.1)	APL(-4.3)	EPL(-15.4)	PT(-34.1)	PT(-14.4)	BRAR(-6.1)	BRAR(-4.2)
13	BRA(-4)	BRA(-4.7)	BRA(-5.7)	BRA(-4.8)	ECU(-19.6)	BB(-50.1)	ECRL(-15.8)	ECRL(-9.4)	BRA(-9.1)
14	BRAR(-6.7)	BRAR(-7.5)	BRAR(-7.9)	BRAR(-6.9)	SUP(-43.8)	FCR(-51.4)	BRA(-16.7)	BRA(-11.6)	ECRL(-11.2)
15	BB(-12)	BB(-12.2)	BB(-13.7)	BB(-11.8)	APL(-72.7)	FCU(-66)	BB(-44.9)	BB(-35.3)	BB(-31.9)

Table A.5. Muscle Contributions to DRUJ Transverse Forces During Forearm Supination

	MaxP	75P	50P	25P	Neutral	25S	50S	75S	MaxS
1	SUP(38.8)	SUP(39.6)	SUP(38)	SUP(43)	SUP(38.5)	SUP(40.8)	SUP(38.7)	SUP(37.3)	SUP(38.9)
2	PQ(32.6)	PQ(26.4)	PQ(25.3)	PQ(19.2)	PQ(26.1)	PQ(21.5)	PQ(30.1)	PQ(33)	PQ(32)
3	APL(18.5)	APL(21.1)	APL(19.8)	APL(18.6)	APL(17.3)	APL(20.8)	APL(16.5)	APL(11.8)	PT(14)
4	ECRB(14.3)	ECRB(13.3)	ECRB(11)	EPL(10)	EPL(10)	EPL(10.5)	EPL(10.3)	PT(11.5)	FCR(12.4)
5	EPL(9.2)	EPL(8.5)	EPL(8.8)	ECRB(9.6)	EI(6.8)	FCR(7.3)	PT(7.1)	FCR(11.4)	APL(9.9)
6	ECRL(8.5)	ECU(8.4)	ECU(8.6)	EI(6.3)	ECRB(5.3)	EI(5.6)	FCR(7)	EPL(8.6)	EPL(9.8)
7	ECU(7.3)	ECRL(5.7)	EI(6.1)	ECU(5.9)	FCR(4.5)	PT(5.1)	FCU(6.5)	FCU(7.3)	FCU(6.7)
8	EI(4.8)	EI(5.1)	ECRL(2.9)	FCR(2.7)	PT(3.6)	FCU(4.7)	EI(6.1)	EI(4.2)	EI(4)
9	BRAR(3.5)	BRAR(1.1)	PT(1.1)	PT(2.5)	ECU(2.4)	ECRB(3.5)	PL(2.2)	PL(2.6)	PL(2.8)
10	BRA(0)	PT(-0.6)	PL(-0.6)	ECRL(1.1)	FCU(1.7)	PL(1.5)	ECRB(-0.5)	ECRL(0)	BB(2.4)
11	PT(-1.5)	BRA(-1.2)	FCR(-0.8)	PL(0.3)	PL(0.9)	ECRL(-0.8)	ECRL(-0.7)	BRAR(-0.4)	ECRL(1.6)
12	BB(-1.7)	PL(-2.1)	BRAR(-1.4)	FCU(-2.5)	ECRL(0.1)	BRAR(-2.4)	BRAR(-1.6)	BRA(-2.6)	BRAR(0.6)
13	PL(-2.5)	BB(-4.7)	BRA(-2.9)	BRAR(-2.7)	BRAR(-3.5)	ECU(-3)	BRA(-4.4)	BB(-4.1)	BRA(-0.6)
14	FCR(-7.5)	FCR(-5.4)	FCU(-7.2)	BRA(-3.3)	BRA(-3.7)	BRA(-3.6)	ECU(-8.2)	ECRB(-4.3)	ECRB(-5.9)
15	FCU(-24.4)	FCU(-15.2)	BB(-8.7)	BB(-10.6)	BB(-9.9)	BB(-11.2)	BB(-9.1)	ECU(-16.2)	ECU(-28.4)

Table A.6. Muscle Contributions to DRUJ Resultant Forces During Forearm Supination

	MaxP	75P	50P	25P	Neutral	25S	50S	75S	MaxS
1	SUP(34.7)	SUP(34.8)	SUP(34.2)	SUP(39)	SUP(36.7)	SUP(39.5)	SUP(38.8)	SUP(41.5)	SUP(45.2)
2	ECU(16.4)	APL(14.6)	PQ(16.98)	PQ(16.4)	PQ(25.1)	APL(21.2)	PQ(25.9)	PQ(23.9)	PQ(18.9)
3	ECRB(15.1)	ECU(13.6)	APL(14.89)	APL(15.3)	APL(16.1)	PQ(20.3)	APL(18.8)	APL(19.3)	APL(18)
4	APL(12.2)	ECRB(13.4)	ECRB(10.8)	ECRB(9.3)	EPL(9.7)	EPL(10.8)	EPL(11)	EPL(10.7)	EPL(11.3)
5	PQ(8.7)	PQ(11)	ECU(10.52)	EPL(9)	EI(7)	FCR(6.5)	EI(6.4)	FCR(9.5)	FCR(10)
6	EPL(6.8)	EPL(6.7)	EPL(7.38)	EI(6.7)	ECRB(5.3)	EI(5.7)	FCR(6.2)	FCU(7.8)	FCU(8.8)
7	EI(6.4)	EI(6.4)	EI(6.94)	ECU(6)	FCR(4.9)	PT(4.3)	FCU(5.9)	PT(7)	PT(7.8)
8	ECRL(3.9)	FCR(4.5)	FCR(5.53)	FCR(5.6)	PT(3.7)	ECRB(3.9)	PT(5.2)	EI(5.1)	EI(4.9)
9	FCR(3.3)	ECRL(3.2)	PT(2.7)	PT(3.5)	ECU(2.4)	FCU(3.8)	PL(1.9)	PL(2.1)	PL(2.1)
10	PT(1)	PT(1.9)	ECRL(2.12)	FCU(1.6)	FCU(2.3)	PL(1.3)	ECRB(0.8)	ECRB(-1.5)	BRAR(-1.5)
11	PL(0.1)	PL(0.4)	FCU(0.86)	ECRL(1.2)	PL(1)	ECRL(-1)	ECRL(-1.5)	BRAR(-2.2)	ECRB(-2.2)
12	FCU(-0.5)	FCU(0.3)	PL(0.7)	PL(0.9)	ECRL(0.3)	ECU(-1.9)	BRAR(-2.1)	ECRL(-2.7)	ECRL(-3.4)
13	BRA(-2.4)	BRA(-2.9)	BRAR(-3.24)	BRAR(-3.2)	BRAR(-3.5)	BRAR(-2.5)	BRA(-5)	BRA(-5.2)	BRA(-4.1)
14	BRAR(-3)	BRAR(-3.3)	BRA(-3.6)	BRA(-3.5)	BRA(-3.6)	BRA(-3.6)	ECU(-5.3)	ECU(-8.2)	ECU(-12.4)
15	BB(-8)	BB(-8.5)	BB(-9.93)	BB(-10.6)	BB(-9.7)	BB(-11.6)	BB(-11.3)	BB(-14.2)	BB(-13)

APPENDIX B: MUSCLE DATA PLOTS

These figures show the percent change that each muscle causes on transverse and shear DRUJ forces during pronation and supination when the muscle is removed. The positive and negative sides of the bars combine to equal 100% of the force observed at that particular position. Because resultant forces are quantitative and don't represent a direction, they do not add up to 100% and are not included.

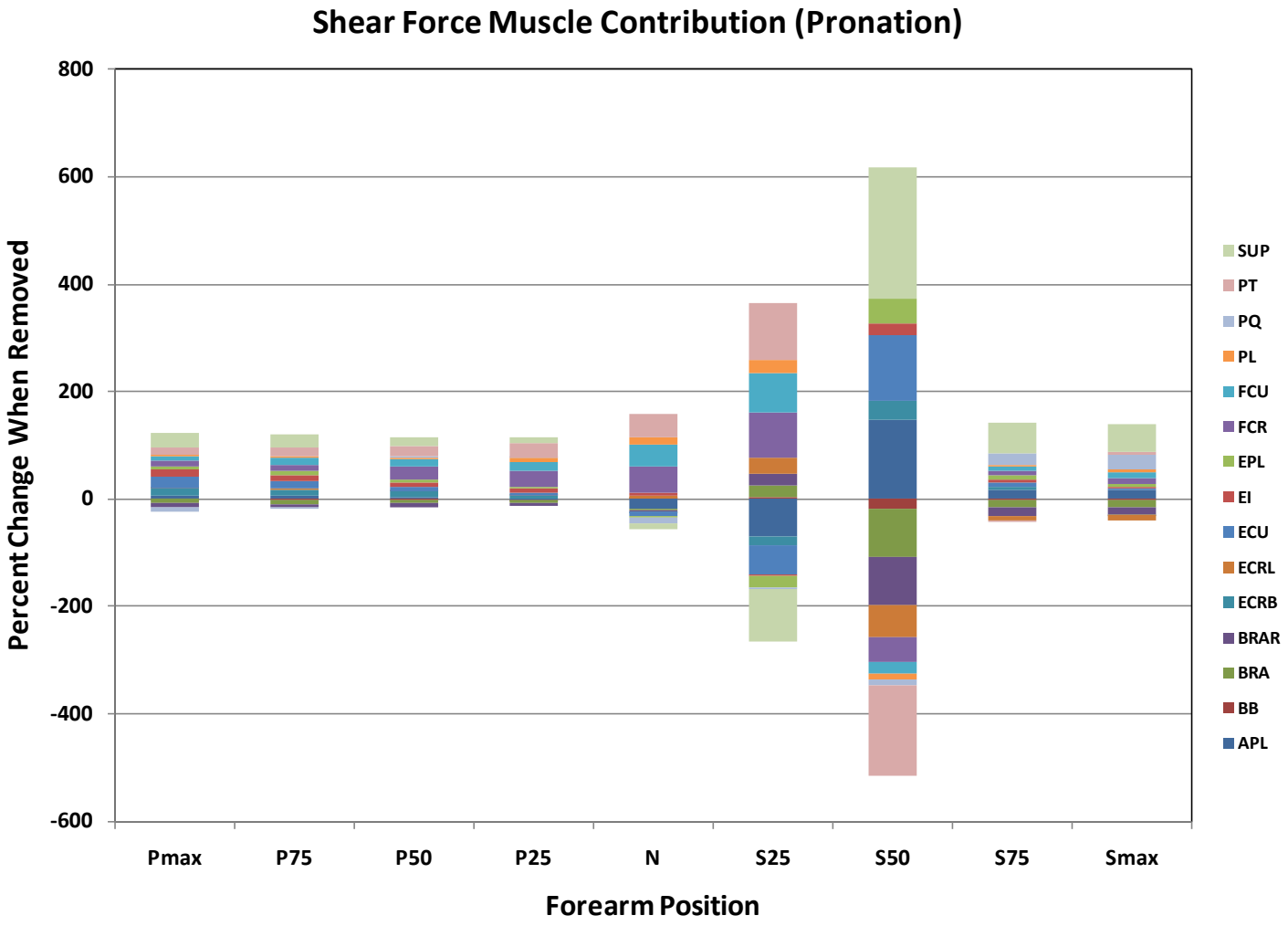

Figure B.1. Shear Force Muscle Contribution during Pronation

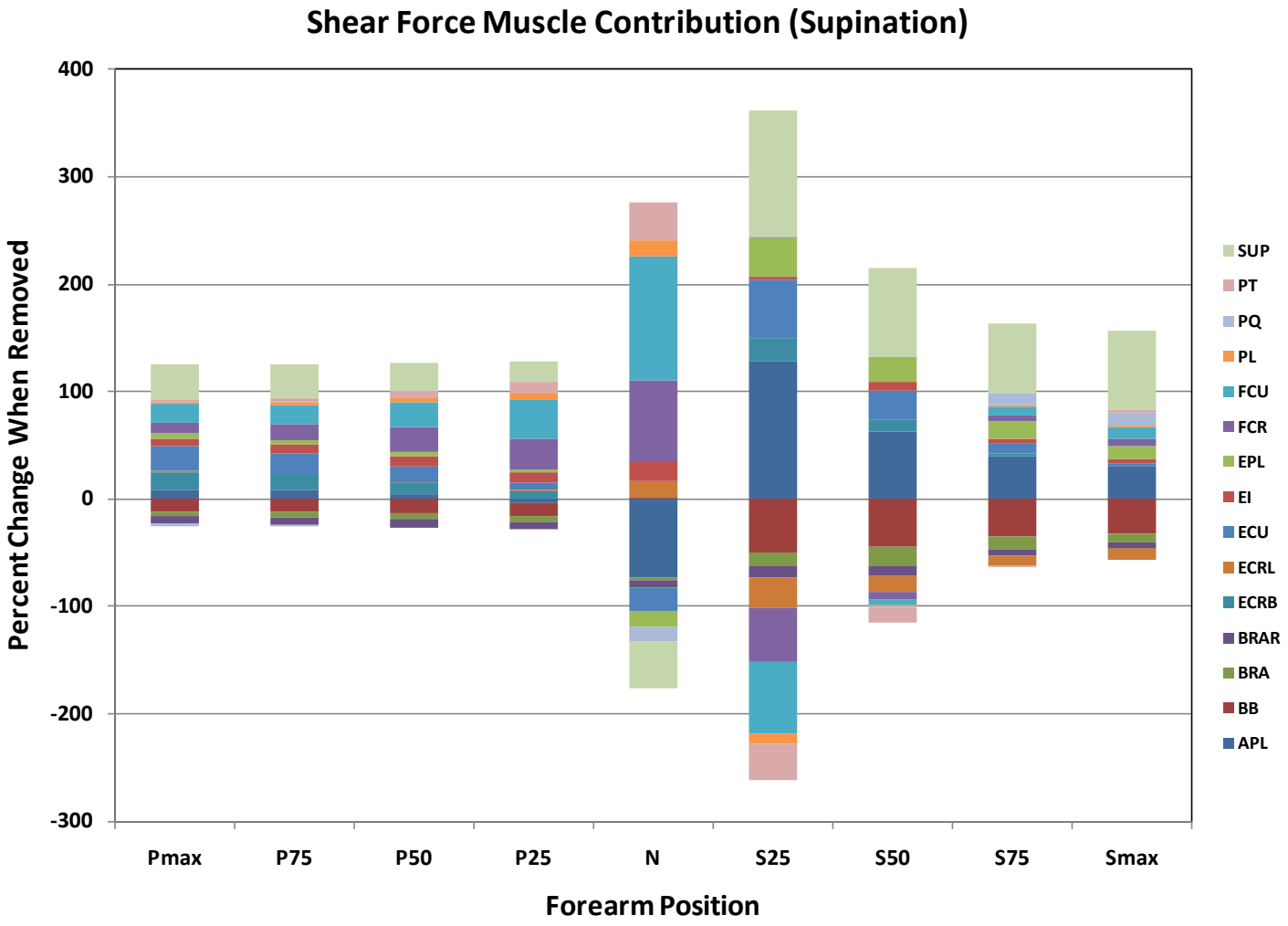

Figure B.2. Shear Force Muscle Contribution during Supination

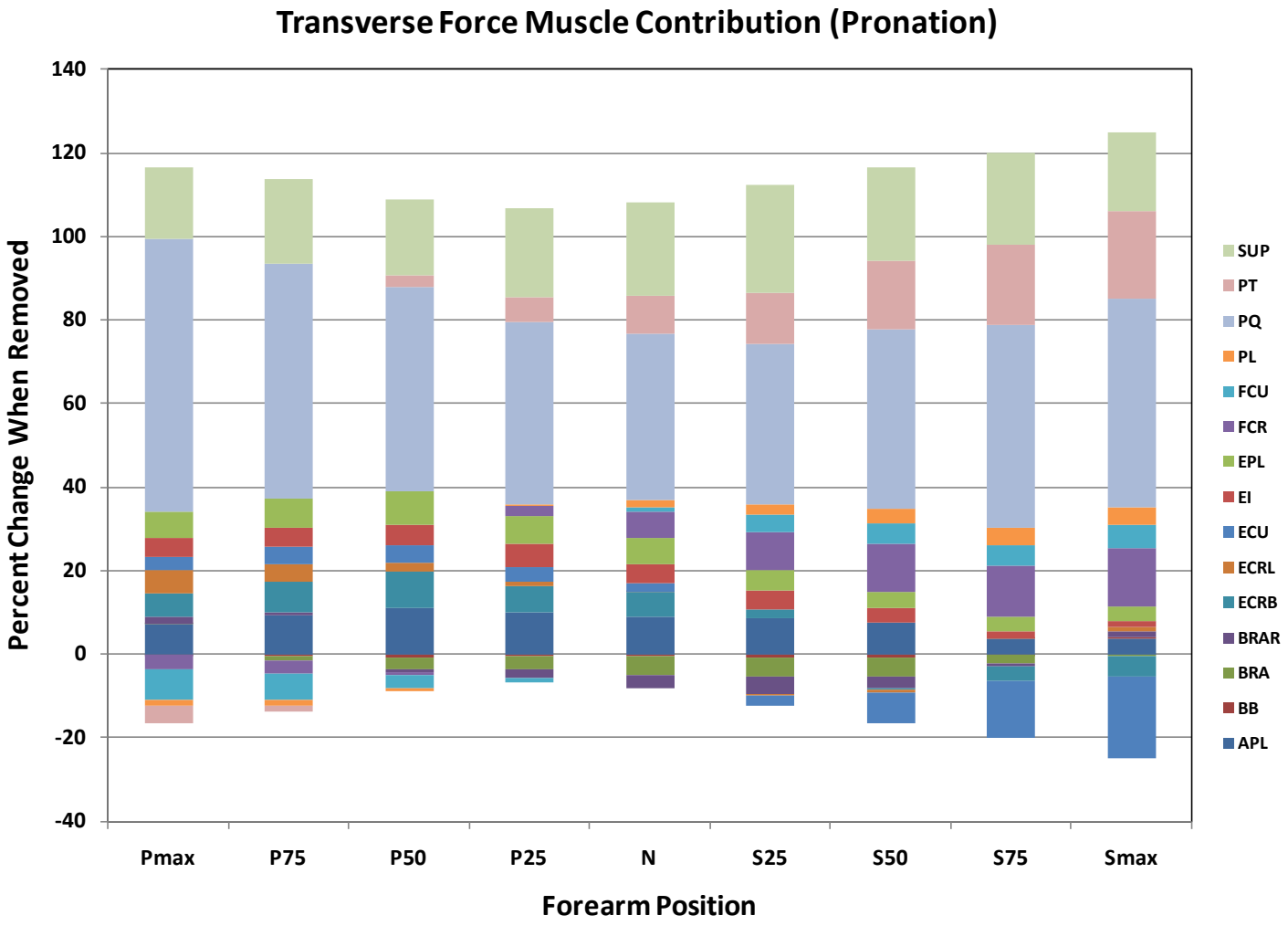

Figure B.3. Transverse Force Muscle Contribution during Pronation

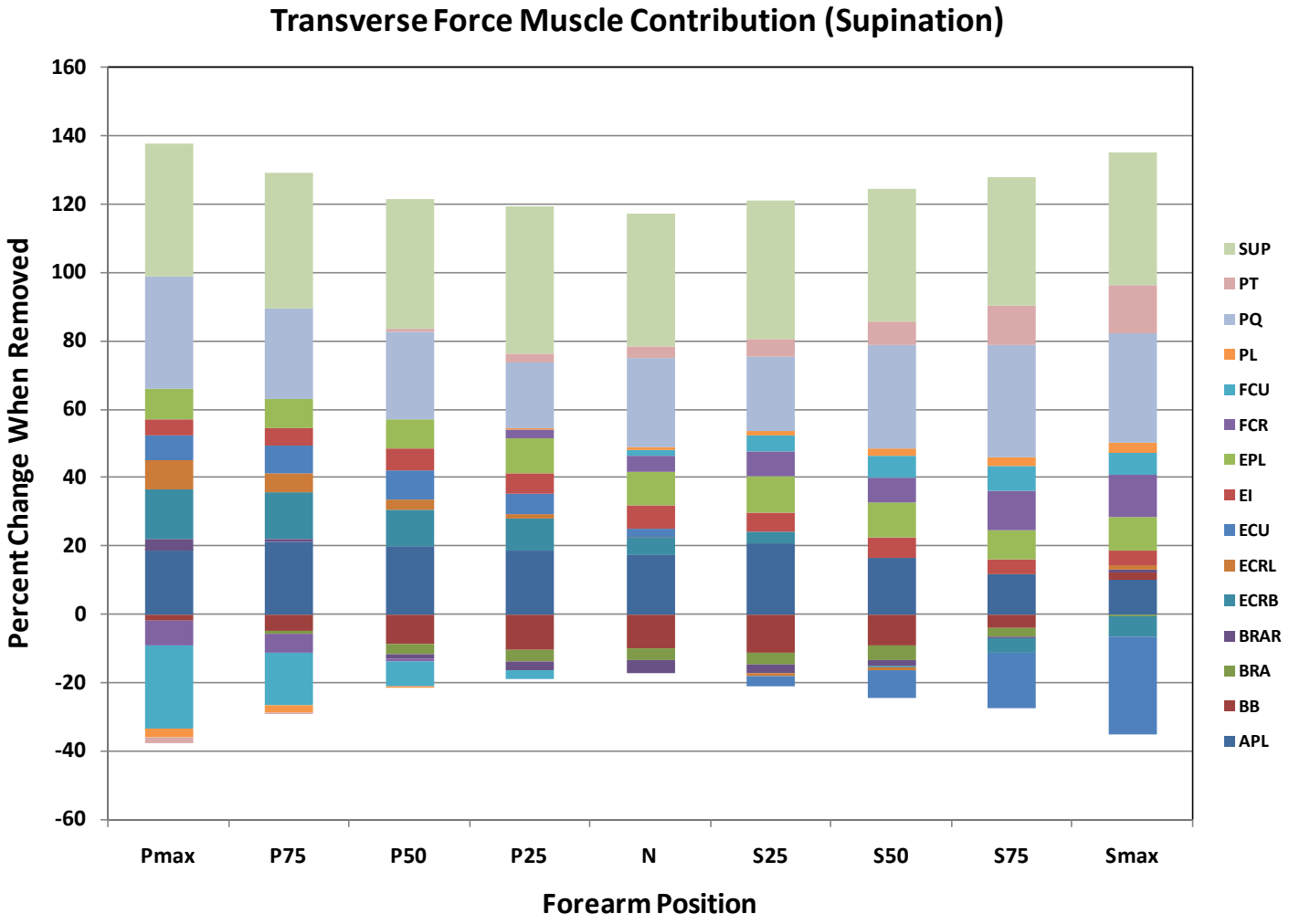

Figure B.4. Transverse Force Muscle Contribution during Supination

APPENDIX C: INDIVIDUAL MUSCLE DATA OVERVIEW

These tables show the percent change in force, extracted from Appendix A for each individual muscle. In addition they also contain muscle length and EMG data. "R" indicates the radial origin, "U" indicates the ulnar origin and "H" indicates the humeral origin. "P" indicates pronating tests and "S" indicates supinating tests. Shaded boxes indicate that a significant difference was observed when the muscle was removed from the model. Red numbers indicate that the change was negative. A "*" indicates that the muscle was the largest loader or unloader in that particular situation.

Table C.1. Abductor Pollicis Longus Data Overview

	Forearm Angle		MaxP	75P	50P	25P	Neutral	25S	50S	75S	MaxS
	EMG (% of Maximum)	P	23.9	33.2	37.4	34.2	33.7	32.5	34.4	30.2	33.6
		S	42.2	48.5	45.4	43.1	48.2	52.9	53.9	51.6	44.5
	Length (% of Maximum)	R	96.3	96.6	97.1	97.4	97.4	95.6	94.5	94.8	97.3
		U	98.6	98.5	98.2	98.1	98.1	96.2	95.1	95.9	96.7
% Δ Force	Shear	P	6.6	6.3	3.2	-2.5	-17.9*	-68.9	146.2	18.3	16.8
		S	8.8	9.1	4.7	-4.3	-72.7*	128*	63.2	39.8	30.2
	Transverse	P	7.2	9.4	11.0	9.9	9.0	8.6	7.5	3.8	3.9
		S	18.5	21.1	19.8	18.6	17.3	20.8	16.5	11.8	9.9
	Resultant	P	7.0	8.4	9.2	8.4	7.9	7.9	7.8	6.1	7.4
		S	12.2	14.6	14.9	15.3*	16.1	21.2	18.8	19.3	18.0
Contribution Rank	Shear	P	9	9	10	13	15	14	2	3	3
		S	6	6	8	12	15	1	2	2	2
	Transverse	P	3	3	3	3	4	5	5	7	7
		S	3	3	3	3	3	3	3	3	5
	Resultant	P	6	4	3	3	4	5	5	5	6
		S	4	2	3	1	3	2	3	3	3

Table C.2. Biceps Brachii Data Overview

	Forearm Angle		MaxP	75P	50P	25P	Neutral	25S	50S	75S	MaxS
	EMG (% of Maximum)	P	1.7	5.7	6.9	4.1	3.6	4.5	6.5	6.4	6.1
		S	44.6	45.7	50.0	48.7	48.9	49.3	58.6	64.9	58.1
	Length (% of Maximum)		98.2	98.5	98.3	97.3	95.6	94.7	93.4	92.3	92.3
% Δ Force	Shear	P	-0.6	-1.5	-1.6	-0.7	0.1	4.0	-18.0	-2.7	-2.5
		S	-12*	-12.2*	-13.7*	-11.8*	2.1	-50.1	-44.9*	-35.3*	-31.9*
	Transverse	P	0.0	-0.4	-0.8	-0.6	-0.5	-0.7	-0.7	-0.2	0.1
		S	-1.7	-4.7	-8.7	-10.6	-9.9	-11.2*	-9.1*	-4.1	2.4
	Resultant	P	-0.2	-0.7	-1.0	-0.6	-0.5	-0.7	-0.8	-0.7	-0.6
		S	-8*	-8.5*	-9.9*	-10.62*	-9.7*	-11.6*	-11.3*	-14.2*	-13*
Contribution Rank	Shear	P	12	12	13	12	7	8	9	12	12
		S	15	15	15	15	7	13	15	15	15
	Transverse	P	11	10	12	12	13	12	12	11	12
		S	12	13	15	15	15	15	15	13	10
	Resultant	P	11	12	13	13	13	12	12	10	10
		S	15	15	15	15	15	15	15	15	15

Table C.3. Brachialis Data Overview

	Forearm Angle		MaxP	75P	50P	25P	Neutral	25S	50S	75S	MaxS
	EMG (% of Maximum)	P	21.2	24.9	24.7	21.3	28.9	28.1	33.9	30.8	29.2
		S	14.2	16.0	17.9	15.6	17.2	14.5	22.7	20.3	15.6
	Length (% of Maximum)		95.5	96.0	95.3	95.4	95.9	97.0	98.3	99.0	98.7
% Δ Force	Shear	P	-7.9	-7.4*	-6.5	-4.7	-1.8	20.5	-90.5	-13.8	-12.5
		S	-4.0	-4.7	-5.7	-4.8	-3.0	-12.1	-16.7	-11.6	-9.1
	Transverse	P	0.0	-1.2	-2.7	-3.1*	-4.6*	-4.7*	-4.7	-2.1	-0.6
		S	0.0	-1.2	-2.9	-3.3	-3.7	-3.6	-4.4	-2.6	-0.6
	Resultant	P	-2.4*	-3.1*	-3.4*	-3.2*	-4.5*	-4.5*	-4.9	-4.2	-3.9
		S	-2.4	-2.9	-3.6	-3.5	-3.6	-3.6	-5.0	-5.2	-4.1
Contribution Rank	Shear	P	14	15	14	14	9	7	14	14	14
		S	13	13	13	13	9	10	14	14	13
	Transverse	P	10	11	14	15	15	15	14	13	13
		S	10	11	13	14	14	14	13	12	13
	Resultant	P	15	15	15	15	15	15	14	14	14
		S	13	13	14	14	14	14	13	13	13

Table C.4. Brachioradialis Data Overview

	Forearm Angle		MaxP	75P	50P	25P	Neutral	25S	50S	75S	MaxS
	EMG (% of Maximum)	P	21.2	29.7	28.4	27.6	30.3	37.6	38.3	37.9	36.2
		S	30.4	32.0	27.5	23.2	25.8	15.3	15.1	13.0	8.7
	Length (% of Maximum)		98.7	97.8	97.9	95.2	93.7	94.4	95.7	96.2	96.8
% Δ Force	Shear	P	-6.2	-7.0	-6.8*	-6*	-2.9	22.4	-87.9	-14*	-12.9*
		S	-6.7	-7.5	-7.9	-6.9	-7.1	-10.4	-9.6	-6.1	-4.2
	Transverse	P	1.7	0.7	-1.0	-2.1	-3.1	-4.0	-2.9	-0.7	1.3
		S	3.5	1.1	-1.4	-2.7	-3.5	-2.4	-1.6	-0.4	0.6
	Resultant	P	-0.8	-1.7	-2.2	-2.5	-3.0	-3.9	-3.2	-3.1	-2.9
		S	-3.0	-3.3	-3.2	-3.2	-3.5	-2.5	-2.1	-2.2	-1.5
Contribution Rank	Shear	P	13	14	15	15	10	6	13	15	15
		S	14	14	14	14	10	9	11	12	12
	Transverse	P	9	9	13	14	14	14	13	12	10
		S	9	9	12	13	13	12	12	11	12
	Resultant	P	13	14	14	14	14	14	13	13	13
		S	14	14	13	13	13	13	12	11	10

Table C.5. Extensor Carpi Radialis Brevis Data Overview

	Forearm Angle		MaxP	75P	50P	25P	Neutral	25S	50S	75S	MaxS
	EMG (% of Maximum)	P	23.8	34.1	42.8	36.9	43.0	29.1	26.7	31.1	30.8
		S	40.7	39.5	36.0	36.4	28.7	31.5	28.8	21.9	19.7
	Length (% of Maximum)		97.8	98.3	98.9	99.0	99.3	99.1	99.0	98.9	98.7
% Δ Force	Shear	P	12.4	12.1	10.5	5.5	-0.9	-17.1	35.6	3.6	-0.5
		S	16.0	13.8	10.6	7.5	-1.7	21.1	10.6	3.2	-0.5
	Transverse	P	5.8	7.4	8.8	6.5	5.9	2.2	-0.3	-3.3	-4.8
		S	14.3	13.3	11.0	9.6	5.3	3.5	-0.5	-4.3	-5.9
	Resultant	P	7.7	8.8	9.1	6.4	5.7	2.1	0.1	-1.8	-2.7
		S	15.1	13.4	10.8	9.3	5.3	3.9	0.8	-1.5	-2.2
Contribution Rank	Shear	P	4	5	5	6	8	5	5	9	11
		S	5	5	5	7	8	11	5	8	11
	Transverse	P	5	4	4	5	7	10	10	14	14
		S	4	4	4	5	6	9	10	14	14
	Resultant	P	4	3	4	5	7	10	10	12	12
		S	3	4	4	4	6	8	10	10	11

Table C.6. Extensor Carpi Radialis Longus Data Overview

	Forearm Angle		MaxP	75P	50P	25P	Neutral	25S	50S	75S	MaxS
	EMG (% of Maximum)	P	30.5	34.7	33.8	37.5	34.5	34.1	27.6	27.6	30.0
		S	33.4	32.1	31.2	31.4	34.2	29.5	26.4	23.5	23.3
	Length (% of Maximum)		98.0	98.0	98.0	98.0	97.8	98.2	99.0	99.4	99.6
% Δ Force	Shear	P	1.6	0.9	0.1	0.9	5.0	28.7	-60.0	-8.7	-10.6
		S	1.3	0.8	0.1	1.1	14.0	-28.4	-15.8	-9.4	-11.2
	Transverse	P	5.4	4.0	2.1	0.9	0.1	-0.6	-0.5	0.0	1.0
		S	8.5	5.7	2.9	1.1	0.1	-0.8	-0.7	0.0	1.6
	Resultant	P	4.2	3.0	1.7	0.9	0.3	-0.4	-0.6	-1.4	-1.9
		S	3.9	3.2	2.1	1.2	0.3	-1.0	-1.5	-2.7	-3.4
Contribution Rank	Shear	P	11	11	12	11	6	4	12	13	13
		S	11	11	12	10	6	11	13	13	14
	Transverse	P	6	8	9	10	12	11	11	10	11
		S	6	7	8	10	12	11	11	10	11
	Resultant	P	8	9	10	11	12	11	11	11	11
		S	8	9	10	11	12	11	11	12	12

Table C.7. Extensor Carpi Ulnaris Data Overview

	Forearm Angle		MaxP	75P	50P	25P	Neutral	25S	50S	75S	MaxS
	EMG (% of Maximum)	P	39.4	46.4	45.7	48.3	55.5	49.7	51.1	52.1	54.7
		S	60.0	59.0	61.2	54.0	51.0	44.2	41.2	33.7	41.1
	Length (% of Maximum)		97.7	98.3	99.1	99.4	99.6	99.1	98.8	98.6	98.3
% Δ Force	Shear	P	19.6	15.0	9.2	3.9	-7.5	-54.4	122.1	10.0	2.1
		S	22.5	18.9	14.8	6.1	-19.6	55.2	27.2	8.3	2.2
	Transverse	P	3.3	4.3	4.3	3.5	1.9	-2.3	-7.3*	-13.6*	-19.5*
		S	7.3	8.4	8.6	5.9	2.4	-3.0	-8.2	-16.2*	-28.4*
	Resultant	P	8.0	7.4	5.4	3.6	1.7	-2.5	-6.6	-9.1	-12.0
		S	16.4	13.6	10.5	6.0	2.4	-1.9	-5.3*	-8.2*	-12.4*
Contribution Rank	Shear	P	2	3	6	8	12	13	3	4	10
		S	2	2	4	7	13	3	3	5	9
	Transverse	P	8	7	7	8	9	13	15	15	15
		S	7	6	6	7	9	13	14	15	15
	Resultant	P	3	5	8	9	11	13	15	15	15
		S	2	3	5	7	9	12	14	14	14

Table C.8. Extensor Indicis Data Overview

	Forearm Angle		MaxP	75P	50P	25P	Neutral	25S	50S	75S	MaxS
	EMG (% of Maximum)	P	40.2	41.5	38.9	42.5	33.9	35.3	33.1	27.6	29.4
		S	29.0	29.7	33.3	32.6	37.9	29.6	42.8	34.8	35.4
	Length (% of Maximum)		96.4	96.9	98.3	99.1	99.5	98.8	97.9	97.3	96.7
% Δ Force	Shear	P	13.6	10.7	8.8	9.2	5.9	-2.9	22.2	3.4	2.4
		S	7.3	6.4	5.6	5.9	4.6	4.6	3.6	2.3	2.3
	Transverse	P	4.5	4.6	4.8	5.5	4.6	4.5	3.4	1.8	1.7
		S	7.4	7.6	9.1	9.8	18.8	2.8	7.9	5.4	4.0
	Resultant	P	7.3	6.4	5.6	5.9	4.6	4.6	3.6	2.3	2.3
		S	6.4	6.4	6.9	6.7	7.0	5.7	6.4	5.1	4.9
Contribution Rank	Shear	P	3	7	7	5	5	9	6	9	9
		S	7	7	6	5	4	6	6	7	7
	Transverse	P	7	6	6	7	8	7	9	9	9
		S	8	8	7	6	5	6	8	8	8
	Resultant	P	5	7	7	7	8	6	8	9	9
		S	7	7	7	6	5	6	5	8	8

Table C.9. Extensor Pollicis Longus Data Overview

	Forearm Angle		MaxP	75P	50P	25P	Neutral	25S	50S	75S	MaxS
	EMG (% of Maximum)	P	30.3	36.8	41.5	35.1	33.1	24.4	23.7	26.5	26.4
		S	30.3	28.9	30.2	34.7	38.6	36.9	42.4	38.4	38.0
	Length (% of Maximum)		96.5	97.7	97.7	98.2	97.0	97.4	96.5	96.7	96.0
% Δ force	Shear	P	7.3	6.4	5.0	1.8	-4.6	-20.9	46.6	8.4	6.7
		S	5.5	5.0	4.4	2.4	-15.4	36.0	23.0	15.5	13.1
	Transverse	P	6.3	7.1	8.1	6.8	6.4	4.7	4.1	3.2	3.5
		S	9.2	8.5	8.8	10.0	10.0	10.5	10.3	8.6	9.8
	Resultant	P	6.6	6.8	7.4	6.2	6.0	4.5	4.2	4.2	4.5
		S	6.8	6.7	7.4	9.0	9.7	10.8	11.0	10.7	11.3
Contribution Rank	Shear	P	8	8	8	9	11	12	4	5	6
		S	8	8	9	9	12	4	4	3	3
	Transverse	P	4	5	5	4	5	6	7	8	8
		S	5	5	5	4	4	4	4	6	6
	Resultant	P	7	6	5	6	6	7	7	7	7
		S	6	6	6	5	4	4	4	4	4

Table C.10. Flexor Carpi Radialis Data Overview

	Forearm Angle		MaxP	75P	50P	25P	Neutral	25S	50S	75S	MaxS
	EMG (% of Maximum)	P	20.0	31.3	47.7	45.5	49.0	50.2	49.7	53.3	56.0
		S	28.6	35.3	37.9	31.5	27.1	26.4	21.9	26.6	25.7
	Length (% of Maximum)		98.5	98.8	99.2	99.2	98.9	98.4	98.2	98.3	98.6
% Δ Force	Shear	P	9.4	13.2	23.8*	30.2*	48.2*	85.6	-46.9	8.3	11.2
		S	10.1	14.8	22.7	29.0	75.6	-51.4	-5.7	5.3	7.0
	Transverse	P	-3.6	-3.1	-0.7	2.6	6.1	9.3	11.4	12.3	14.0
		S	-7.5	-5.4	-0.8	2.7	4.5	7.3	7.0	11.4	12.4
	Resultant	P	0.3	1.6	4.1	5.2	7.4	9.7	11.3	11.8	13.6
		S	3.3	4.5	5.5	5.6	4.9	6.5	6.2	9.5	10.0
Contribution Rank	Shear	P	6	4	1	1	1	2	11	6	5
		S	5	4	3	2	2	14	10	8	6
	Transverse	P	13	14	11	9	6	4	4	4	4
		S	14	14	11	8	7	5	6	5	4
	Resultant	P	10	10	9	8	5	4	4	4	4
		S	9	8	8	8	7	5	6	5	5

Table C.11. Flexor Carpi Ulnaris Data Overview

	Forearm Angle		MaxP	75P	50P	25P	Neutral	25S	50S	75S	MaxS
	EMG (% of Maximum)	P	13.3	17.9	16.5	16.8	25.9	29.2	25.5	29.3	35.0
		S	31.1	27.6	25.3	25.5	25.0	22.9	23.8	23.0	22.5
	Length (% of Maximum)		99.3	99.5	99.5	99.6	99.1	97.7	96.7	96.6	97.0
% Δ Force	Shear	P	9.3	11.4	12.6	17.6	42.0	73.7	-21.0	8.1	11.3
		S	16.4	17.4	23.3	37*	114.8*	-66*	-5.4	8.1	9.8
	Transverse	P	-7.2*	-6.4*	-3.2*	-1.1	1.3	4.0	5.0	5.0	5.3
		S	-24.4*	-15.2*	-7.2	-2.5	1.7	4.7	6.5	7.3	6.7
	Resultant	P	-2.3	-1.3	0.0	0.8	2.6	4.4	5.1	5.8	7.8
		S	-0.5	0.3	0.9	1.6	2.3	3.8	5.9	7.8	8.8
Contribution Rank	Shear	P	7	6	4	3	3	3	10	7	4
		S	3	3	2	1	1	15	9	6	5
	Transverse	P	15	15	15	13	11	8	6	5	5
		S	15	15	14	12	10	8	7	7	7
	Resultant	P	14	13	13	13	9	8	6	6	5
		S	12	12	11	10	10	9	7	6	6

Table C.12. Palmaris Longus Data Overview

	Forearm Angle		MaxP	75P	50P	25P	Neutral	25S	50S	75S	MaxS
	EMG (% of Maximum)	P	28.7	33.6	39.9	46.0	56.7	56.6	56.4	65.9	58.2
		S	29.8	38.1	33.1	25.9	23.9	21.2	25.6	21.8	20.0
	Length (% of Maximum)		99.4	99.2	99.0	98.6	98.2	97.7	97.8	98.2	98.6
% Δ Force	Shear	P	2.2	2.6	4.0	6.7	12.9	22.8	-12.1	3.0	3.8
		S	1.7	2.9	4.0	5.3	15.4	-9.8	-1.5	1.3	1.8
	Transverse	P	-1.6	-1.2	-0.5	0.4	1.5	2.6	3.5	4.2	4.1
		S	-2.5	-2.1	-0.6	0.3	0.9	1.5	2.2	2.6	2.8
	Resultant	P	-0.5	-0.1	0.4	1.0	1.9	2.7	3.4	4.0	3.9
		S	0.1	0.4	0.7	0.9	1.0	1.3	1.9	2.1	2.1
Contribution Rank	Shear	P	10	10	9	6	4	5	8	10	8
		S	10	10	10	8	5	8	8	10	10
	Transverse	P	12	12	10	11	10	9	8	6	6
		S	13	12	10	11	11	10	9	9	9
	Resultant	P	12	11	11	10	10	9	9	8	8
		S	11	11	12	12	11	10	9	9	9

Table C.13. Pronator Quadratus Data Overview

	Forearm Angle		MaxP	75P	50P	25P	Neutral	25S	50S	75S	MaxS
	EMG (% of Maximum)	P	65.4	68.2	66.4	63.3	58.5	51.3	52.9	54.9	47.1
		S	22.5	20.8	23.2	18.7	28.6	19.4	26.5	20.3	15.5
	Length (% of Maximum)		56.5	60.7	66.6	72.8	79.9	86.8	95.5	97.6	98.6
% Δ Force	Shear	P	-8.4*	-3.1	1.7	1.5	-9.3	-4.6	-10.7	22.8	27.6
		S	-2.2	-0.9	0.7	0.6	-13.0	2.0	-1.5	10.7	12.3
	Transverse	P	65.1*	56.2*	48.8*	43.5*	39.9*	38.3*	43*	48.3*	50.1*
		S	32.6	26.4	25.3	19.2	26.1	21.5	30.1	33.0	32.0
	Resultant	P	32.3*	32.1*	35.4*	37.3*	36.9*	37.3*	41.3*	41.7*	38.3*
		S	8.7	11.0	17.0	16.4	25.1	20.3	25.9	23.9	18.9
Contribution Rank	Shear	P	15	13	11	10	13	10	7	2	2
		S	12	12	11	11	11	7	7	4	4
	Transverse	P	1	1	1	1	1	1	1	1	1
		S	2	2	2	2	2	2	2	2	2
	Resultant	P	1	1	1	1	1	1	1	1	1
		S	5	5	2	2	2	3	2	2	2

Table C.14. Pronator Teres Data Overview

	Forearm Angle		MaxP	75P	50P	25P	Neutral	25S	50S	75S	MaxS
	EMG (% of Maximum)	P	51.3	55.1	53.8	50.8	53.7	54.1	56.0	50.9	46.6
		S	12.9	14.6	14.4	14.8	15.6	15.1	17.3	16.3	16.2
	Length (% of Maximum)	H	98.2	98.5	98.3	97.3	95.6	94.7	93.4	92.3	92.3
		U	92.1	92.0	93.2	93.8	94.3	96.8	97.8	98.4	98.6
% Δ Force	Shear	P	13.2	16.2	20.4	26.7	42.9	107.1*	-169.1*	-2.0	5.0
		S	2.5	4.3	6.6	10.8	35.4	-34.1	-14.4	-0.8	2.3
	Transverse	P	-4.0	-1.4	2.9	5.8	9.1	12.3	16.4	19.4	20.8
		S	-1.5	-0.6	1.1	2.5	3.6	5.1	7.1	11.5	14.0
	Resultant	P	0.9	3.6	6.4	7.9	10.1	12.3	14.8	14.7	15.4
		S	1.0	1.9	2.7	3.5	3.7	4.3	5.2	7.0	7.8
Contribution Rank	Shear	P	4	2	2	2	2	1	15	11	7
		S	9	9	7	4	3	12	12	11	8
	Transverse	P	14	13	8	6	3	3	3	3	2
		S	11	10	9	9	8	7	5	4	3
	Resultant	P	9	8	6	4	3	3	3	3	3
		S	10	10	9	9	8	7	8	7	7

Table C.15. Supinator Data Overview

	Forearm Angle		MaxP	75P	50P	25P	Neutral	25S	50S	75S	MaxS
	EMG (% of Maximum)	P	31.4	38.4	33.7	40.4	42.1	47.1	41.4	49.2	45.1
		S	48.6	49.2	47.9	54.0	54.3	50.2	51.5	45.7	47.5
	Length (% of Maximum)		82.3	86.7	91.6	95.6	96.2	94.9	89.0	81.8	81.8
% Δ Force	Shear	P	28*	24.3*	15.4	9.9	-12.0	-96.3*	243.5*	55.5*	52*
		S	32.6*	30.8*	26.2*	18.4	-43.8	117.1	83.6*	65.7*	74.1*
	Transverse	P	17.2	20.0	18.0	21.6	22.3	25.8	22.2	21.8	19.0
		S	38.8*	39.6*	38*	43*	38.5*	40.8*	38.7*	37.3*	38.9*
	Resultant	P	20.3	21.3	17.4	20.2	20.7	24.1	21.7	25.6	25.2
		S	34.7*	34.8*	34.2*	39*	36.7*	39.5*	38.8*	41.5*	45.2*
Contribution Rank	Shear	P	1	1	3	4	14	15	1	1	1
		S	1	1	1	3	14	2	1	1	1
	Transverse	P	2	2	2	2	2	2	2	2	3
		S	1	1	1	1	1	1	1	1	1
	Resultant	P	2	2	2	2	2	2	2	2	2
		S	1	1	1	1	1	1	1	1	1

APPENDIX D: INDIVIDUAL MUSCLE PLOTS

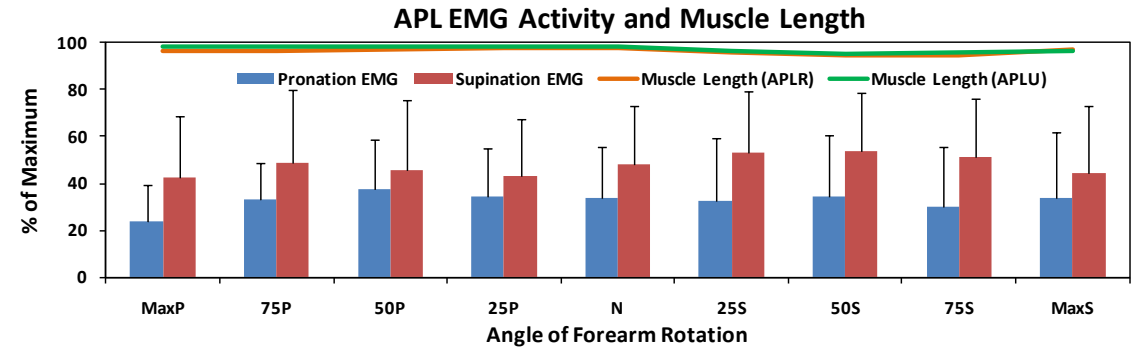

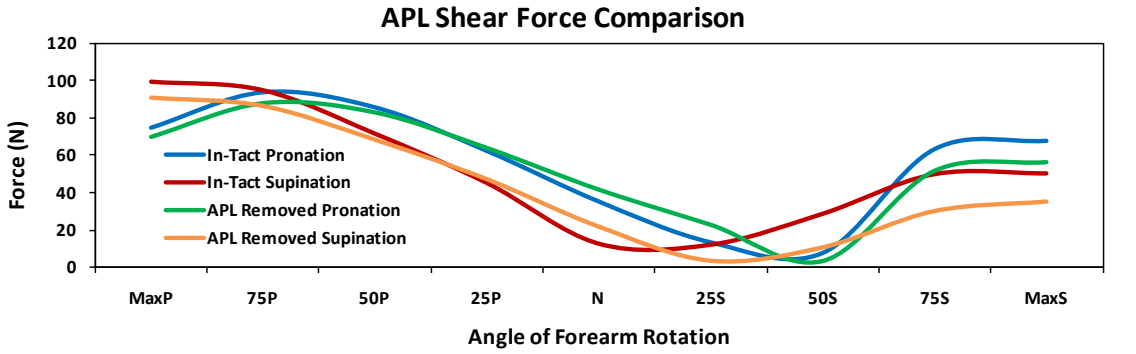

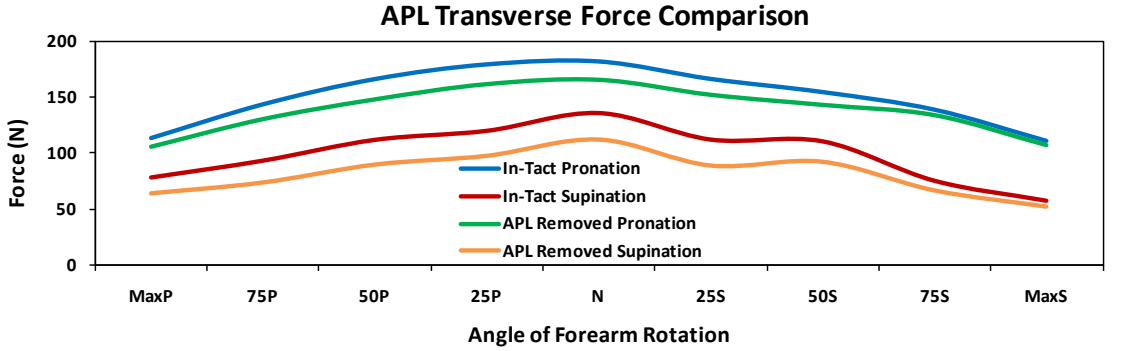

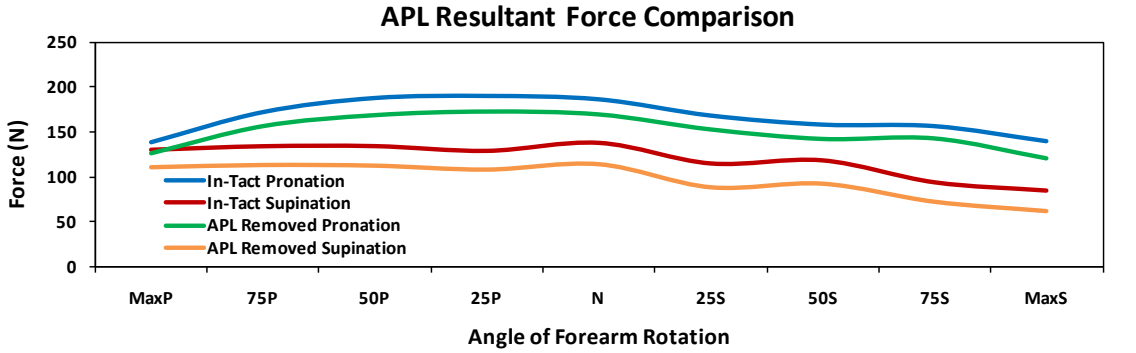

Figure D.1. Mean Abductor Pollicis Longus Plots

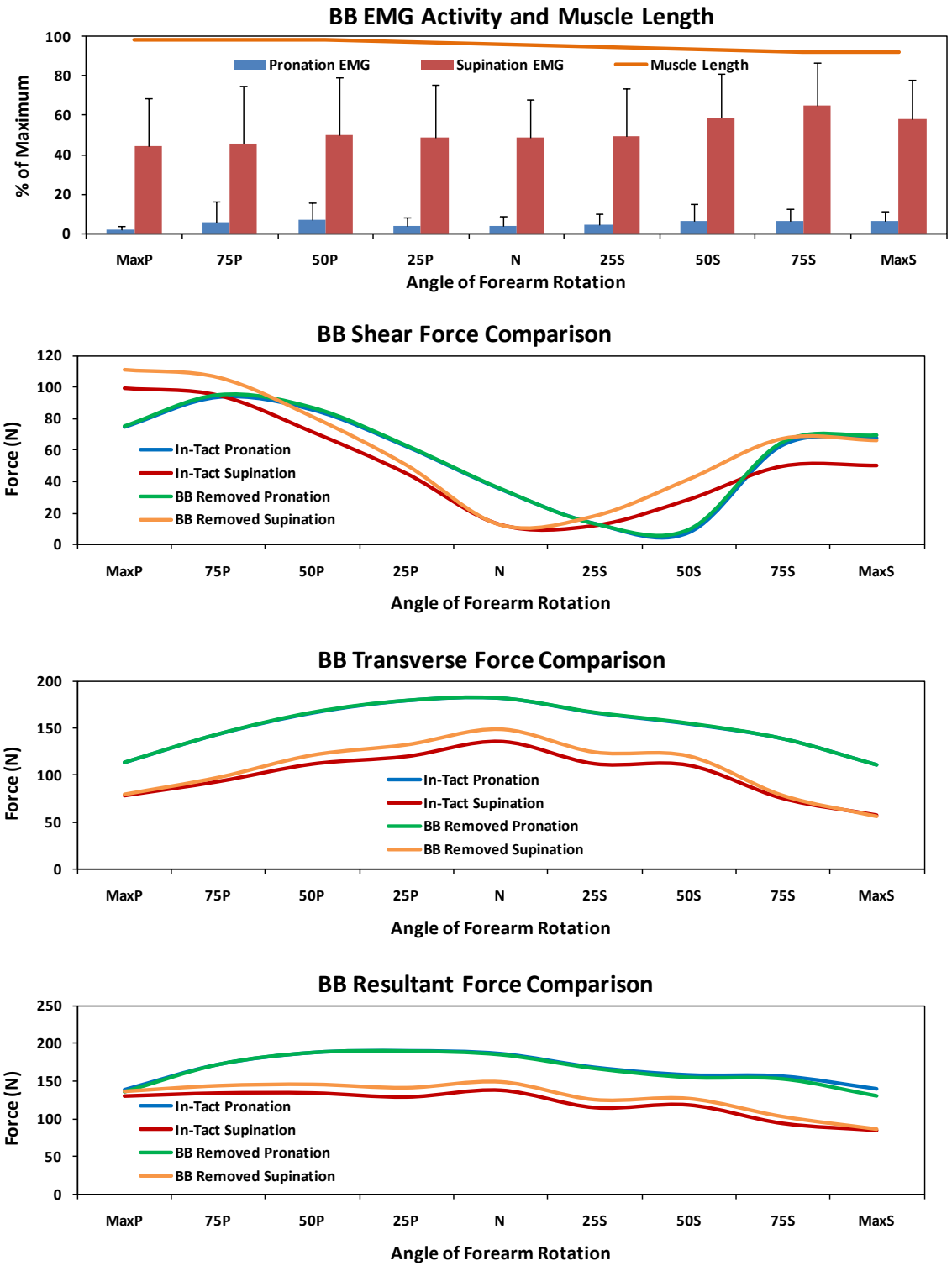

Figure D.2. Mean Biceps Brachii Plots

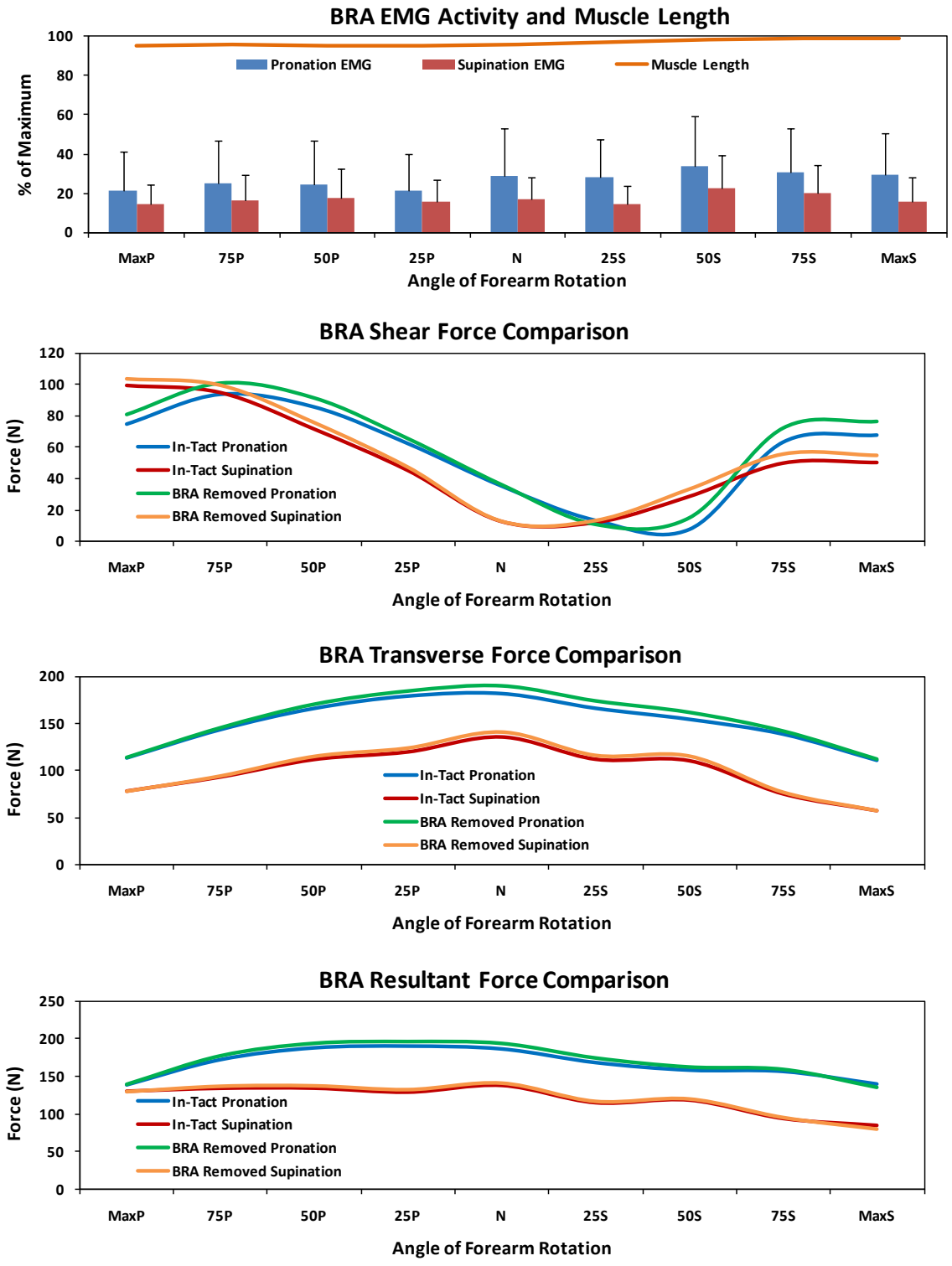

Figure D.3. Mean Brachialis Plots

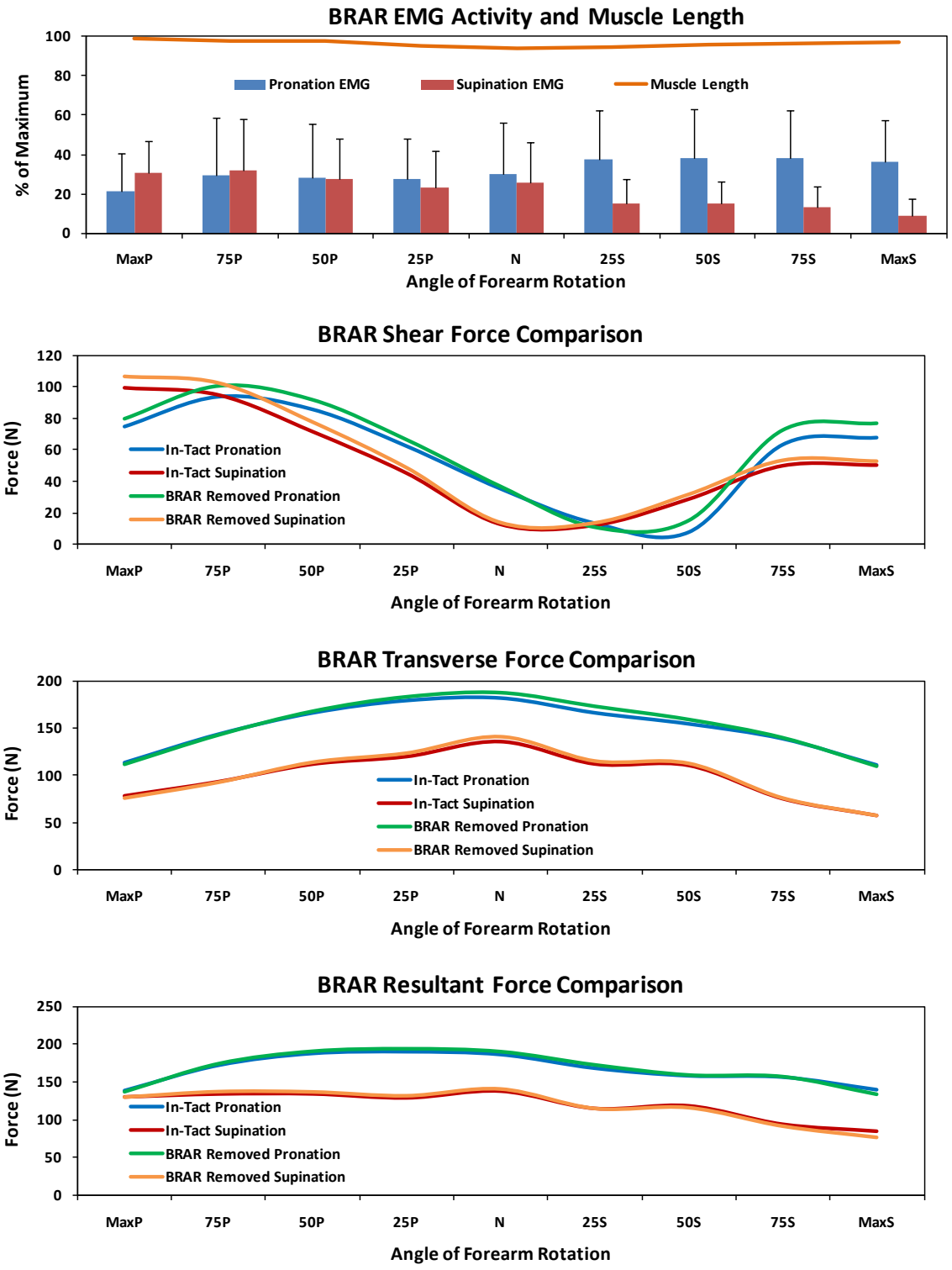

Figure D.4. Mean Brachioradialis Plots

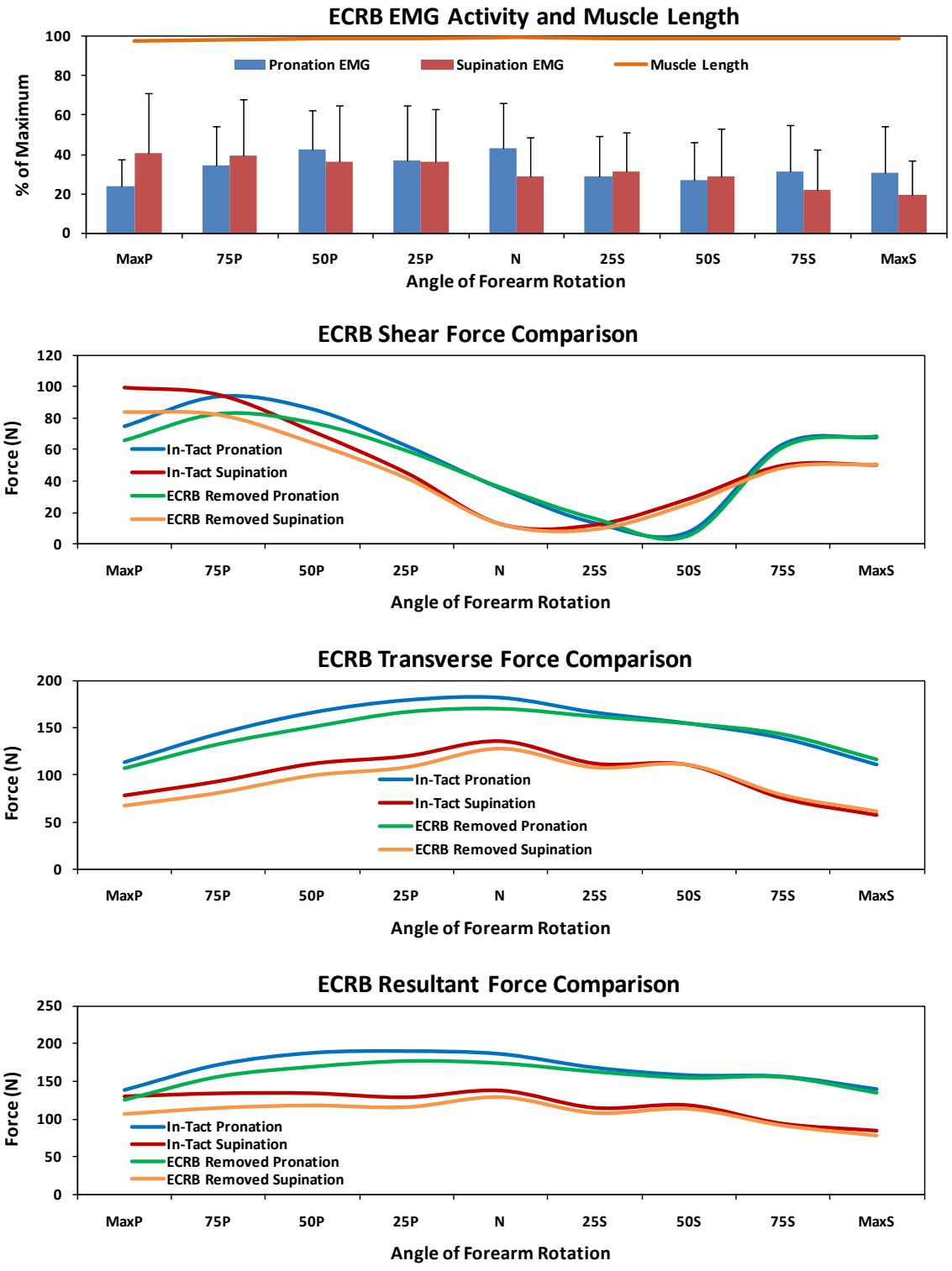

Figure D.5. Mean Extensor Carpi Radialis Brevis Plots

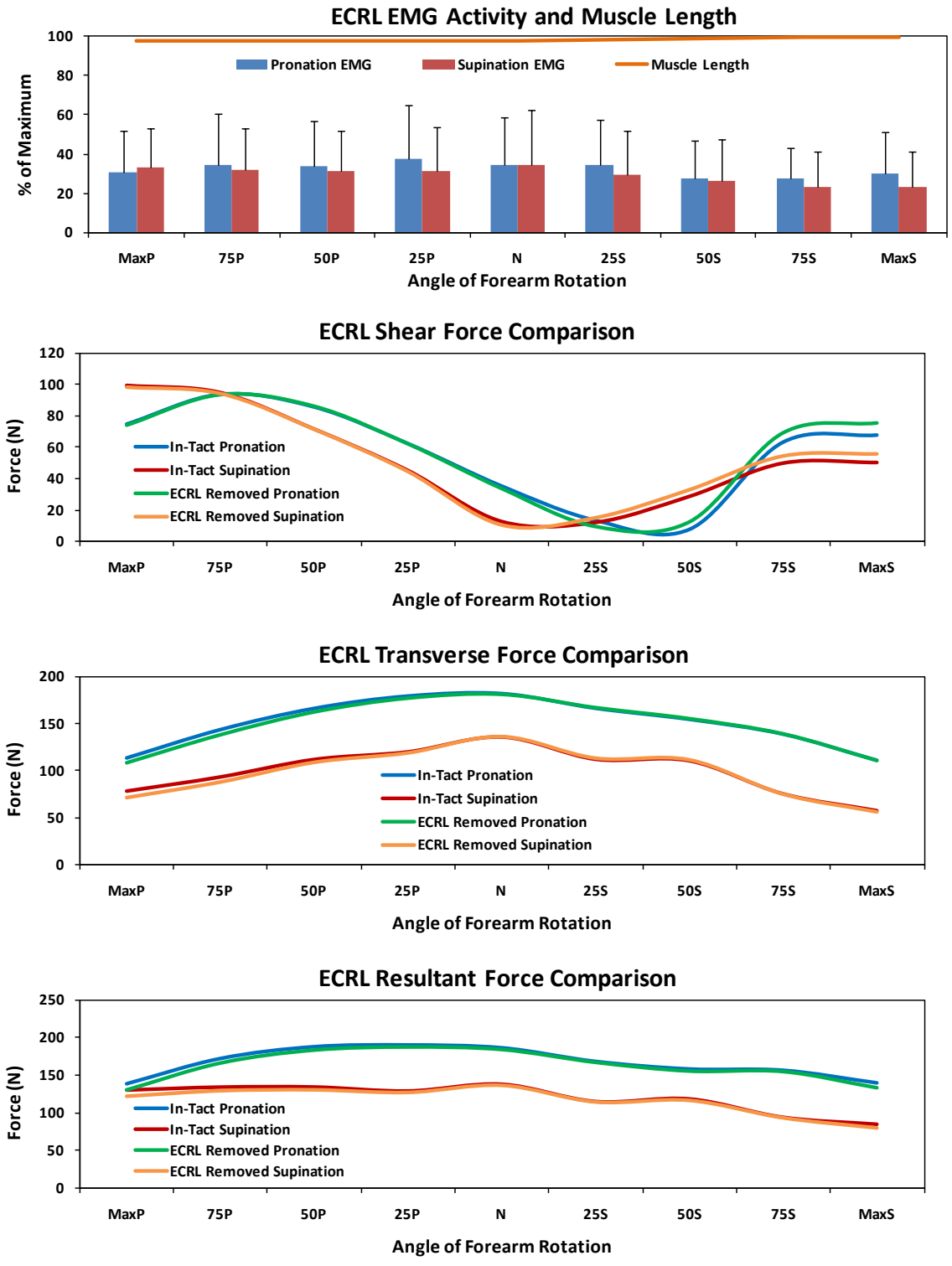

Figure D.6. Mean Extensor Carpi Radialis Longus Plots

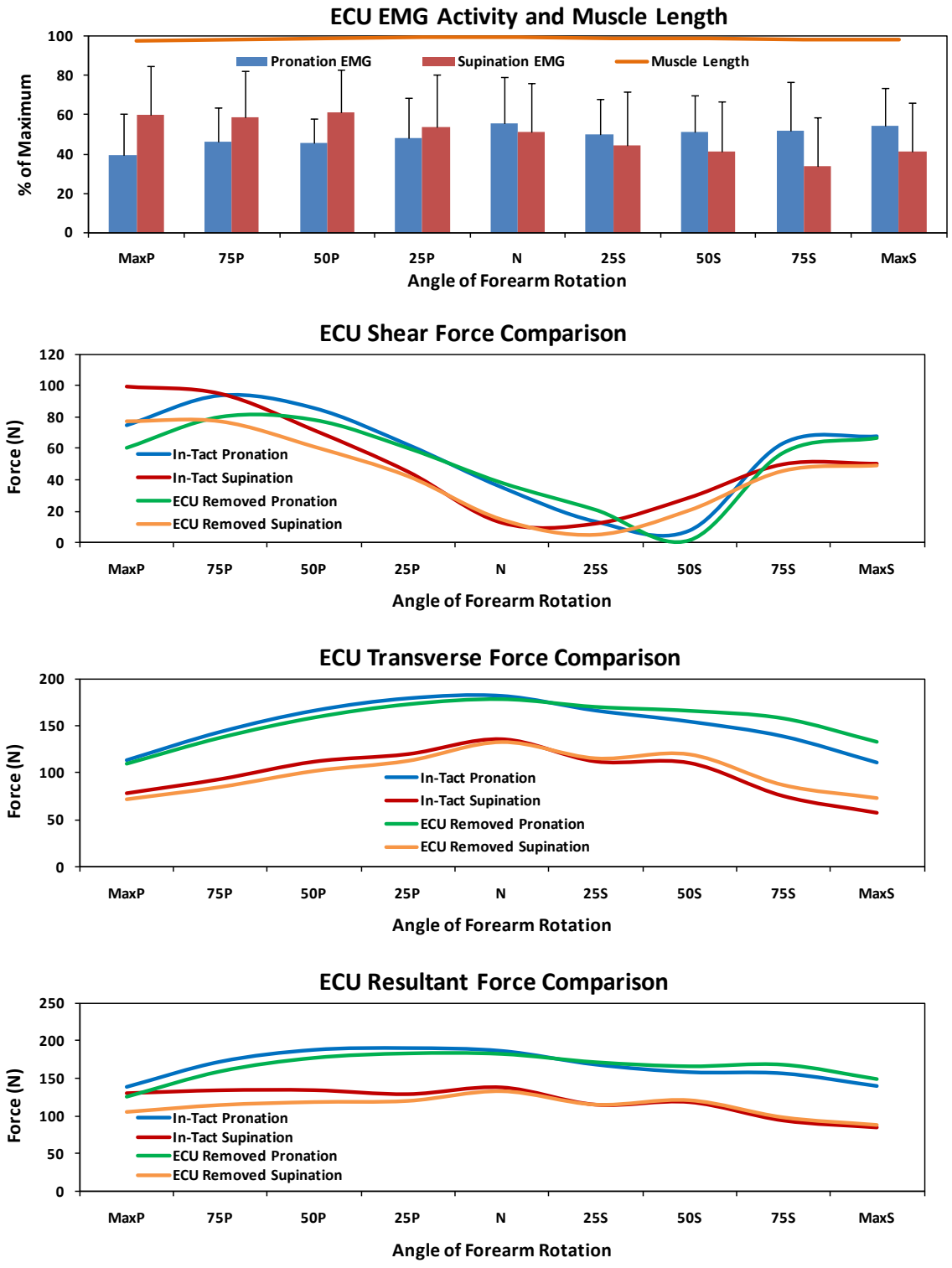

Figure D.7. Mean Extensor Carpi Ulnaris Plots

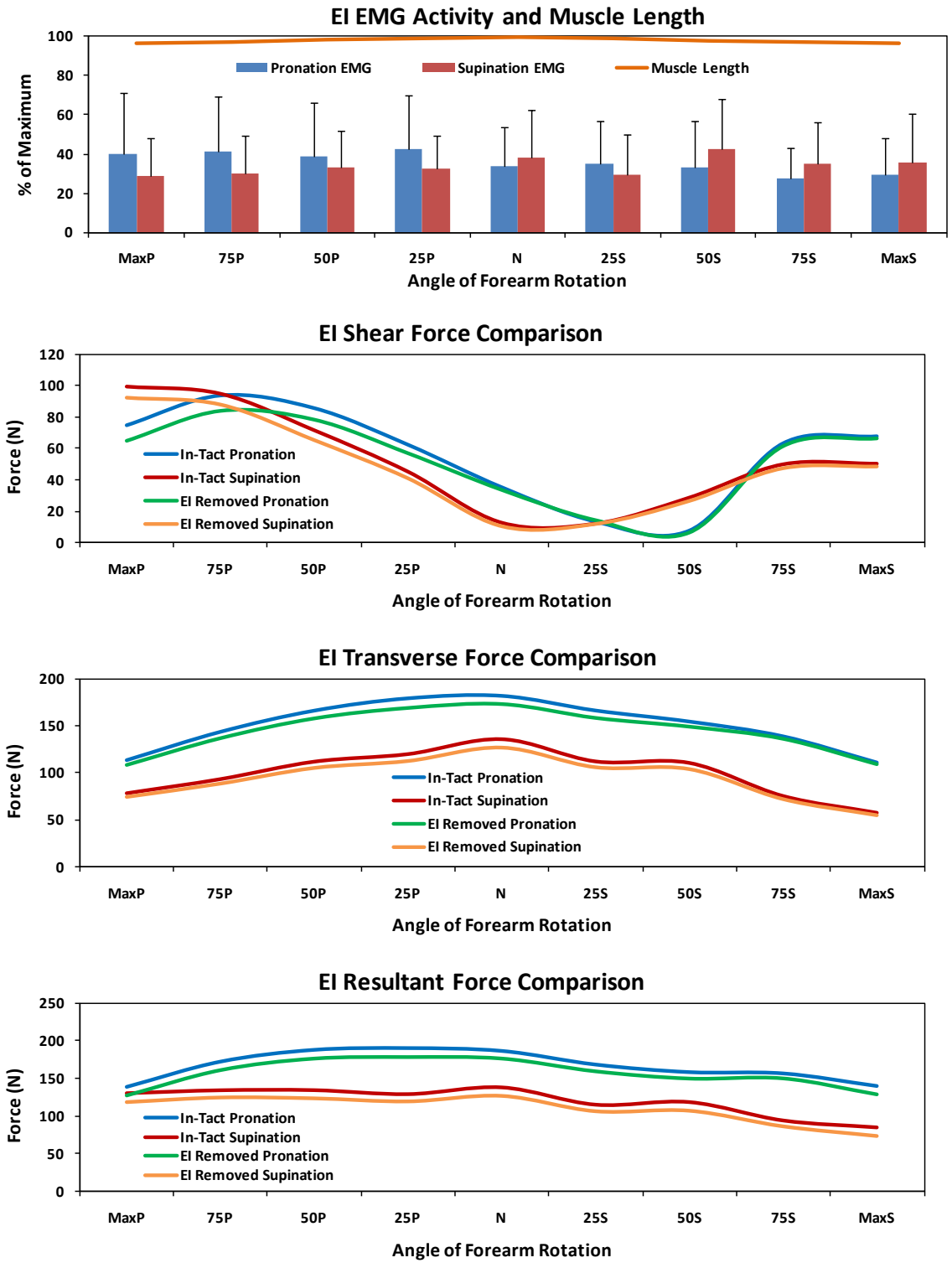

Figure D.8. Mean Extensor Indicis Plots

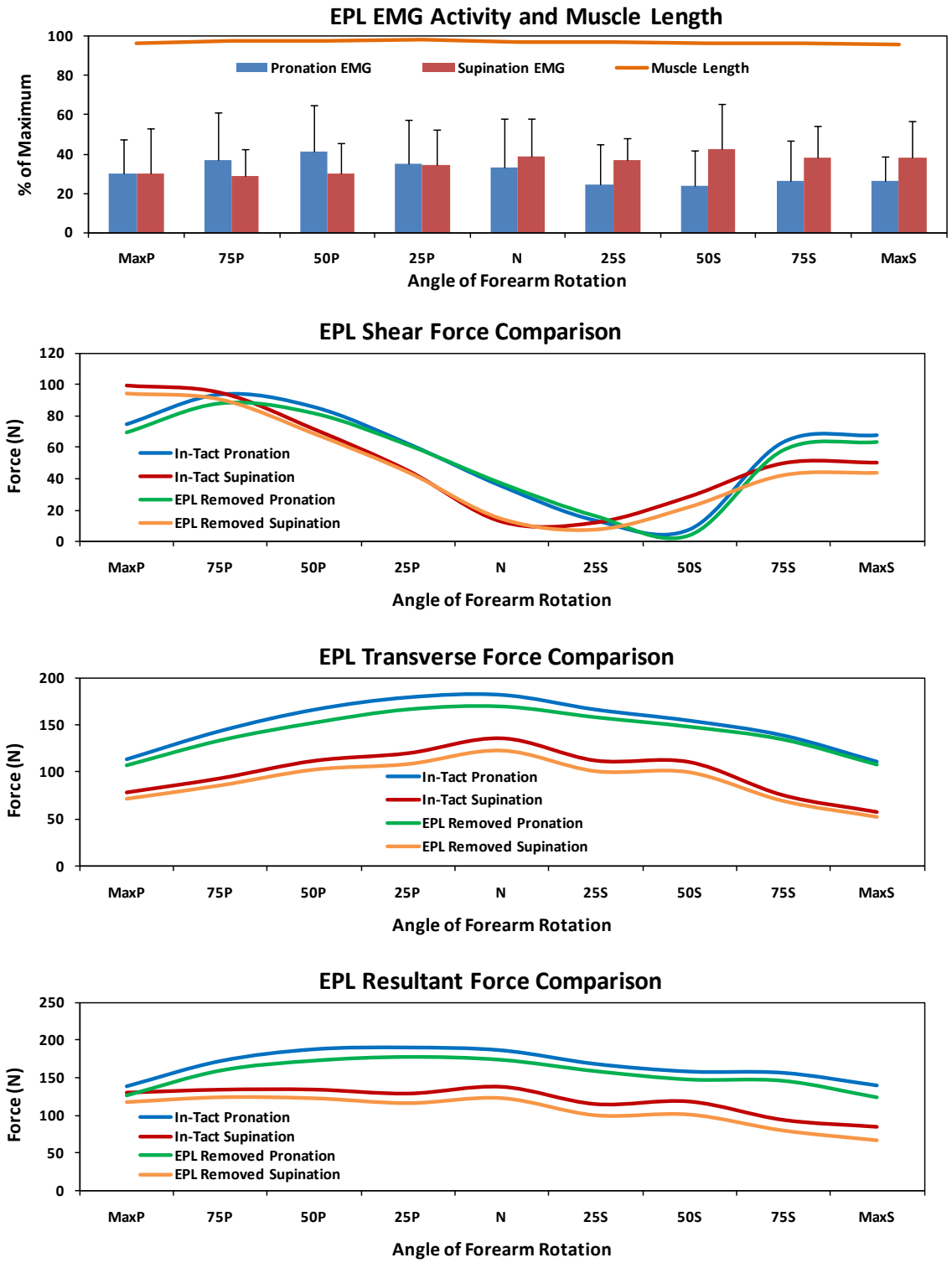

Figure D.9. Mean Extensor Pollicis Longus Plots

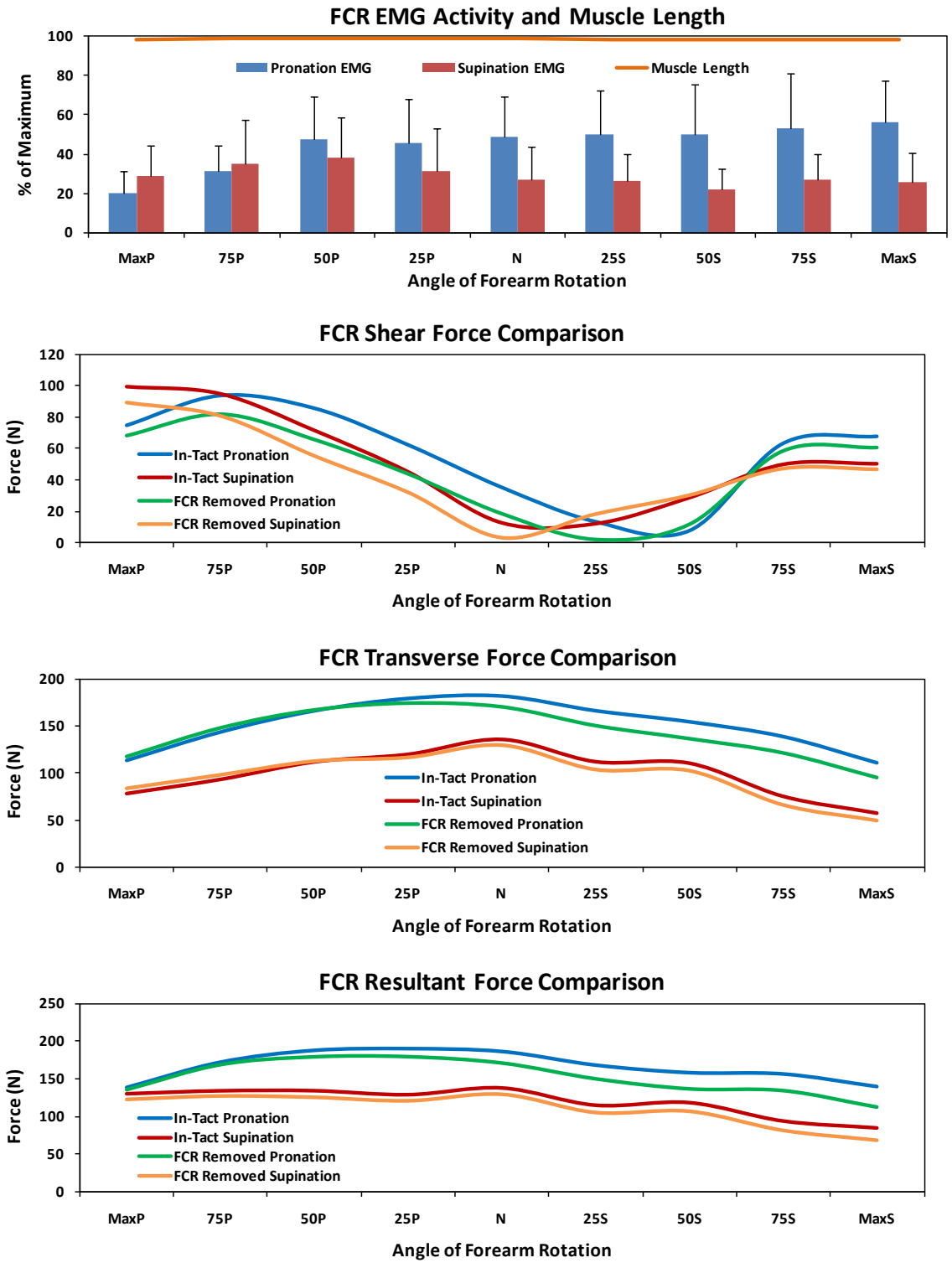

Figure D.10. Mean Flexor Carpi Radialis Plots

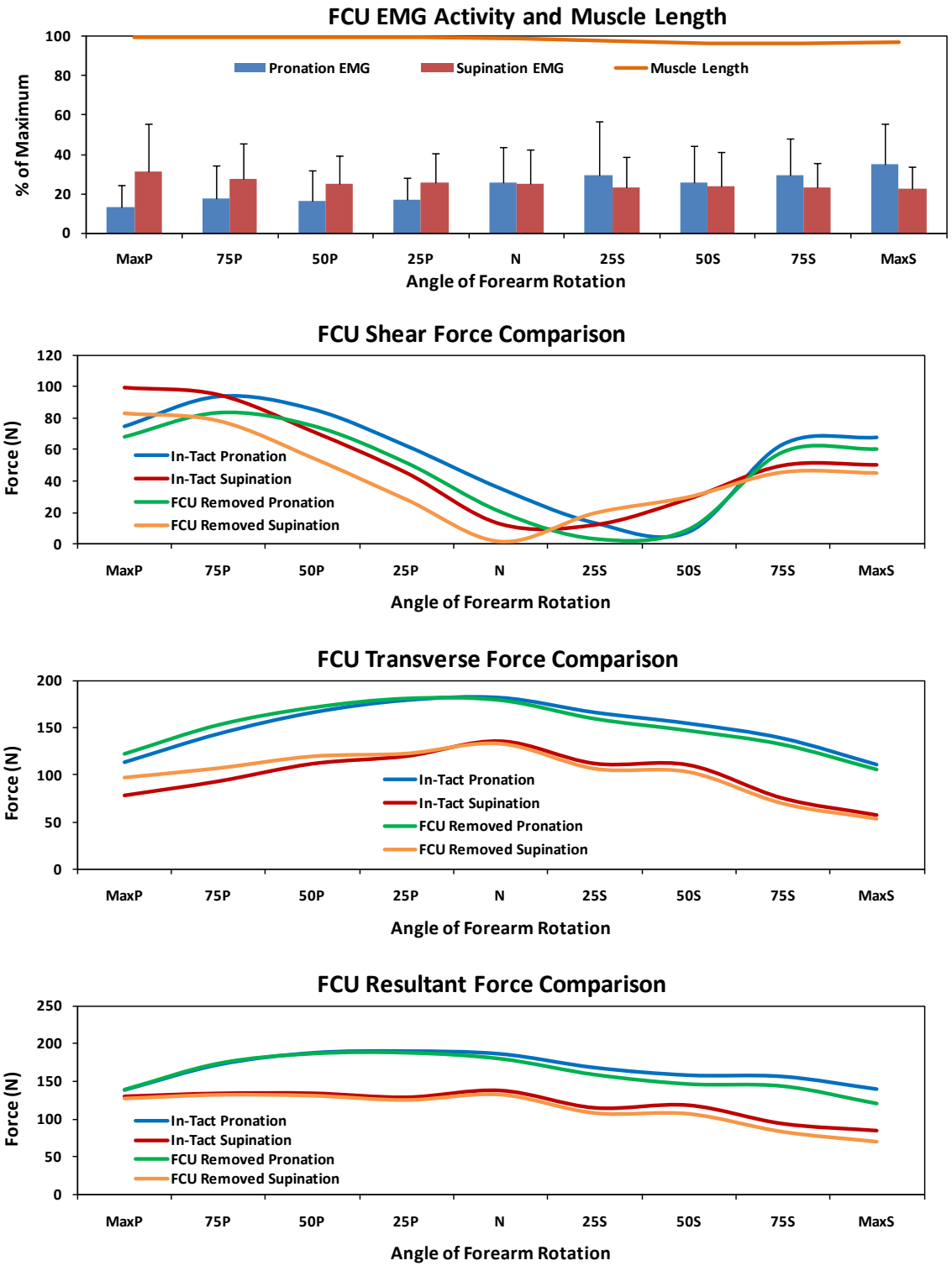

Figure D.11. Mean Flexor Carpi Ulnaris Plots

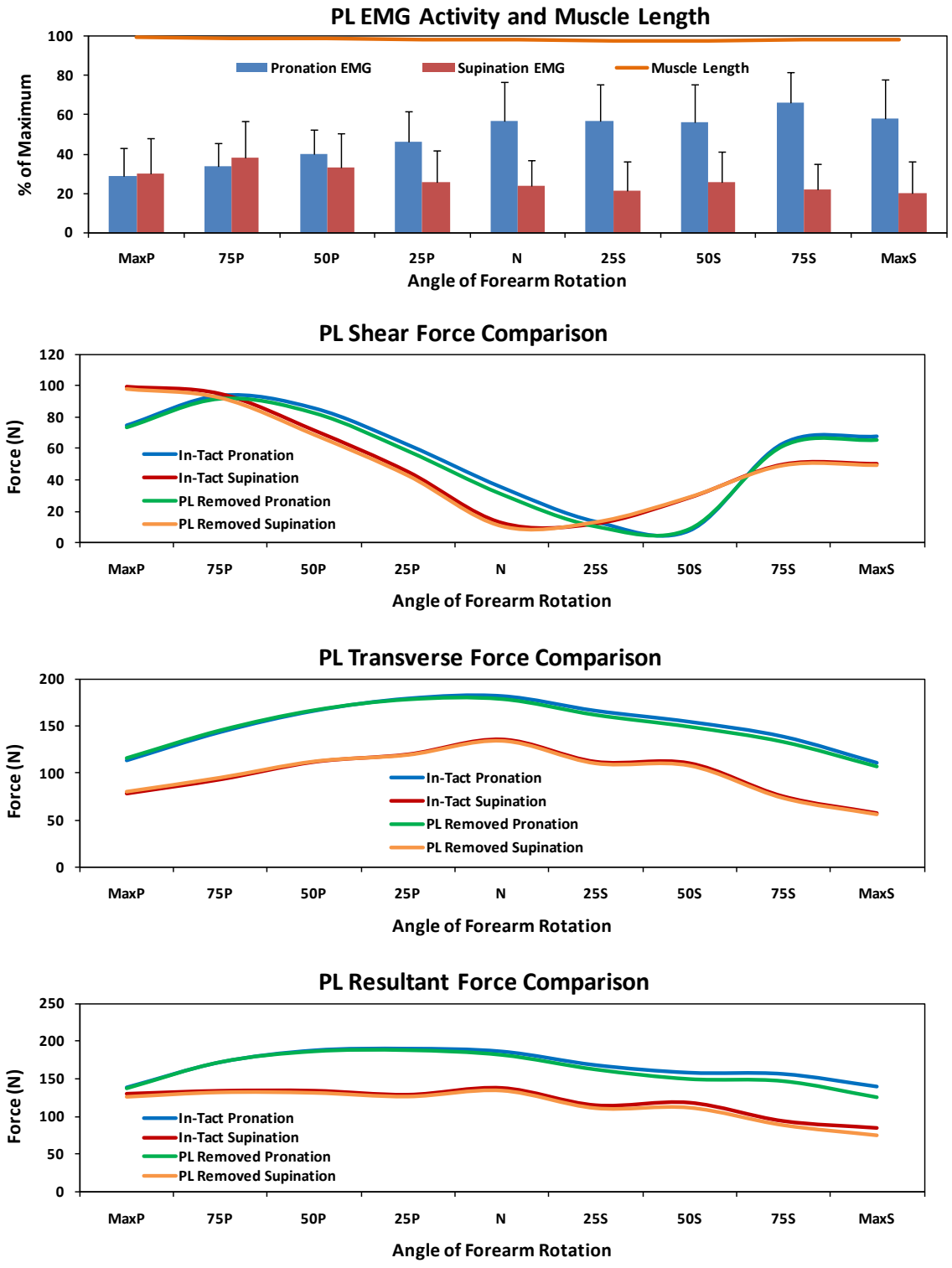

Figure D.12. Mean Palmaris Longus Plots

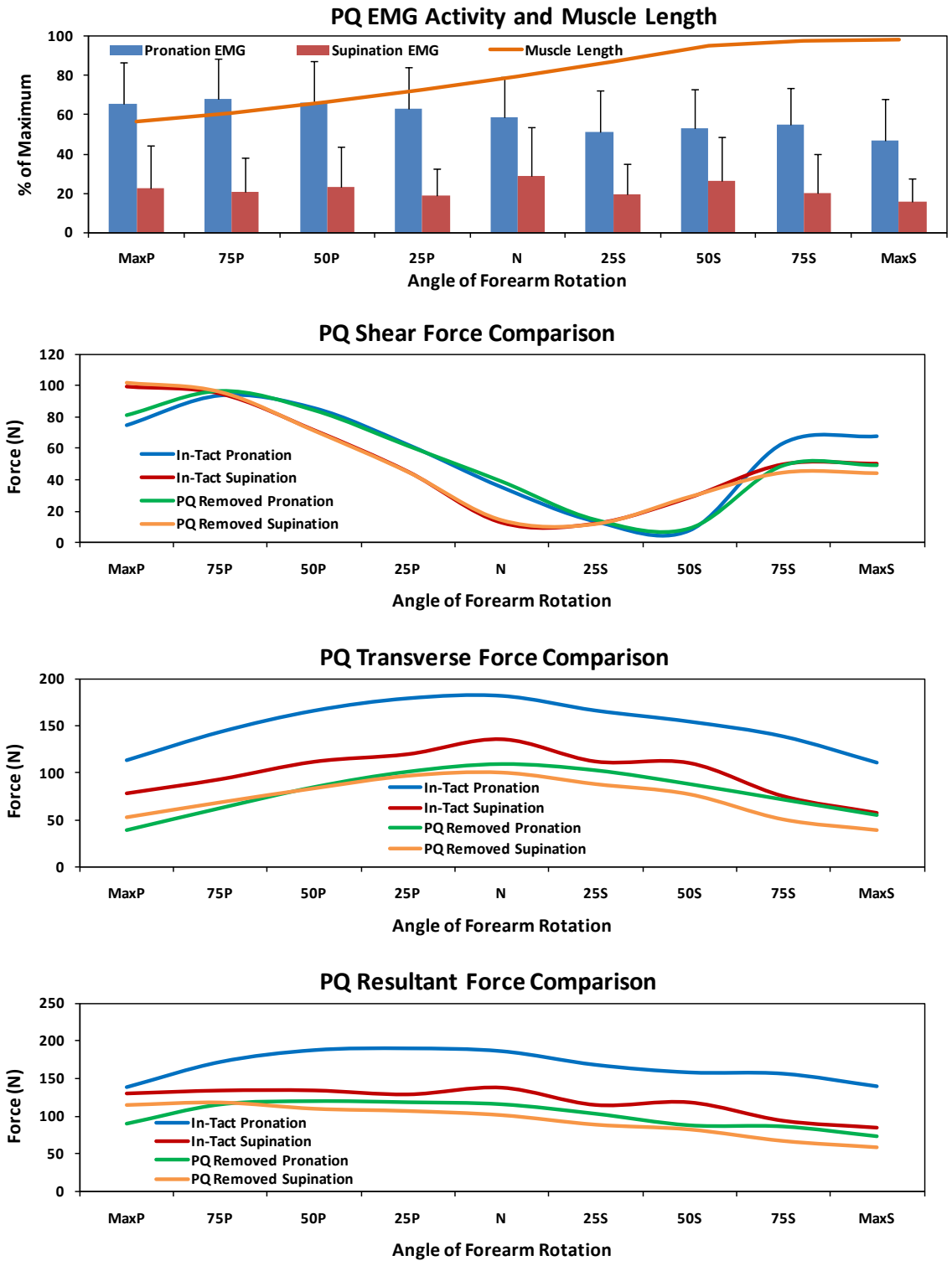

Figure D.13. Mean Pronator Quadratus Plots

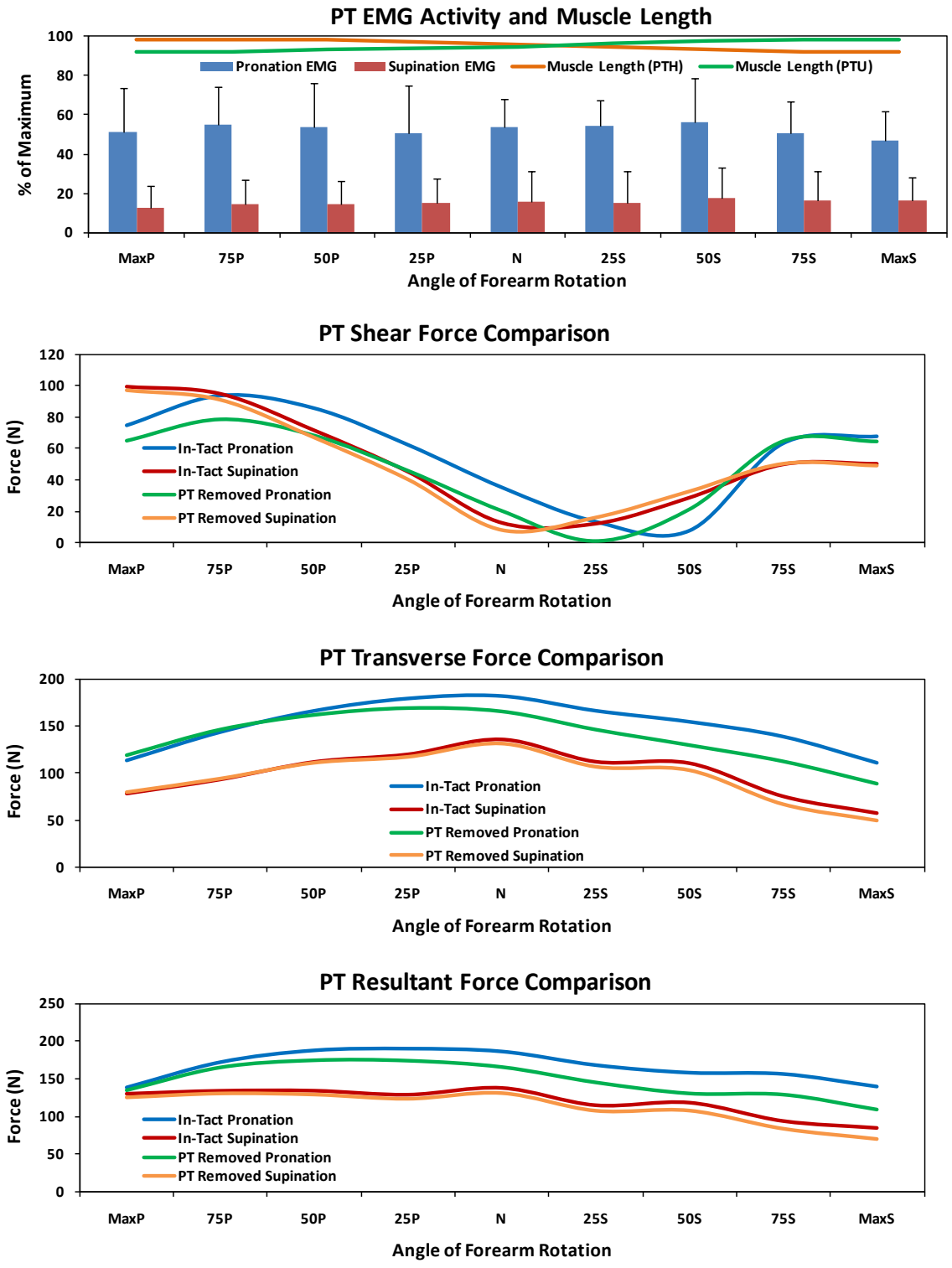

Figure D.14. Mean Pronator Teres Plots

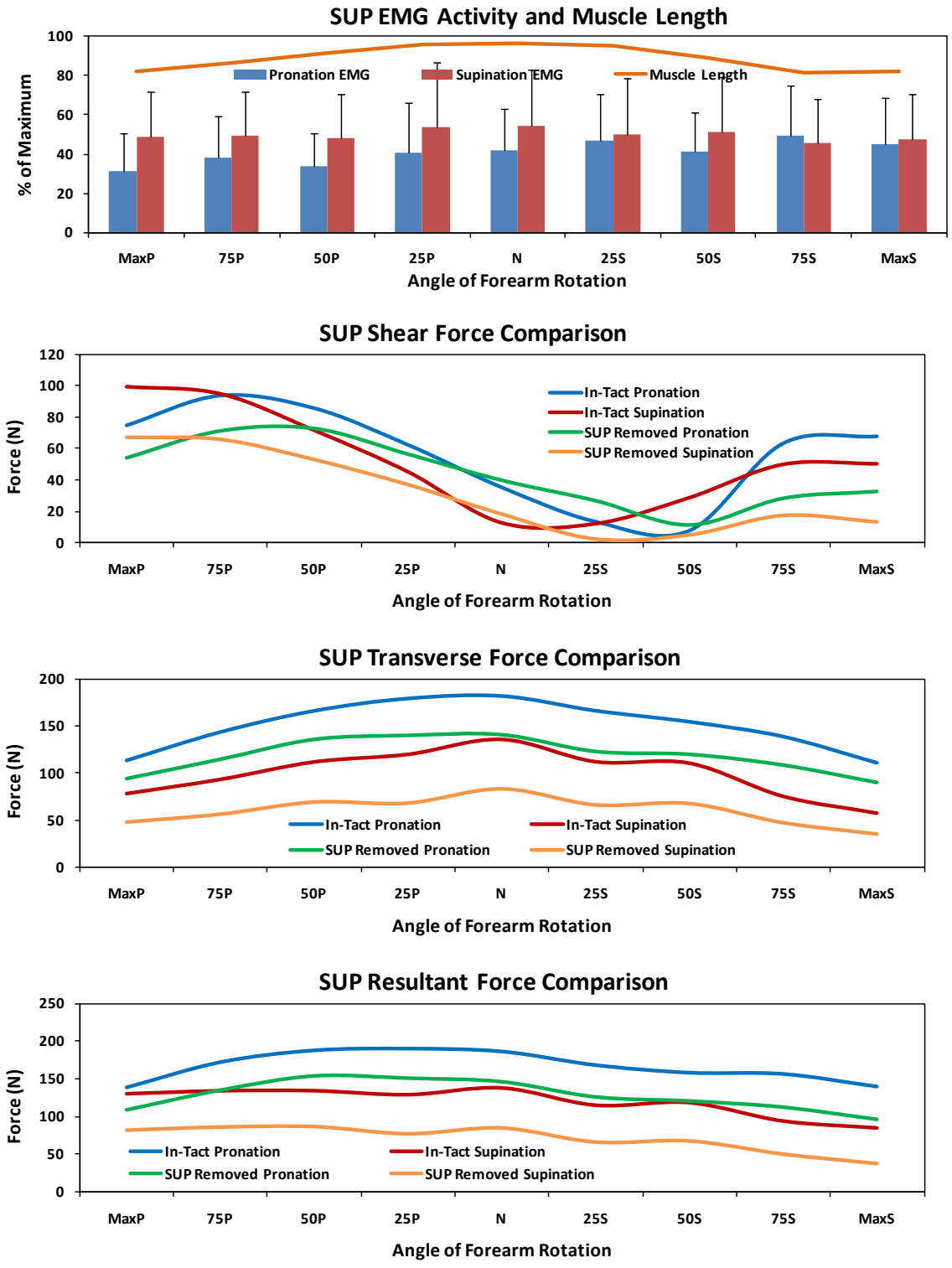

Figure D.15. Mean Supinator Plots

APPENDIX E: CUMULATIVE MUSCLE FORCE CONTRIBUTIONS

The muscles providing a negative force are on the left side of the plot while the positive forces are on the right side of the plot. The positive and negative forces are separately ranked from the largest magnitude to smallest magnitude. The force provided by each muscle is added to the sum of the muscle forces in the bar before it. The horizontal blue line indicates 75% of the combined positive force of all muscles while the horizontal red line indicates 75% of the combined negative force of all the muscles. The total positive force is usually greater than 100% because the positive and negative forces combine to make the overall 100% force. Therefore the lines do not occur at 75% of the total force, but 75% of the total positive and total negative force. Green bars indicate that the muscle contributes to reaching the 75% mark. Red and blue bars indicate that a muscle provides negative force and positive force, respectively, but do not contribute to reaching 75% of the force. In order to rank the muscles, the total number of times that a muscle contributed to reaching 75% of the force (green bars) as well as in individual categories were counted .

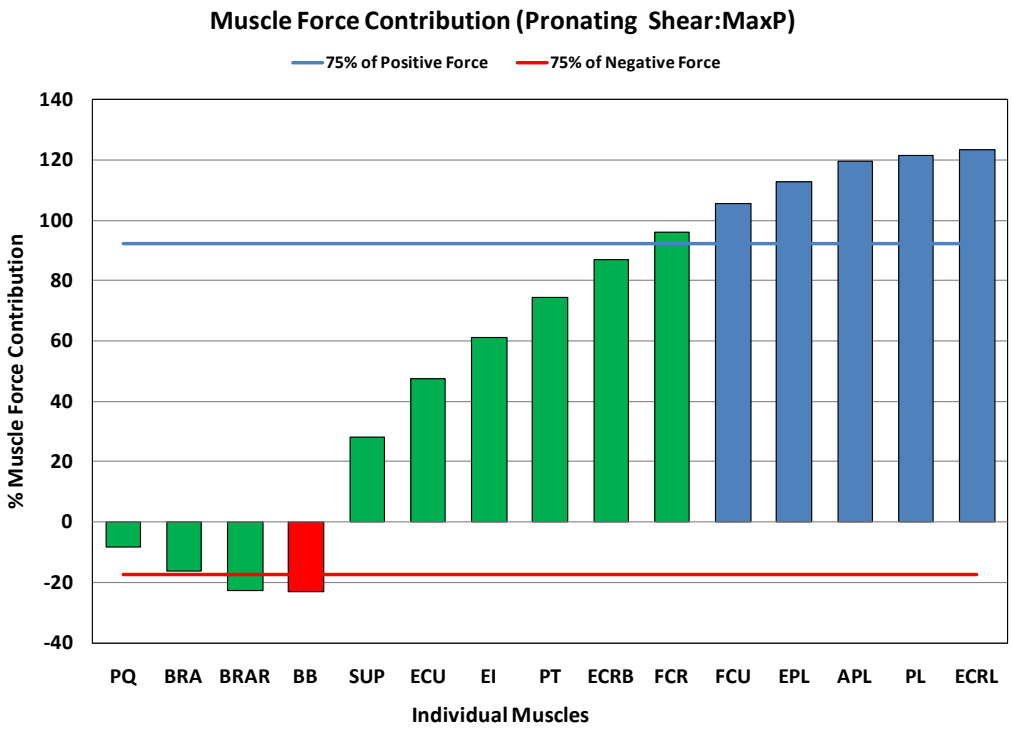

Figure E.1. Shear Force Contributions during Pronation at MaxP

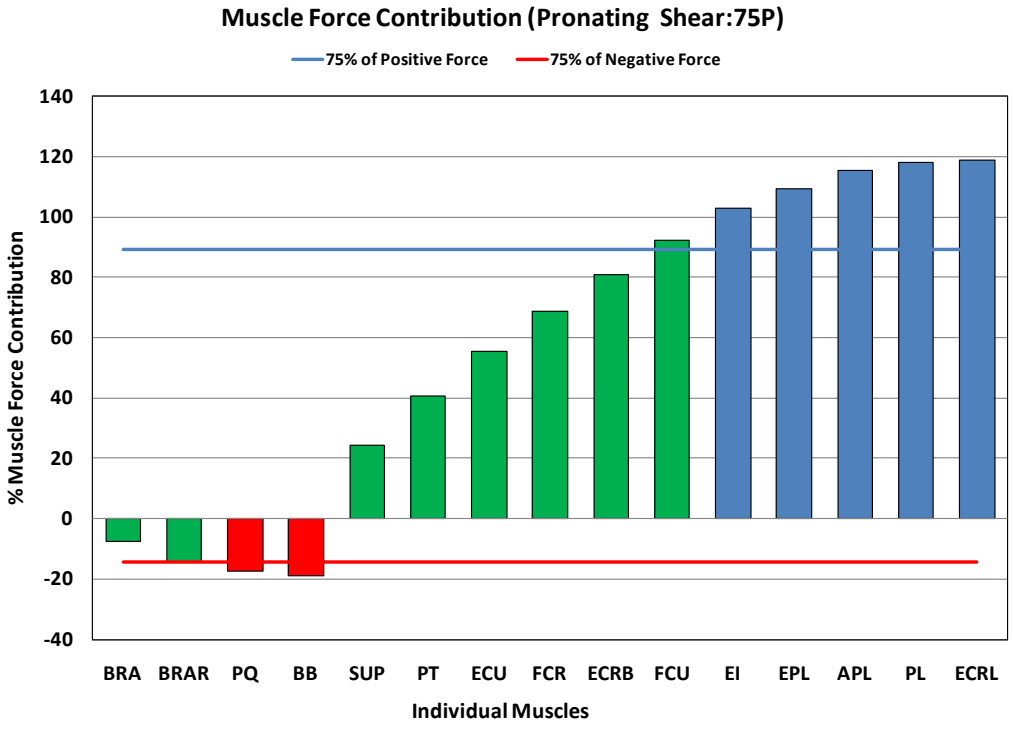

Figure E.2. Shear Force Contributions during Pronation at 75P

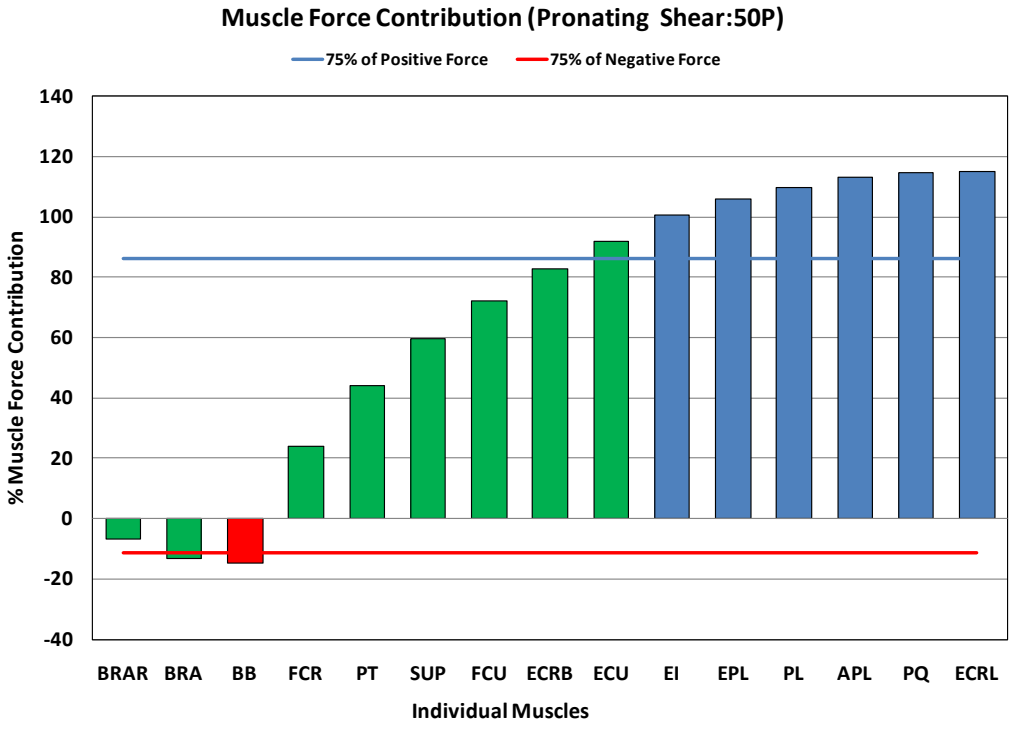

Figure E.3. Shear Force Contributions during Pronation at 50P

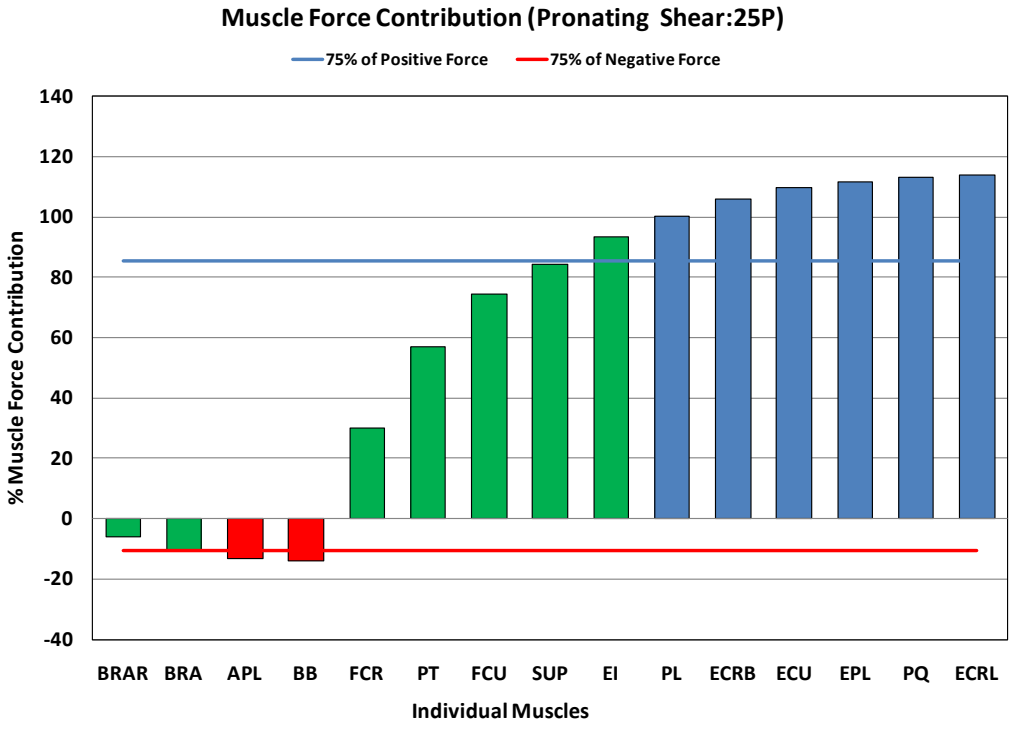

Figure E.4. Shear Force Contributions during Pronation at 25P

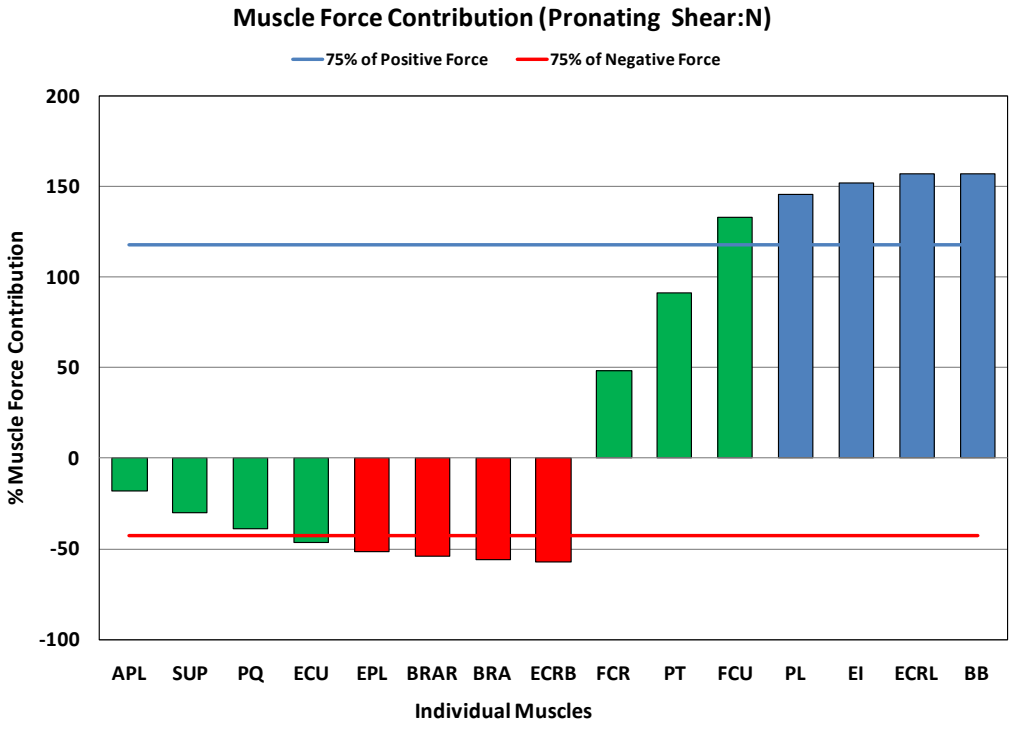

Figure E.5. Shear Force Contributions during Pronation at Neutral

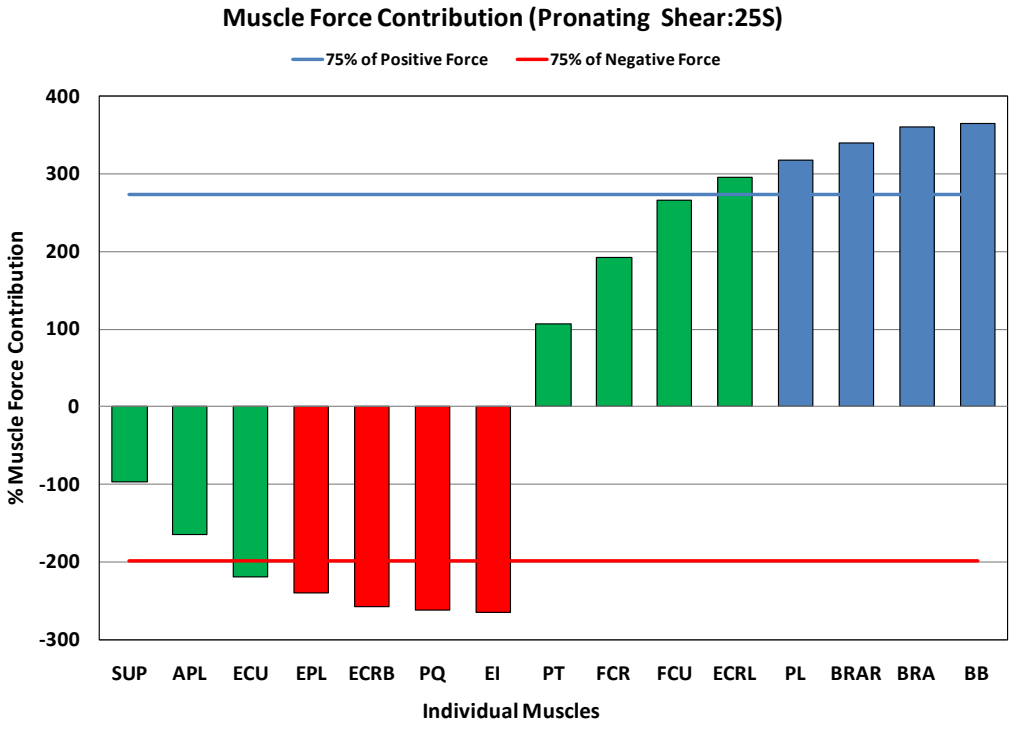

Figure E.6. Shear Force Contributions during Pronation at 25S

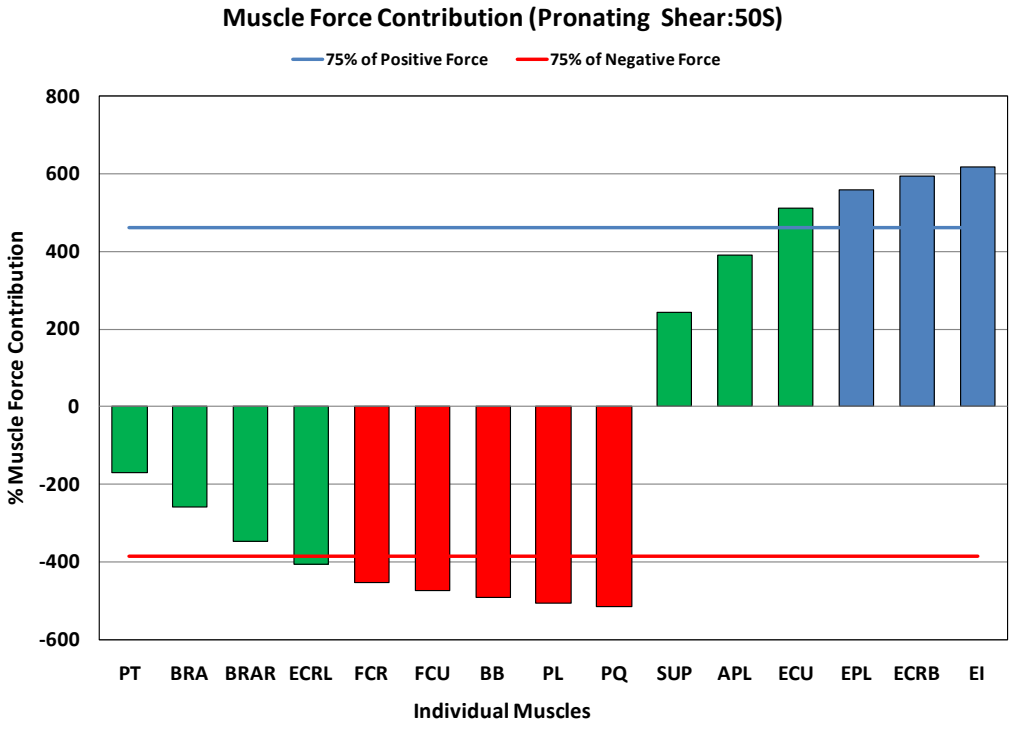

Figure E.7. Shear Force Contributions during Pronation at 50S

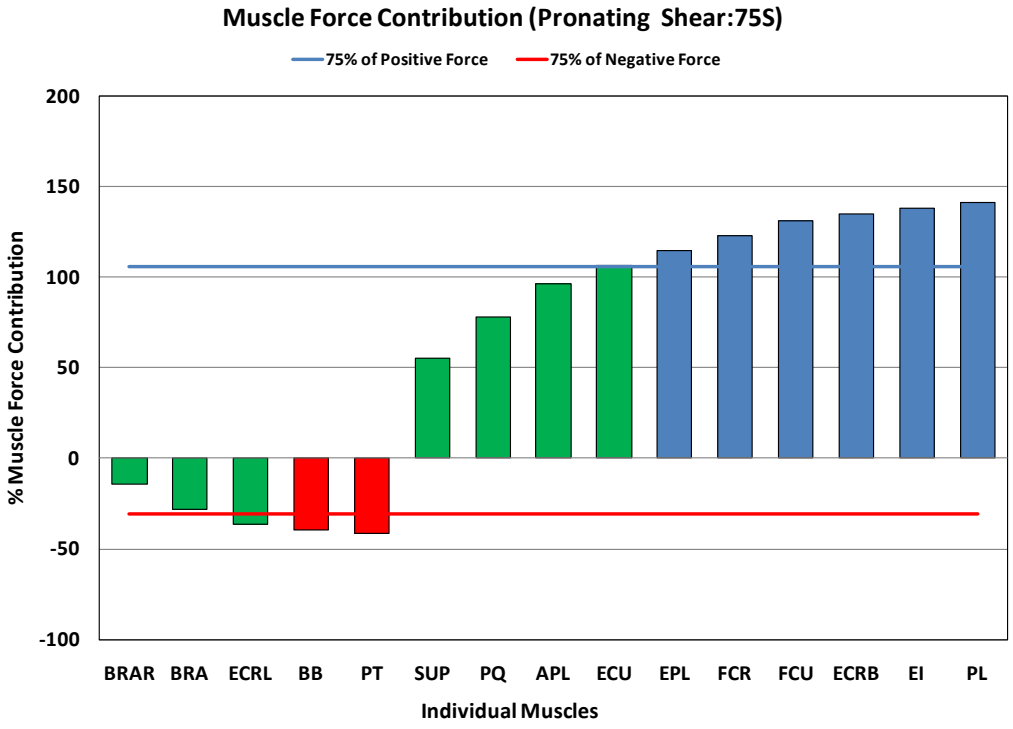

Figure E.8. Shear Force Contributions during Pronation at 75S

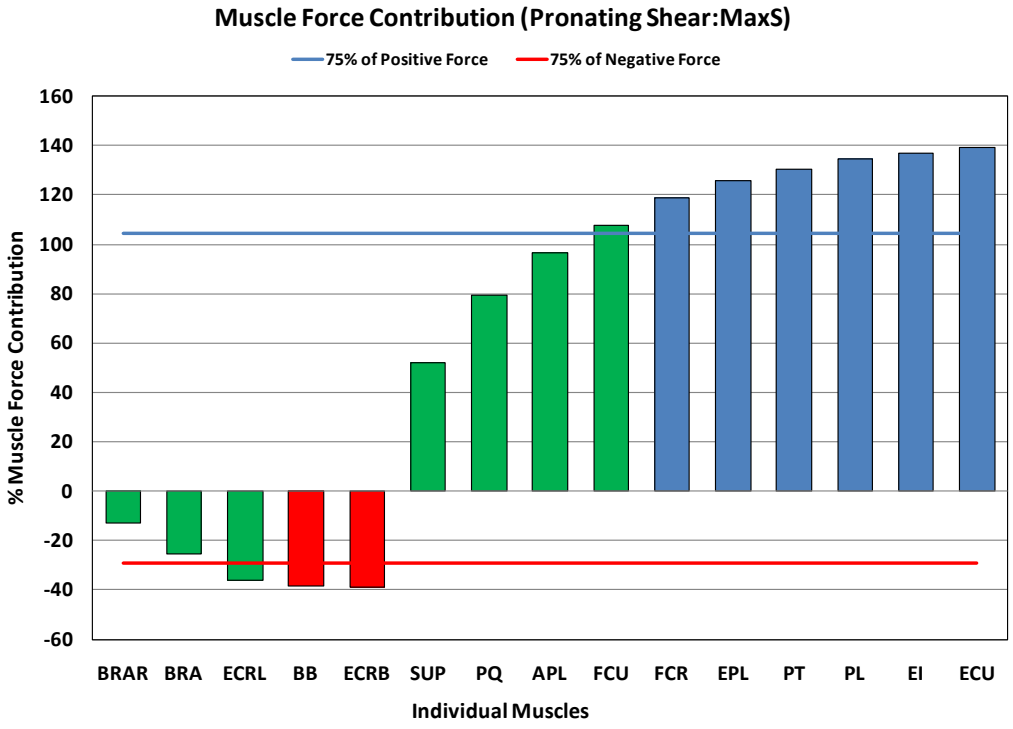

Figure E.9. Shear Force Contributions during Pronation at MaxS

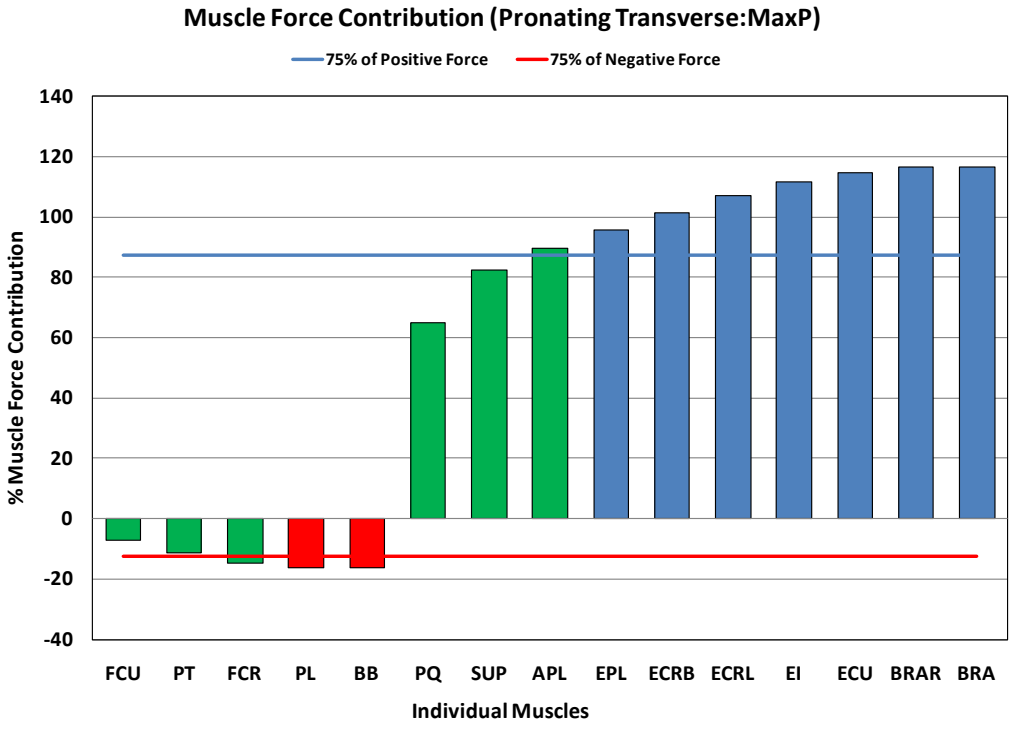

Figure E.10. Transverse Force Contributions during Pronation at MaxP

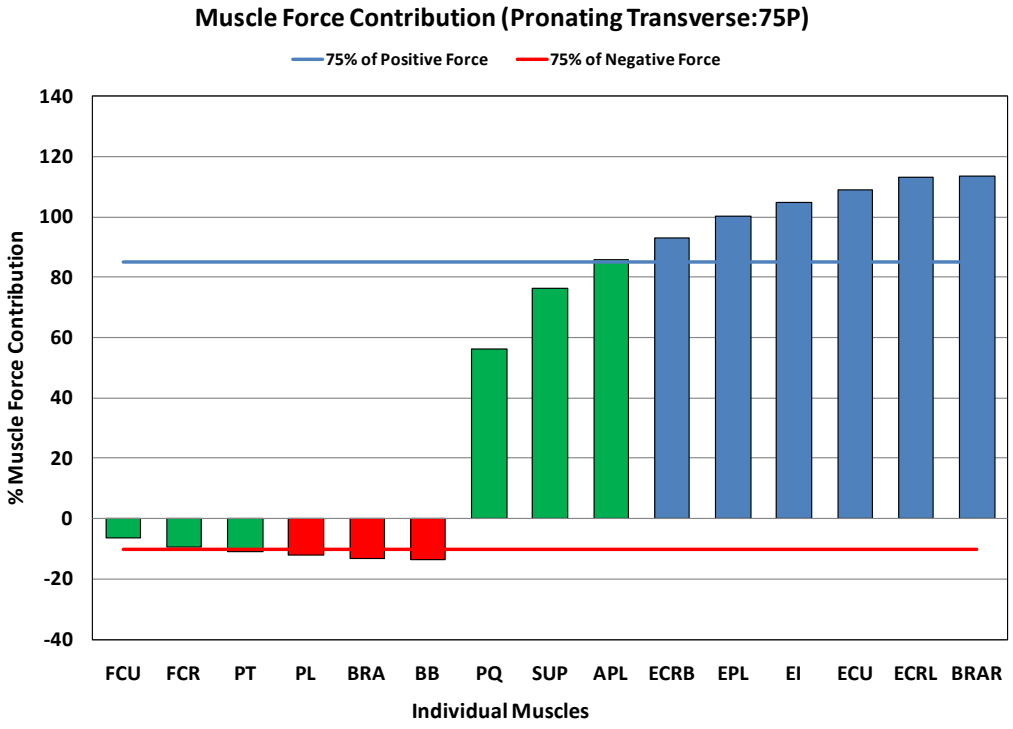

Figure E.11. Transverse Force Contributions during Pronation at 75P

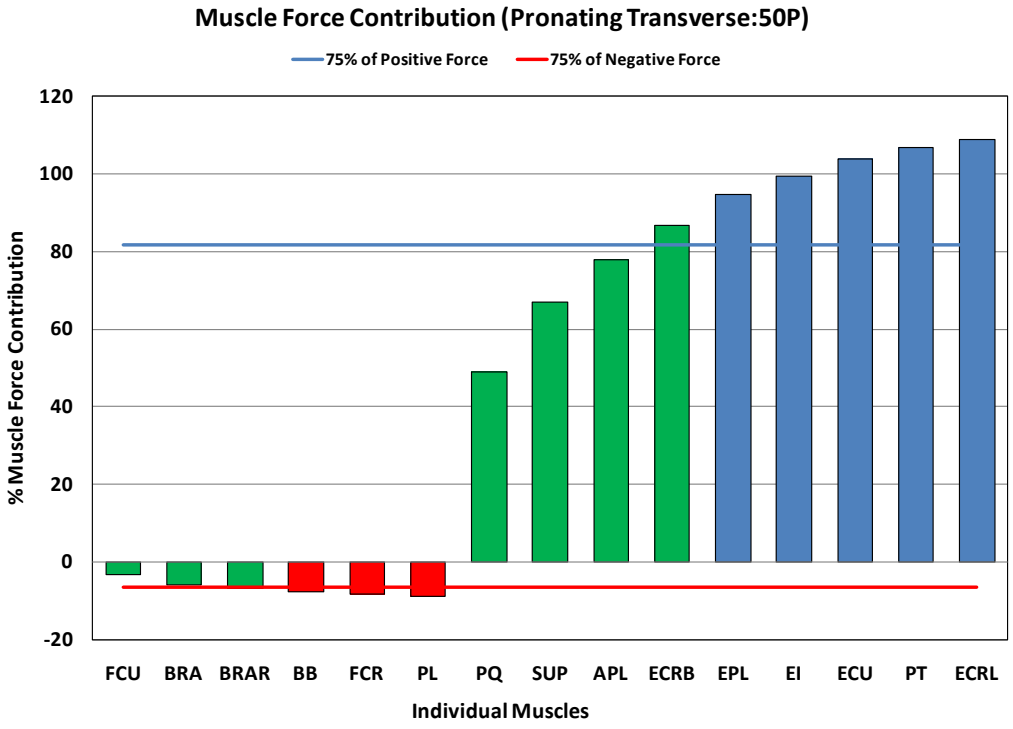

Figure E.12. Transverse Force Contributions during Pronation at 50P

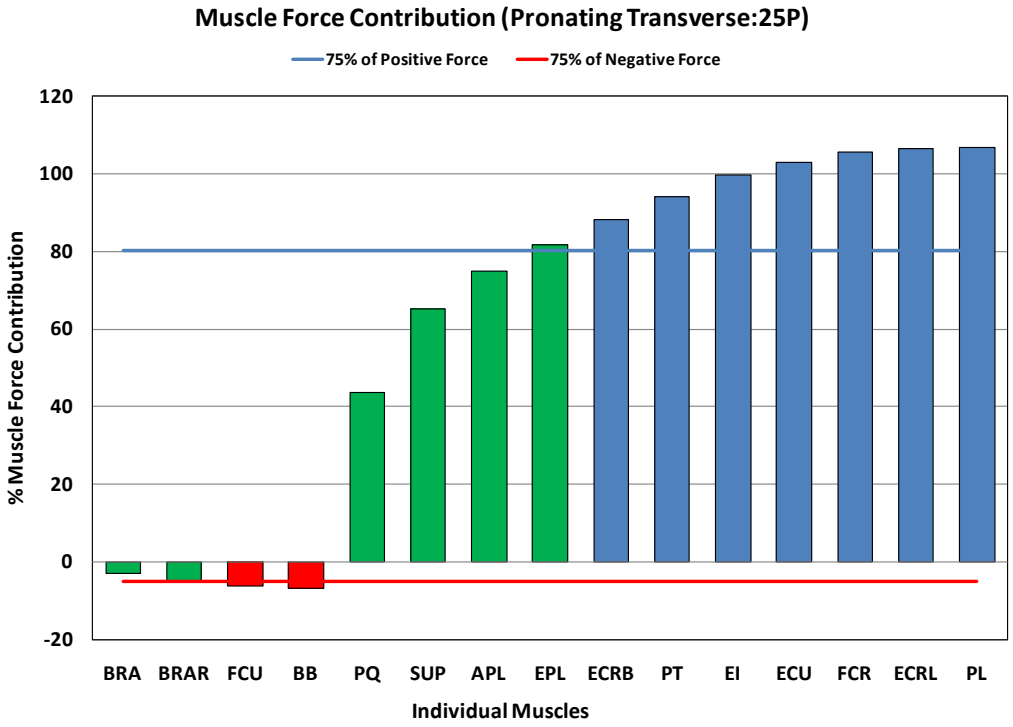

Figure E.13. Transverse Force Contributions during Pronation at 25P

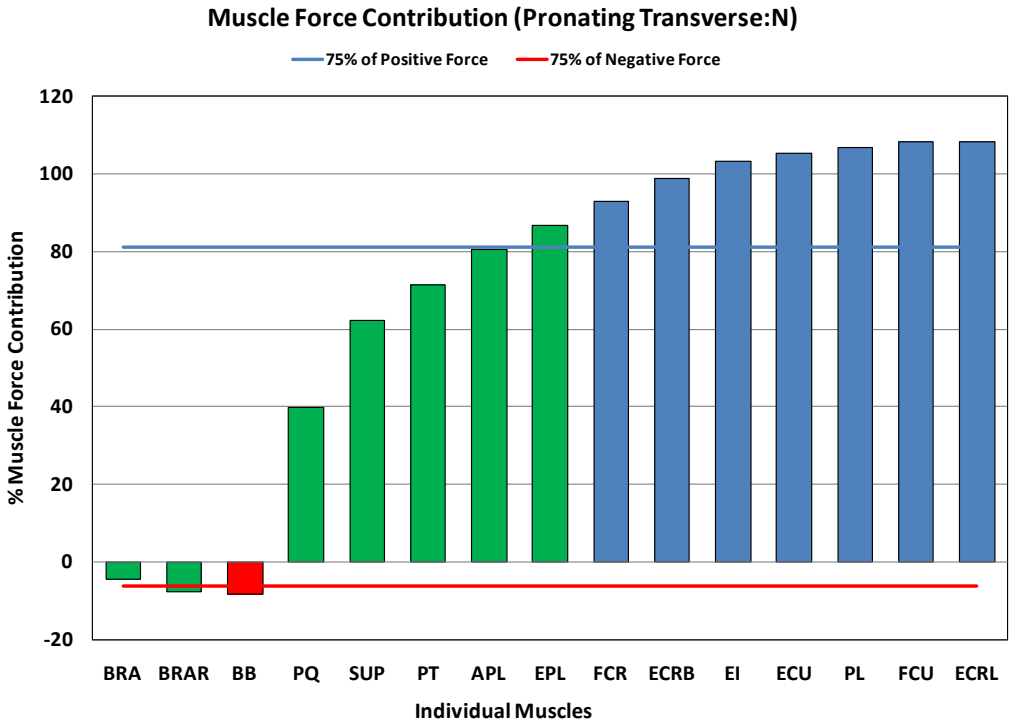

Figure E.14. Transverse Force Contributions during Pronation at Neutral

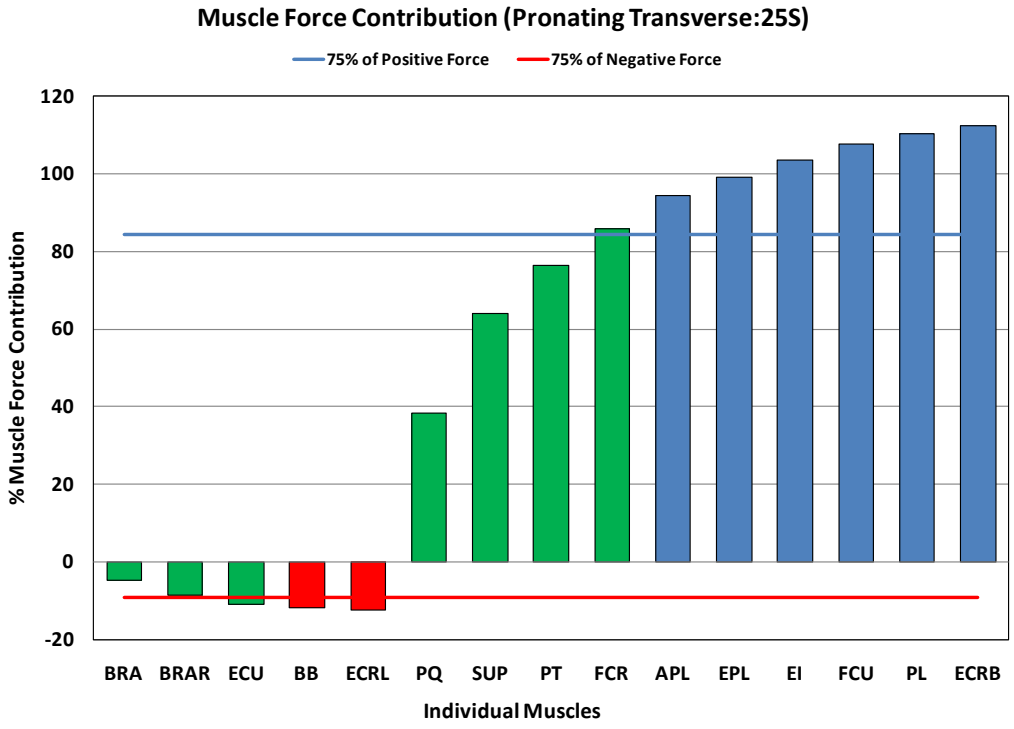

Figure E.15. Transverse Force Contributions during Pronation at 25S

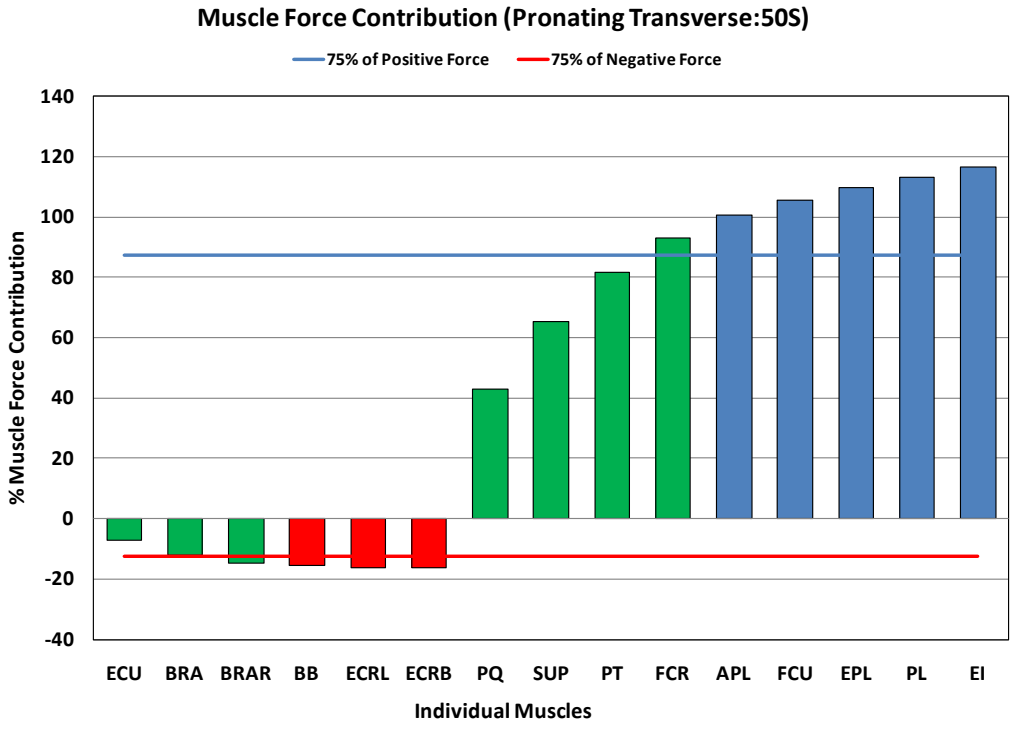

Figure E.16. Transverse Force Contributions during Pronation at 50S

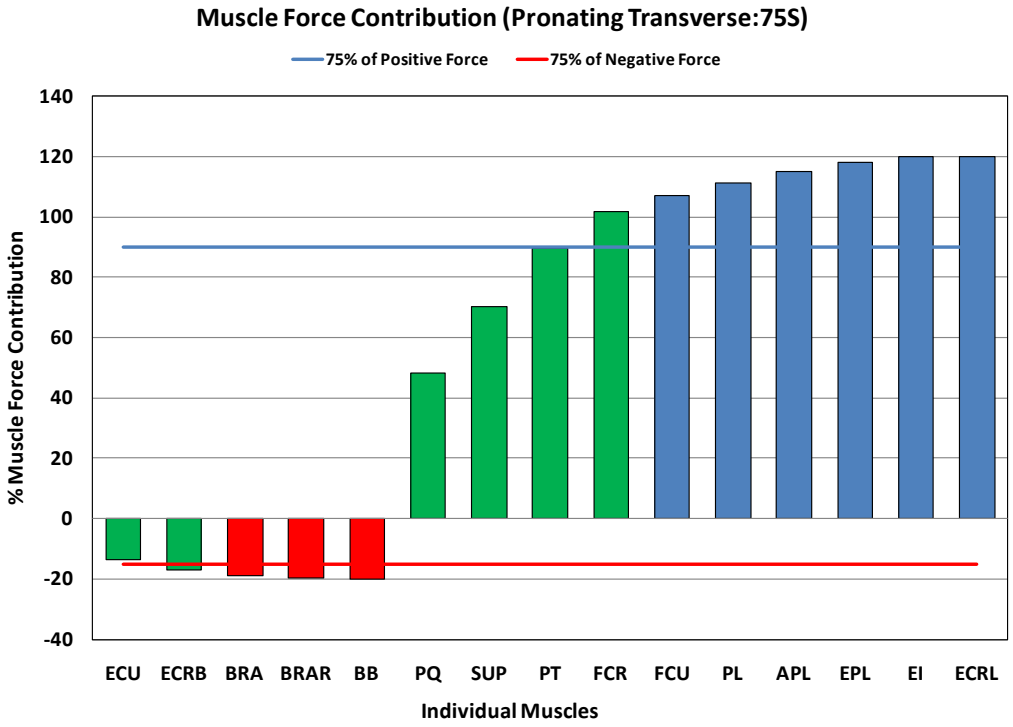

Figure E.17. Transverse Force Contributions during Pronation at 75S

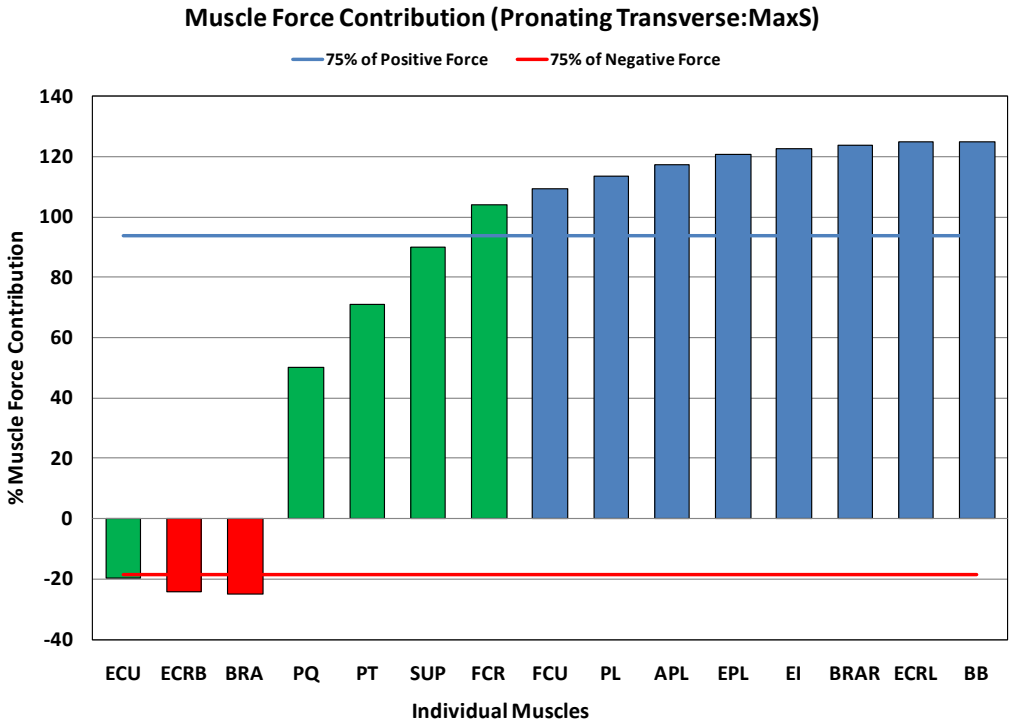

Figure E.18. Transverse Force Contributions during Pronation at MaxS

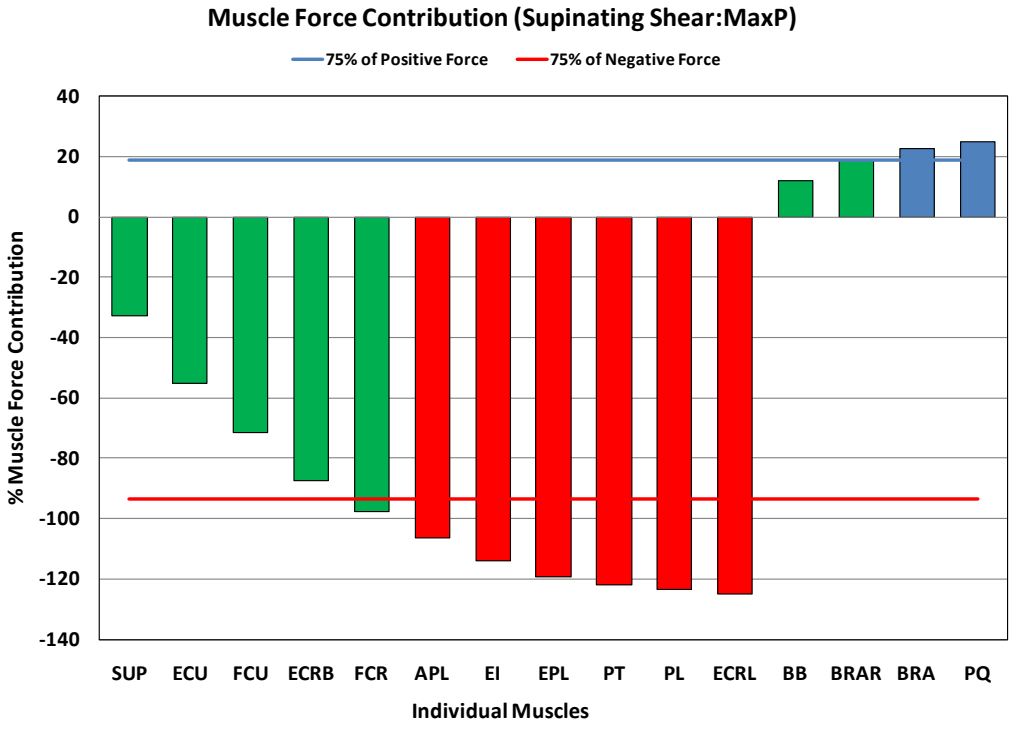

Figure E.19. Shear Force Contributions during Supination at MaxP

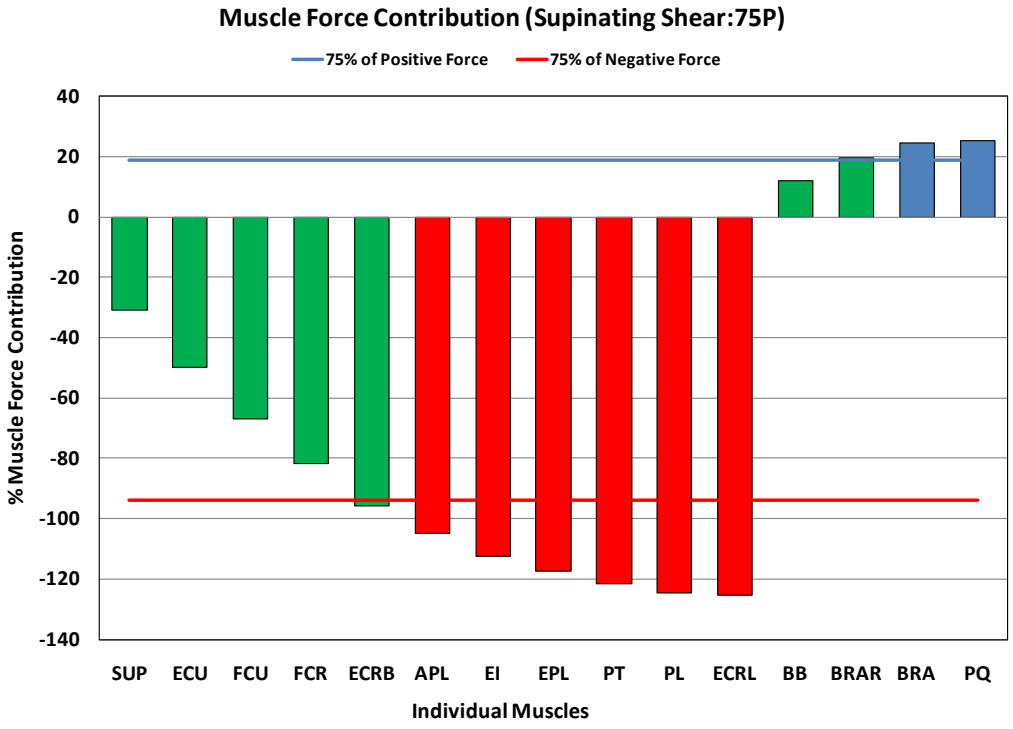

Figure E.20. Shear Force Contributions during Supination at 75P

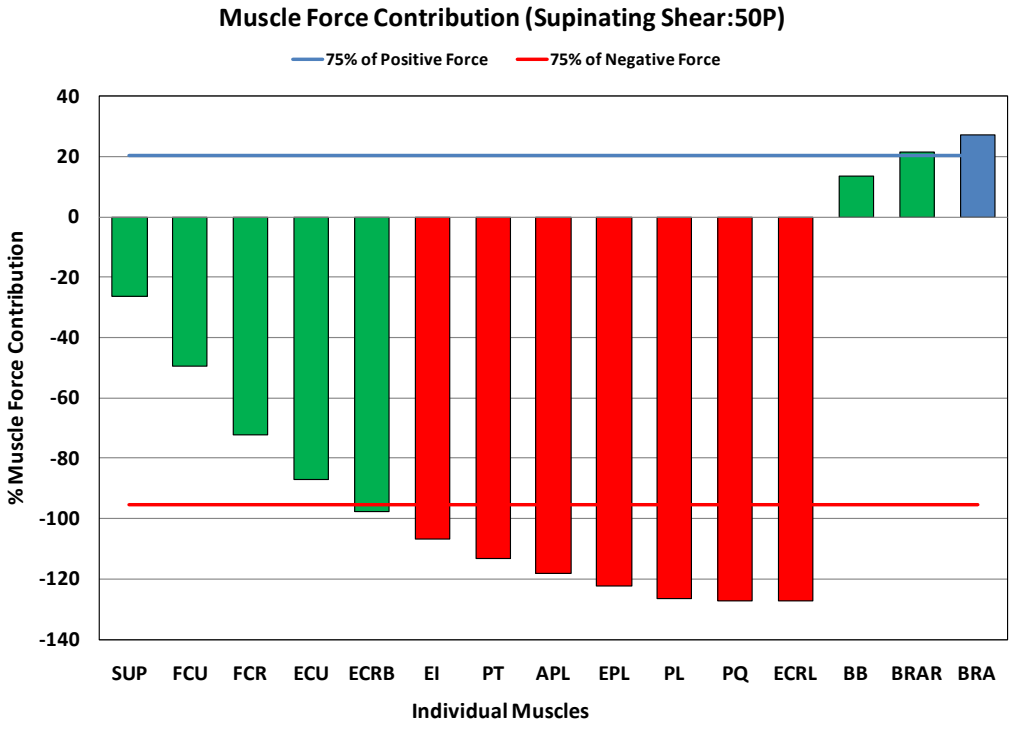

Figure E.21. Shear Force Contributions during Supination at 50P

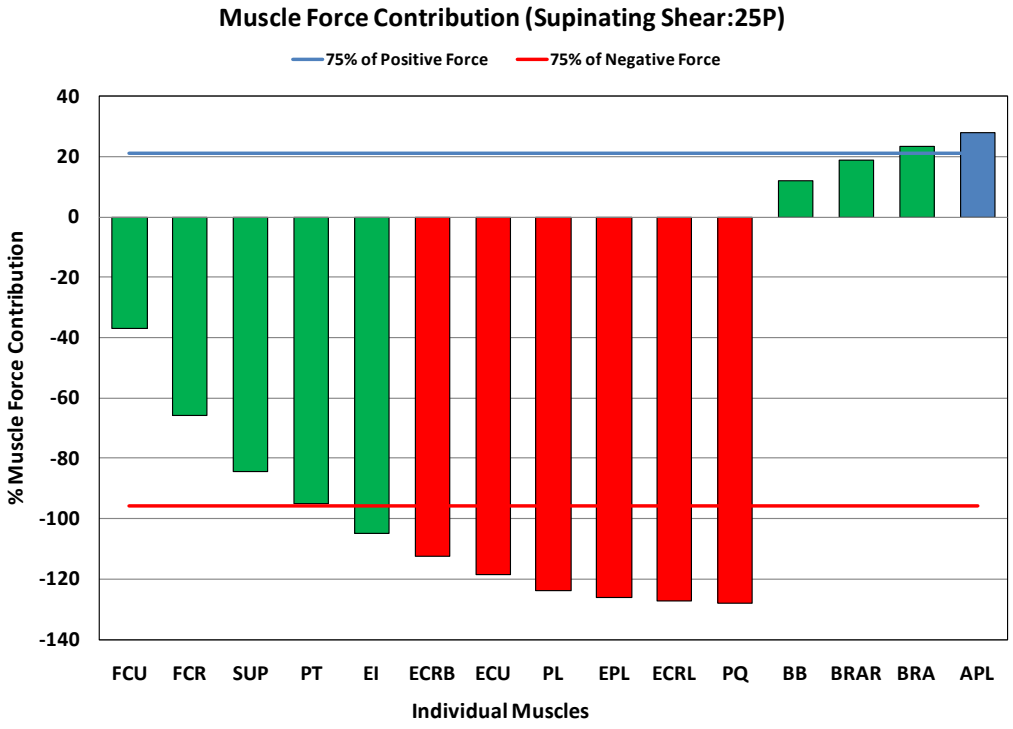

Figure E.22. Shear Force Contributions during Supination at 25P

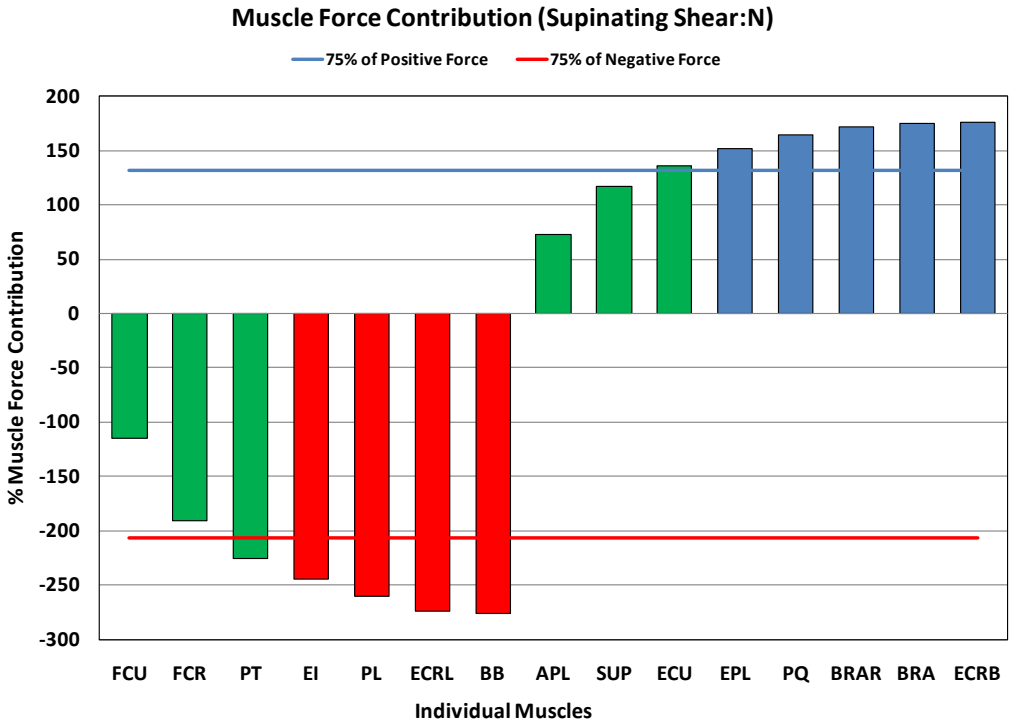

Figure E.23. Shear Force Contributions during Supination at Neutral

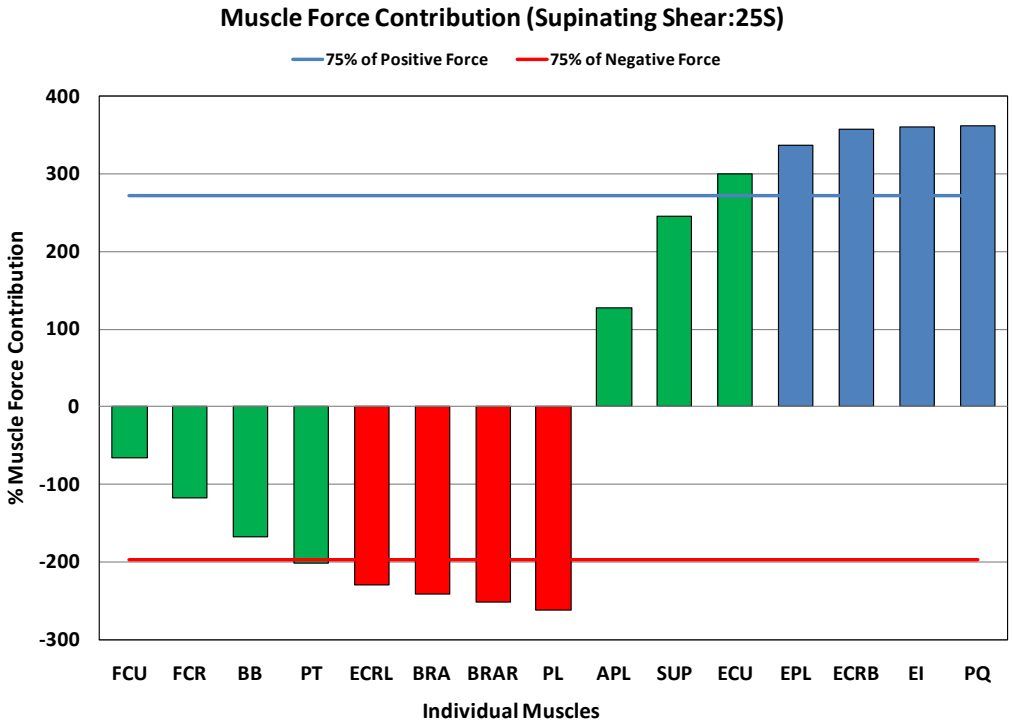

Figure E.24. Shear Force Contributions during Supination at 25S

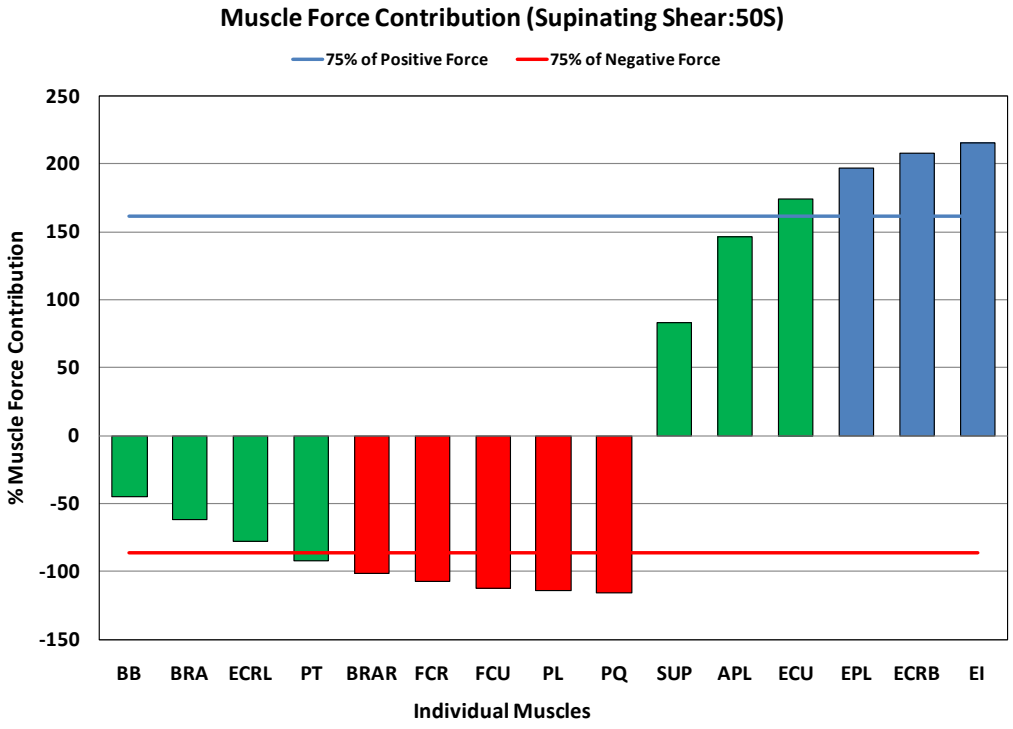

Figure E.25. Shear Force Contributions during Supination at 50S

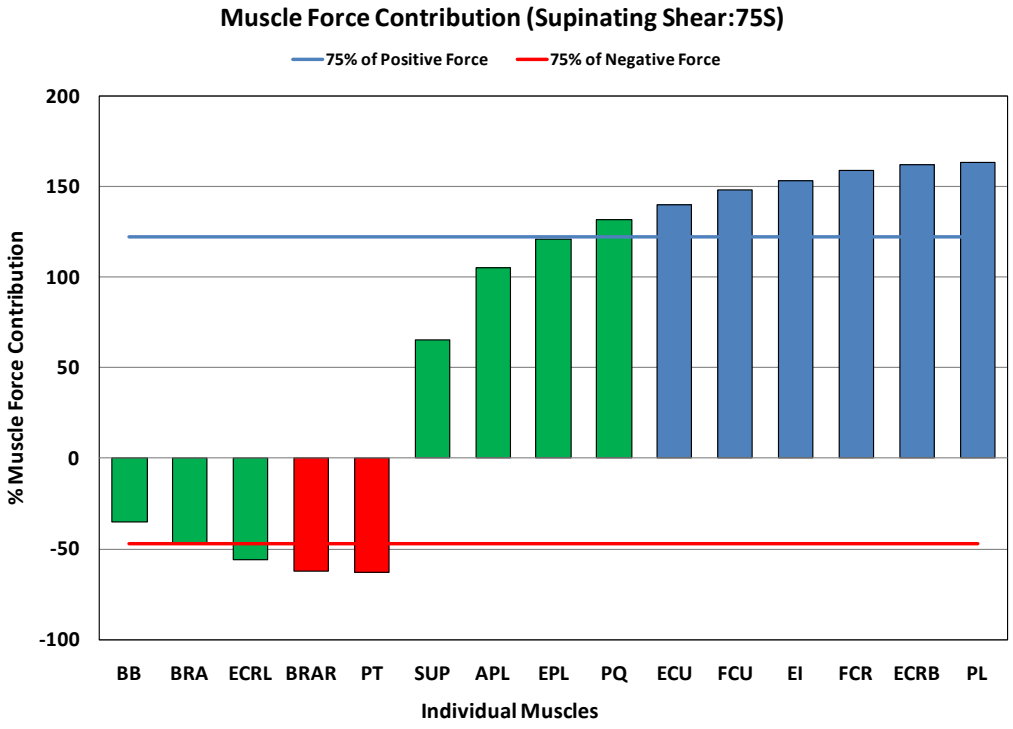

Figure E.26. Shear Force Contributions during Supination at 75S

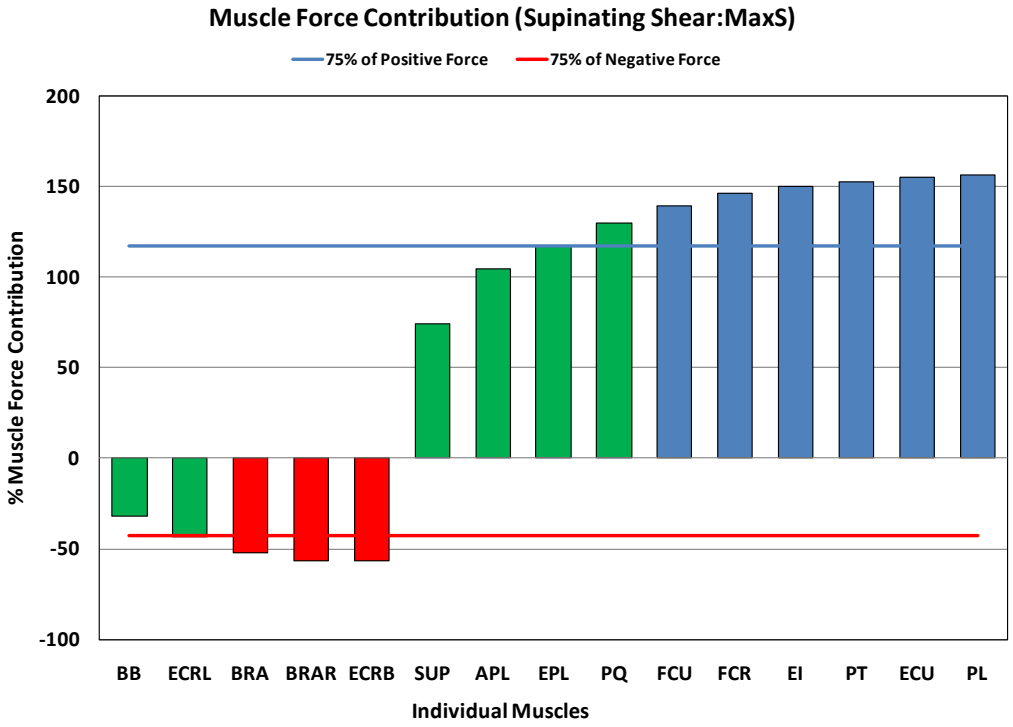

Figure E.27. Shear Force Contributions during Supination at MaxS

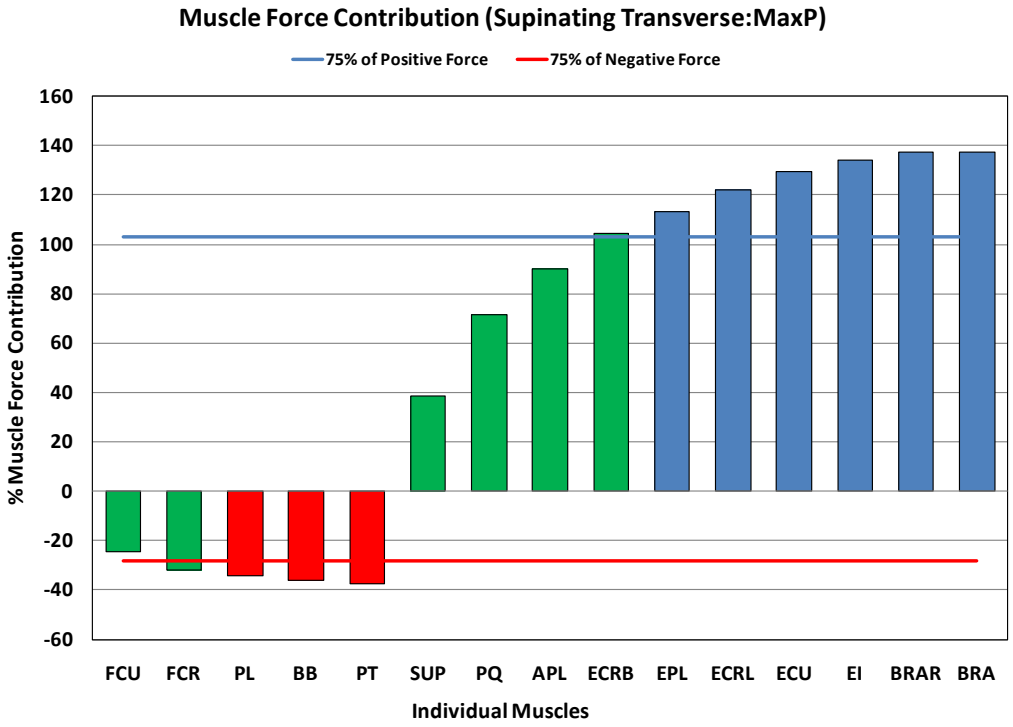

Figure E.28. Transverse Force Contributions during Supination at MaxP

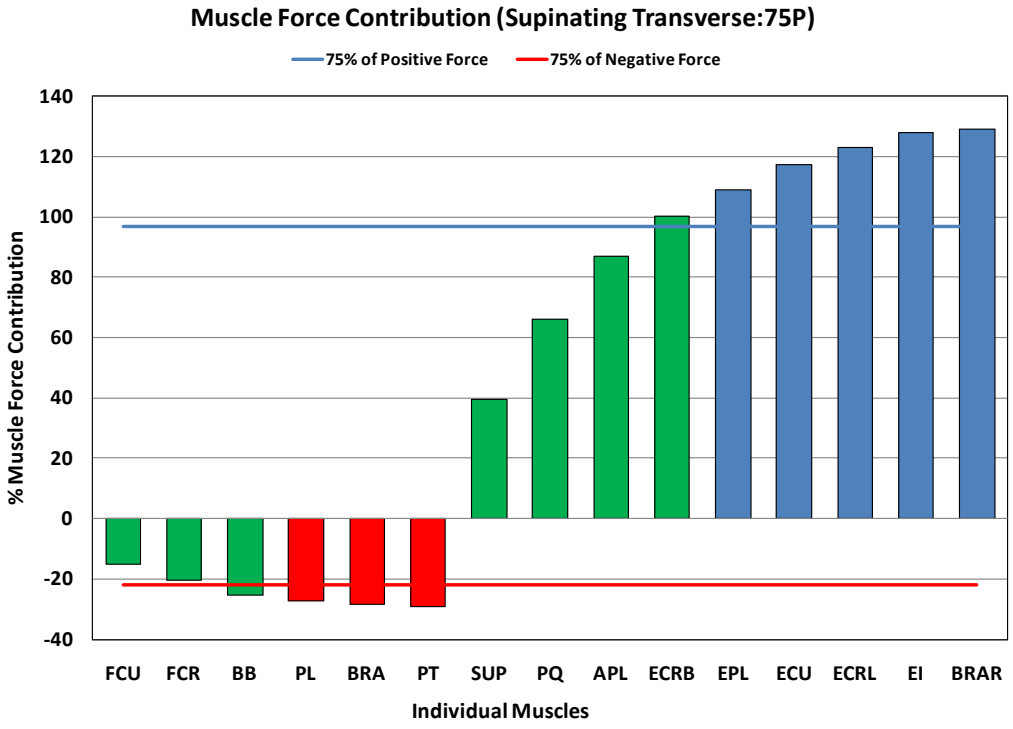

Figure E.29. Transverse Force Contributions during Supination at 75P

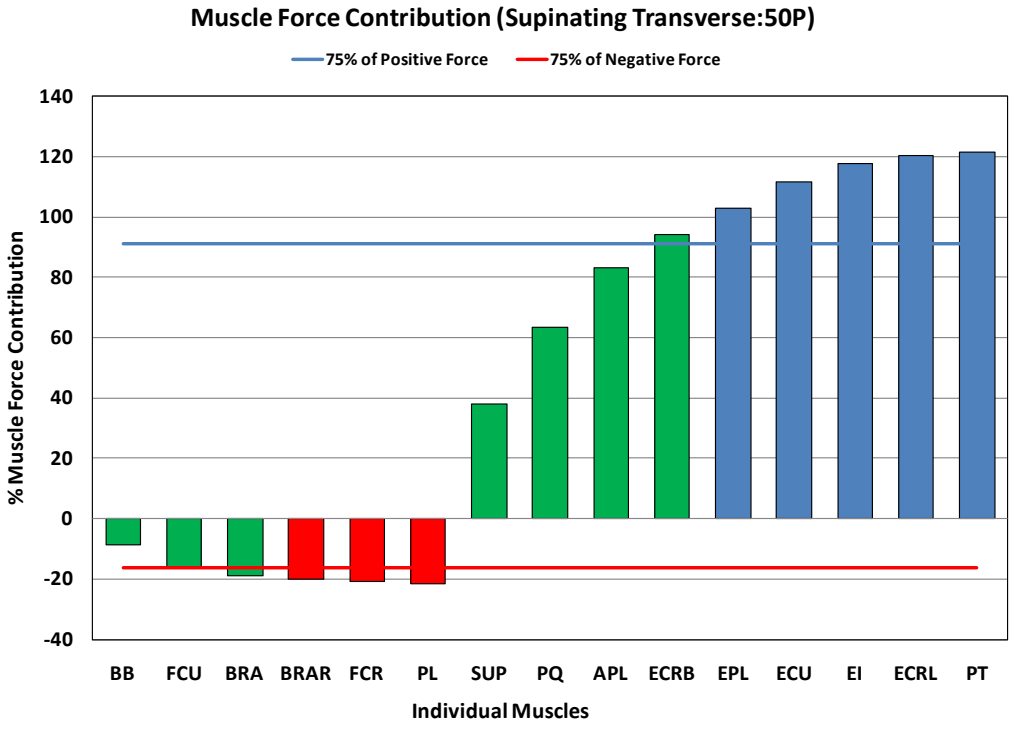

Figure E.30. Transverse Force Contributions during Supination at 50P

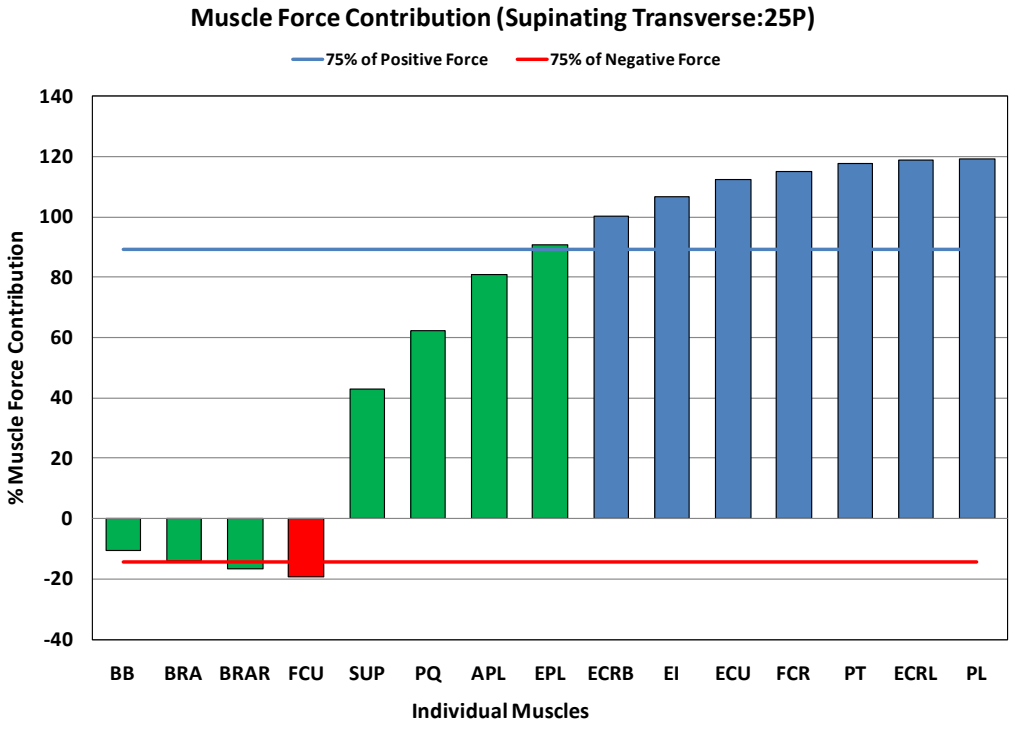

Figure E.31. Transverse Force Contributions during Supination at 25P

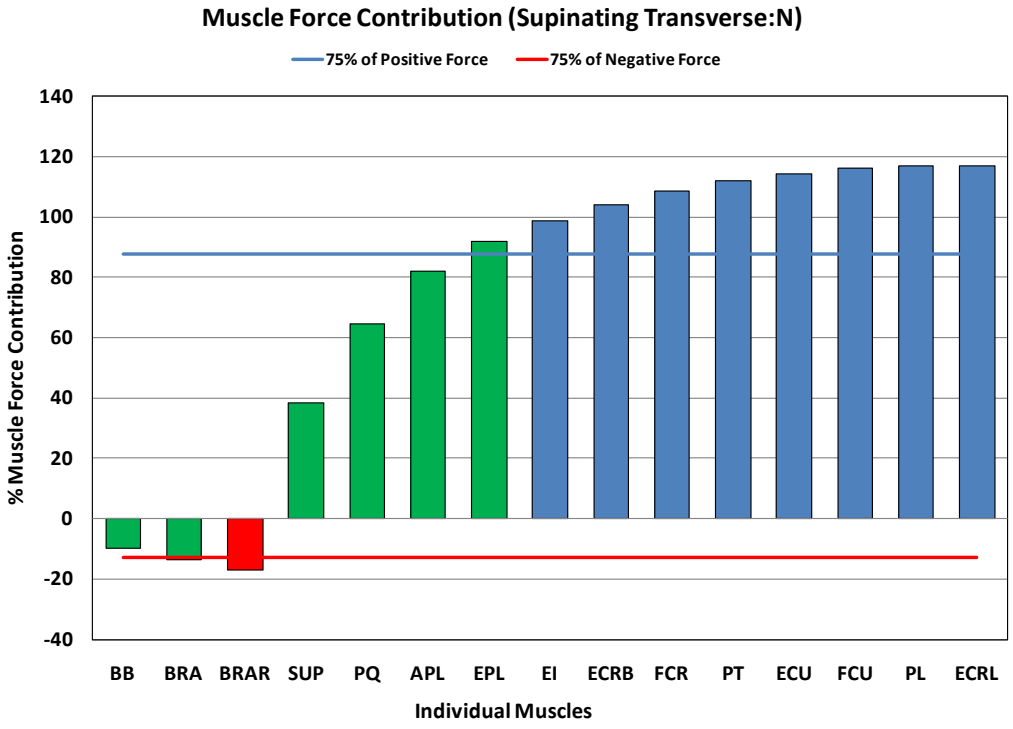

Figure E.32. Transverse Force Contributions during Supination at Neutral

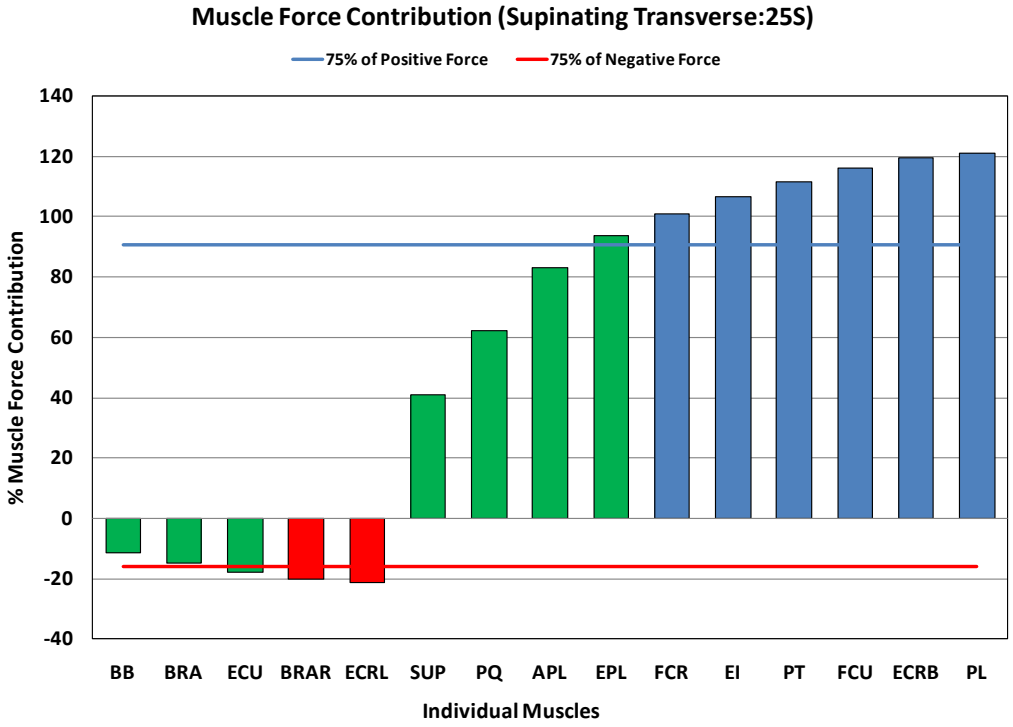

Figure E.33. Transverse Force Contributions during Supination at 25S

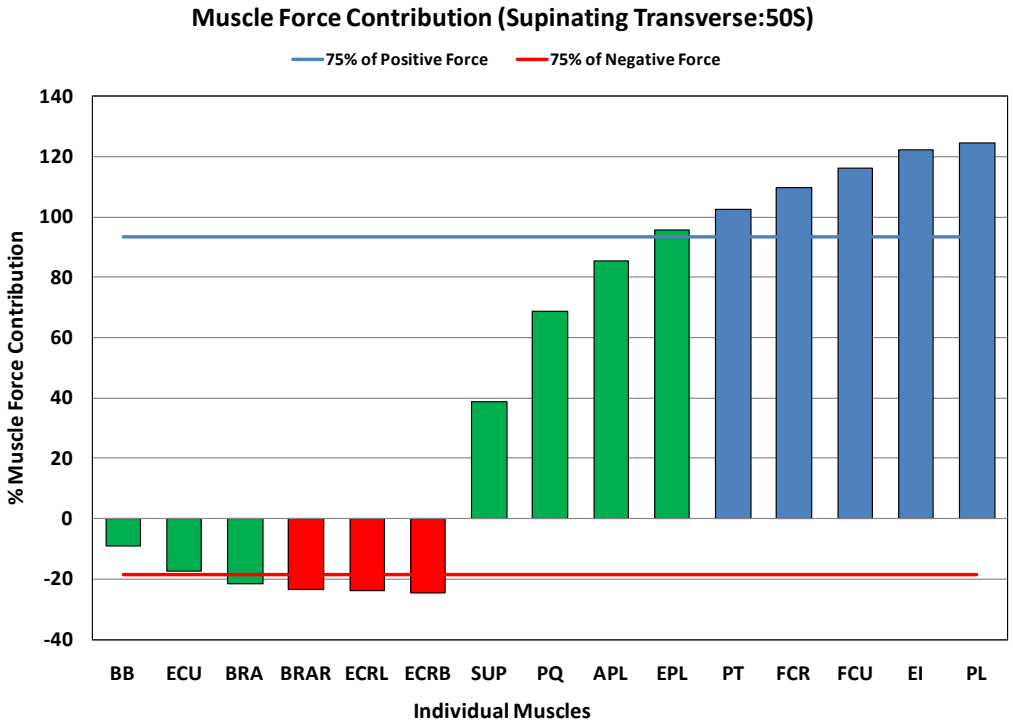

Figure E.34. Transverse Force Contributions during Supination at 50S

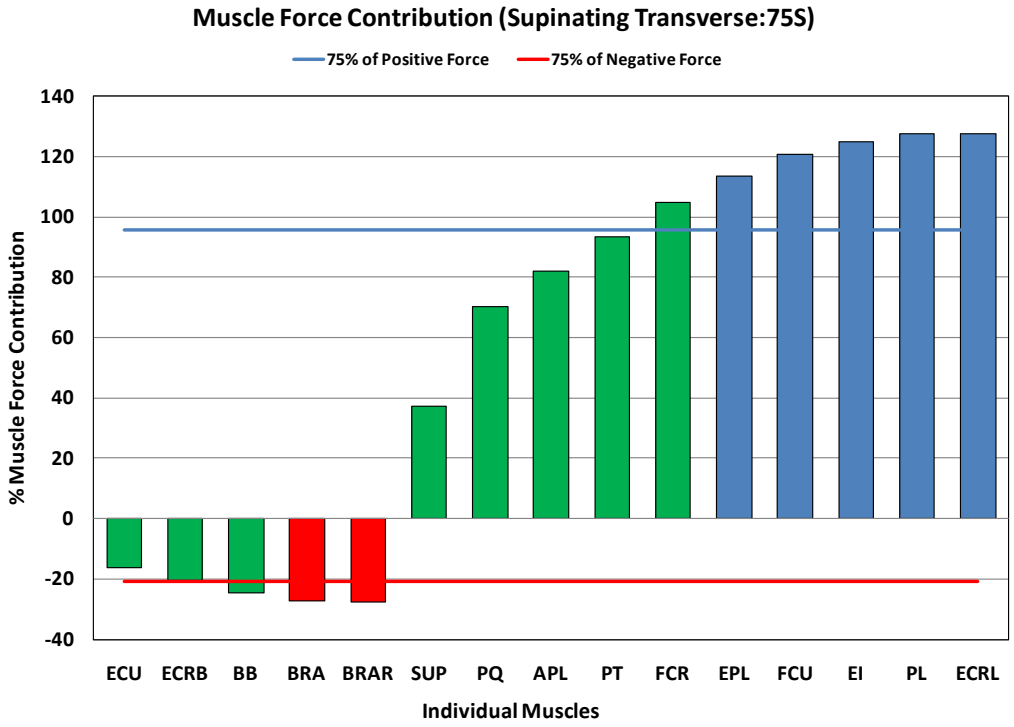

Figure E.35. Transverse Force Contributions during Supination at 75S

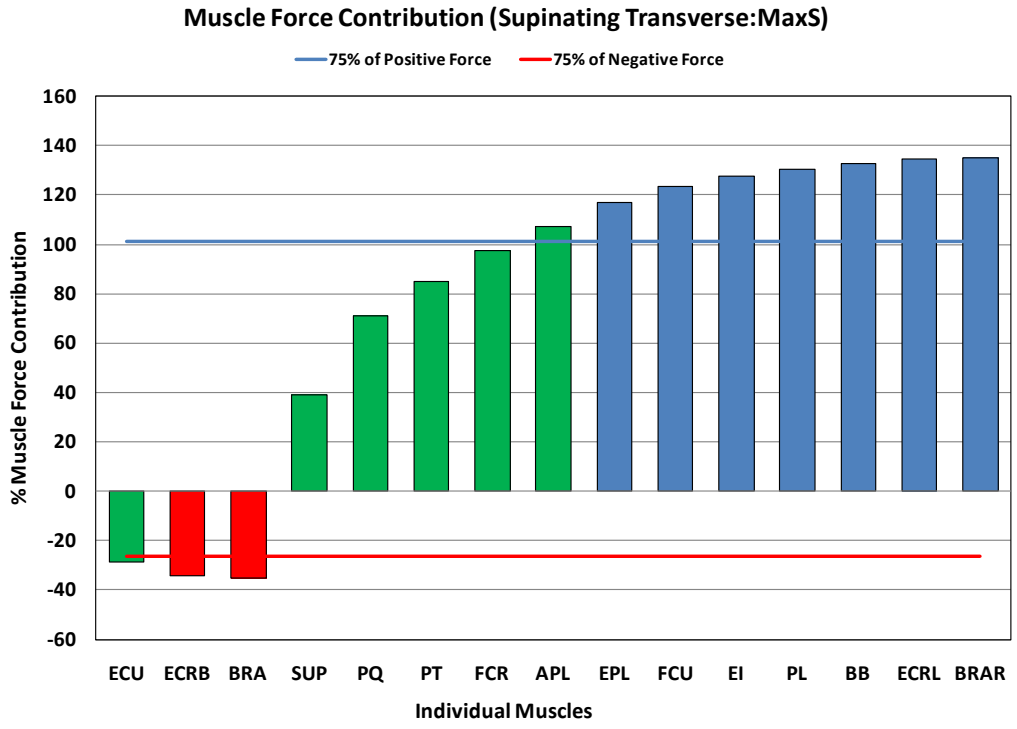

Figure E.36. Transverse Force Contributions during Supination at MaxS

REFERENCES

1. Adams BD**.** Effects of radial deformity on distal radioulnar joint mechanics. The Journal of hand surgery 1993;18(3):492-498.
2. Adams BD**.** Distal radioulnar joint instability. Instructional course lectures 1998;47:209-213.
3. af Ekenstam F, Hagert CG**.** Anatomical studies on the geometry and stability of the distal radio ulnar joint. Scandinavian journal of plastic and reconstructive surgery 1985;19(1):17-25.
4. af Ekenstam F, Hagert CG**.** The distal radio ulnar joint. The influence of geometry and ligament on simulated Colles' fracture. An experimental study. Scandinavian journal of plastic and reconstructive surgery 1985;19(1):27-31.
5. af Ekenstam FW, Palmer AK, Glisson RR**.** The load on the radius and ulna in different positions of the wrist and forearm. A cadaver study. Acta orthopaedica Scandinavica 1984;55(3):363-365.
6. Alffram PA, Bauer GC**.** Epidemiology of fractures of the forearm. A biomechanical investigation of bone strength. The Journal of bone and joint surgery. American volume 1962;44-A:105-114.
7. Amis AA, Dowson D, Wright V**.** Muscle strengths and musculo-skeletal geometry of the upper limb. Eng in Med 1979;8:41-48.
8. Amis AA, Dowson D, Wright V, Miller JH**.** The derivation of elbow joint forces, and their relation to prosthesis design. J Med Eng Technol 1979;3(5):229-234.
9. An KN, Hui FC, Morrey BF, Linscheid RL, Chao EY**.** Muscles across the elbow joint: a biomechanical analysis. J Biomech 1981;14(10):659-669.
10. Anderson DD, Daniel TE**.** A contact-coupled finite element analysis of the radiocarpal joint. Seminars in arthroplasty 1995;6(1):30-36.
11. Anderson DD, Deshpande BR, Daniel TE, Baratz ME**.** A three-dimensional finite element model of the radiocarpal joint: distal radius fracture step-off and stress transfer. The Iowa orthopaedic journal 2005;25:108-117.

12. Bacorn RW, Kurtzke JF. Colles' fracture; a study of two thousand cases from the New York State Workmen's Compensation Board. The Journal of bone and joint surgery. American volume 1953;35-A(3):643-658.
13. Bade H, Koebke J, Schluter M. Morphology of the articular surfaces of the distal radio-ulnar joint. The Anatomical record 1996;246(3):410-414.
14. Bain GI, Pugh DM, MacDermid JC, Roth JH. Matched hemiresection interposition arthroplasty of the distal radioulnar joint. The Journal of hand surgery 1995;20(6):944-950.
15. Basmajian JV, De Luca CJ. Muscles alive : their functions revealed by electromyography. 5th ed. Baltimore: Williams & Wilkins; 1985.
16. Basmajian JV, Latif A. Integrated actions and functions of the chief flexors of the elbow: a detailed electromyographic analysis. J Bone Joint Surg Am 1957;39-A(5):1106-1118.
17. Basmajian JV, Travill A. Electromyography of the pronator muscles in the forearm. Anat Rec 1961;139:45-49.
18. Bechtel R, Caldwell G.E. The influence of task and angle on torque production and muscle activity at the elbow. Journal of Electromyography and Kinesiology 1994:195-204.
19. Bell MJ, Hill RJ, McMurtry RY. Ulnar impingement syndrome. The Journal of bone and joint surgery. British volume 1985;67(1):126-129.
20. Bettinger PC, Smutz WP, Linscheid RL, Cooney WP, 3rd, An KN. Material properties of the trapezial and trapeziometacarpal ligaments. The Journal of hand surgery 2000;25(6):1085-1095.
21. Bieber EJ, Linscheid RL, Dobyns JH, Beckenbaugh RD. Failed distal ulna resections. The Journal of hand surgery 1988;13(2):193-200.
22. Bigland-Ritchie B, Johansson R, Lippold OC, Woods JJ. Contractile speed and EMG changes during fatigue of sustained maximal voluntary contractions. J Neurophysiol 1983;50(1):313-324.

23. Birkbeck DP, Failla JM, Hoshaw SJ, Fyhrie DP, Schaffler M. The interosseous membrane affects load distribution in the forearm. The Journal of hand surgery 1997;22(6):975-980.
24. Boland MR, Spigelman T, Uhl TL. The function of brachioradialis. J Hand Surg Am 2008;33(10):1853-1859.
25. Bowers WH. Distal radioulnar joint arthroplasty: the hemiresection-interposition technique. The Journal of hand surgery 1985;10(2):169-178.
26. Bowers WH. Instability of the distal radioulnar articulation. Hand clinics 1991;7(2):311-327.
27. Brand PW, Beach RB, Thompson DE. Relative tension and potential excursion of muscles in the forearm and hand. The Journal of hand surgery 1981;6(3):209-219.
28. Brand PW, Hollister A. Clinical mechanics of the hand. 2nd ed. St. Louis: Mosby Year Book; 1993.
29. Brandsma JW, van Oudenaarde E, Oostendorp R. The abductores pollicis muscles. Clinical considerations based on electromyographical and anatomical studies. J Hand Ther 1996;9(3):218-222.
30. Bronstein AJ, Trumble TE, Tencer AF. The effects of distal radius fracture malalignment on forearm rotation: a cadaveric study. J Hand Surg Am 1997;22(2):258-262.
31. Buchanan TS, Rovai GP, Rymer WZ. Strategies for muscle activation during isometric torque generation at the human elbow. J Neurophysiol 1989;62(6):1201-1212.
32. Buck-Gramcko D. On the priorities of publication of some operative procedures on the distal end of the ulna. Journal of hand surgery 1990;15(4):416-420.
33. Caldwell GE. Muscle Modeling. In: Robertson D, Caldwell GE, Hamill J, Kamen G, Whittlesey S, eds. Research Methods in Biomechanics. Champaign, IL: Human Kinetics; 2004.

34. Caldwell GE, Chapman A. The general distribution problem: a physiological solution which includes antagonism. Hum Movement Sci 1991;10:355-392.
35. Caldwell GE, Jamison JC, Lee S. Amplitude and frequency measures of surface electromyography during dual task elbow torque production. Eur J Appl Physiol Occup Physiol 1993;66(4):349-356.
36. Caldwell GE, Van Leemputte M. Elbow torques and EMG patterns of flexor muscles during different isometric tasks. Electromyogr Clin Neurophysiol 1991;31(7):433-445.
37. Carrigan SD, Whiteside RA, Pichora DR, Small CF. Development of a three-dimensional finite element model for carpal load transmission in a static neutral posture. Annals of biomedical engineering 2003;31(6):718-725.
38. Carson RG, Riek S, Smethurst CJ, Parraga JF, Byblow WD. Neuromuscular-skeletal constraints upon the dynamics of unimanual and bimanual coordination. Exp Brain Res 2000;131(2):196-214.
39. Chidgey LK. The Distal Radioulnar Joint: Problems and Solutions. The Journal of the American Academy of Orthopaedic Surgeons 1995;3(2):95-109.
40. Cnockaert JC, Lensel G, Pertuzon E. Relative contribution of individual muscles to the isometric contraction of a muscular group. J Biomech 1975;8(3-4):191-197.
41. Colles A. On the fracture of the carpal extremity of the radius. Edinb Med Surg J. 1814;10:181. Clinical orthopaedics and related research 2006;445:5-7.
42. Cooney WP, 3rd, An KN, Daube JR, Askew LJ. Electromyographic analysis of the thumb: a study of isometric forces in pinch and grasp. J Hand Surg Am 1985;10(2):202-210.
43. Cooney WP, 3rd, Dobyns JH, Linscheid RL. Complications of Colles' fractures. The Journal of bone and joint surgery. American volume 1980;62(4):613-619.
44. Cutts A, Seedhom BB. Validity of cadaveric data for muscles physiological cross-sectional area ratios: a comparative study of cadaveric and in-vivo dta in human thigh muscles. Clin Biomech (Bristol, Avon) 1993;8:156-162.

45. Darcus HD. The maximum torques developed in pronation and supination of the right hand. J Anat 1951;85(1):55-67.
46. Darcus HD, Salter N. The amplitude of pronation and supination with the elbow flexed to a right angle. Journal of anatomy 1953;87(2):169-184.
47. Darrach W. Partial excision of lower shaft of ulna for deformity following Colles's fracture. 1913. Clinical orthopaedics and related research 1992(275):3-4.
48. De Luca CJ. The use of surface electromyography in biomechanics. Journal of Applied Biomechanics 1997;13:135-163.
49. de SO, de MJ, Vieira FL. Electromyographic study of the brachioradialis muscle. Anat Rec 1961;139:125-131.
50. Dell PC. Distal radioulnar joint dysfunction. Hand clinics 1987;3(4):563-583.
51. DiTano O, Trumble TE, Tencer AF. Biomechanical function of the distal radioulnar and ulnocarpal wrist ligaments. The Journal of hand surgery 2003;28(4):622-627.
52. Doczi J, Renner A. Epidemiology of distal radius fractures in Budapest. A retrospective study of 2,241 cases in 1989. Acta orthopaedica Scandinavica 1994;65(4):432-433.
53. Drake RL, Vogl W, Mitchell AWM, Gray H. Gray's anatomy for students. 1st ed. Philadelphia, PA: Churchill Livingstone/Elsevier; 2005.
54. Drobner WS, Hausman MR. The distal radioulnar joint. Hand clinics 1992;8(4):631-644.
55. Epner RA, Bowers WH, Guilford WB. Ulnar variance--the effect of wrist positioning and roentgen filming technique. The Journal of hand surgery 1982;7(3):298-305.
56. Fan Z, Swadener JG, Rho JY, Roy ME, Pharr GM. Anisotropic properties of human tibial cortical bone as measured by nanoindentation. Journal of orthopaedic research : official publication of the Orthopaedic Research Society 2002;20(4):806-810.

57. Fernandez DL, Joneschild ES, Abella DM. Treatment of failed Sauve-Kapandji procedures with a spherical ulnar head prosthesis. Clinical orthopaedics and related research 2006;445:100-107.

58. Fujii H, Kobayashi S, Sato T, Shinozaki K, Naito A. Co-contraction of the pronator teres and extensor carpi radialis during wrist extension movements in humans. J Electromyogr Kinesiol 2007;17(1):80-89.

59. Funk DA, An KN, Morrey BF, Daube JR. Electromyographic analysis of muscles across the elbow joint. J Orthop Res 1987;5(4):529-538.

60. Gabl M, Zimmermann R, Angermann P, Sekora P, Maurer H, Steinlechner M, et al. The interosseous membrane and its influence on the distal radioulnar joint. An anatomical investigation of the distal tract. Journal of hand surgery 1998;23(2):179-182.

61. Gans C. Fiber architecture and muscle function. Exercise and sport sciences reviews 1982;10:160-207.

62. Garcia-Elias M. Failed ulnar head resection: prevention and treatment. Journal of hand surgery 2002;27(5):470-480.

63. Garcia-Elias M. Eclypse: partial ulnar head replacement for the isolated distal radio-ulnar joint arthrosis. Techniques in hand & upper extremity surgery 2007;11(1):121-128.

64. Garcia OS, de Carvalho CA. Electromyographic study of the muscles "abductor digiti minimi" and "flexor carpi ulnaris". Electromyogr Clin Neurophysiol 1972;12(4):367-377.

65. Garner BA, Pandy MG. Musculoskeletal model of the upper limb based on the visible human male dataset. Comput Methods Biomech Biomed Engin 2001;4(2):93-126.

66. Geissler WB, Fernandez DL, Lamey DM. Distal radioulnar joint injuries associated with fractures of the distal radius. Clinical orthopaedics and related research 1996(327):135-146.

67. George MS, Kiefhaber TR, Stern PJ**.** The Sauve-Kapandji procedure and the Darrach procedure for distal radio-ulnar joint dysfunction after Colles' fracture. Journal of hand surgery 2004;29(6):608-613.

68. Gielen CC, van Zuylen EJ**.** Coordination of arm muscles during flexion and supination: application of the tensor analysis approach. Neuroscience 1986;17(3):527-539.

69. Gíslason MK, Fowler NK, Nash DH**.** The three dimensional load transfer characteristics of the wrist during maximal gripping. Proceedings of the XXth congress of the international society for biomechanics & 29th meeting of the American society of Biomechanics. Cleveland, OH; 2005:318.

70. Glowacki KA**.** Hemiresection arthroplasty of the distal radioulnar joint. Hand clinics 2005;21(4):591-601.

71. Gofton WT, Gordon KD, Dunning CE, Johnson JA, King GJ**.** Soft-tissue stabilizers of the distal radioulnar joint: an in vitro kinematic study. The Journal of hand surgery 2004;29(3):423-431.

72. Gofton WT, Gordon KD, Dunning CE, Johnson JA, King GJ**.** Comparison of distal radioulnar joint reconstructions using an active joint motion simulator. J Hand Surg Am 2005;30(4):733-742.

73. Goldberg HD, Young JW, Reiner BI, Resnik CS, Gillespie TE**.** Double injuries of the forearm: a common occurrence. Radiology 1992;185(1):223-227.

74. Goldfarb CA, Stern PJ**.** Rheumatoid arthritis-skeletal reconstruction. In: Trumble TE, ed. Handsurgery Update 3. Rosemont (Il): American Society for Surgery of the Hand; 2002:525-533.

75. Gonzalez del Pino J, Fernandez DL**.** Salvage procedure for failed Bowers' hemiresection interposition technique in the distal radioulnar joint. Journal of hand surgery 1998;23(6):749-753.

76. Gordon KD, Dunning CE, Johnson JA, King GJ**.** Kinematics of ulnar head arthroplasty. Journal of hand surgery 2003;28(6):551-558.

77. Gordon KD, Kedgley AE, Ferreira LM, King GJ, Johnson JA**.** Design and implementation of an instrumented ulnar head prosthesis to measure loads in vitro. Journal of biomechanics 2006;39(7):1335-1341.

78. Gordon KD, Kedgley AE, Ferreira LM, King GJ, Johnson JA**.** Design and implementation of an instrumented ulnar head prosthesis to measure loads in vitro. J Biomech 2006;39(7):1335-1341.

79. Gordon KD, Kedgley AE, Ferreira LM, King GJ, Johnson JA**.** Effect of simulated muscle activity on distal radioulnar joint loading in vitro. Journal of orthopaedic research : official publication of the Orthopaedic Research Society 2006;24(7):1395-1404.

80. Gordon KD, Pardo RD, Johnson JA, King GJ, Miller TA**.** Electromyographic activity and strength during maximum isometric pronation and supination efforts in healthy adults. J Orthop Res 2004;22(1):208-213.

81. Gupta R, Allaire RB, Fornalski S, Osterman AL, Lee TQ**.** Kinematic analysis of the distal radioulnar joint after a simulated progressive ulnar-sided wrist injury. The Journal of hand surgery 2002;27(5):854-862.

82. Hagert CG**.** The distal radioulnar joint. Hand clinics 1987;3(1):41-50.

83. Harrison JW, Siddique I, Powell ES, Shaaban H, Stanley JK**.** Does the orientation of the distal radioulnar joint influence the force in the joint and the tension in the interosseous membrane? Clinical biomechanics 2005;20(1):57-62.

84. Hasan Z, Enoka RM**.** Isometric torque-angle relationship and movement-related activity of human elbow flexors: implications for the equilibrium-point hypothesis. Exp Brain Res 1985;59(3):441-450.

85. Haugstvedt JR, Berger RA, Berglund LJ**.** A mechanical study of the moment-forces of the supinators and pronators of the forearm. Acta Orthop Scand 2001;72(6):629-634.

86. Haugstvedt JR, Berger RA, Berglund LJ, Neale PG, Sabick MB**.** An analysis of the constraint properties of the distal radioulnar ligament attachments to the ulna. The Journal of hand surgery 2002;27(1):61-67.

87. Haugstvedt JR, Berglund LJ, Neale PG, Berger RA**.** A dynamic simulator to evaluate distal radio-ulnar joint kinematics. J Biomech 2001;34(3):335-339.

88. Hebert LJ, De Serres SJ, Arsenault AB**.** Cocontraction of the elbow muscles during combined tasks of pronation-flexion and supination-flexion. Electromyogr Clin Neurophysiol 1991;31(8):483-488.

89. Herbert TJ, Van Schoonhoven J**.** Ulnar head prostheses: a new soluton for problems at the distal radioulnar joint. In: Simmen BR, Allieu Y, Lluch A, Stanley J, eds. Hand Arthroplasties. London: Martin Dunitz; 2000:145-149.

90. Herbert TJ, van Schoonhoven J**.** Ulnar head replacement. Techniques in hand & upper extremity surgery 2007;11(1):98-108.

91. Holzbaur KR, Murray WM, Delp SL**.** A model of the upper extremity for simulating musculoskeletal surgery and analyzing neuromuscular control. Ann Biomed Eng 2005;33(6):829-840.

92. Hotchkiss RN, An KN, Sowa DT, Basta S, Weiland AJ**.** An anatomic and mechanical study of the interosseous membrane of the forearm: pathomechanics of proximal migration of the radius. The Journal of hand surgery 1989;14(2 Pt 1):256-261.

93. Hughston JC**.** Fracture of the distal radial shaft; mistakes in management. The Journal of bone and joint surgery. American volume 1957;39-A(2):249-264; passim.

94. Hui FC, Linscheid RL**.** Ulnotriquetral augmentation tenodesis: a reconstructive procedure for dorsal subluxation of the distal radioulnar joint. The Journal of hand surgery 1982;7(3):230-236.

95. Ishii S, Palmer AK, Werner FW, Short WH, Fortino MD**.** Pressure distribution in the distal radioulnar joint. J Hand Surg Am 1998;23(5):909-913.

96. Jacobson MD, Raab R, Fazeli BM, Abrams RA, Botte MJ, Lieber RL**.** Architectural design of the human intrinsic hand muscles. The Journal of hand surgery 1992;17(5):804-809.

97. Jaffe R, Chidgey LK, LaStayo PC**.** The distal radioulnar joint: anatomy and management of disorders. Journal of hand therapy : official journal of the American Society of Hand Therapists 1996;9(2):129-138.

98. Jamison JC, Caldwell GE**.** Muscle synergies and isometric torque production: influence of supination and pronation level on elbow flexion. J Neurophysiol 1993;70(3):947-960.

99. Johnson JA, Rath DA, Dunning CE, Roth SE, King GJ**.** Simulation of elbow and forearm motion in vitro using a load controlled testing apparatus. Journal of biomechanics 2000;33(5):635-639.

100. Johnson RK, Shrewsbury MM**.** The pronator quadratus in motions and in stabilization of the radius and ulna at the distal radioulnar joint. The Journal of hand surgery 1976;1(3):205-209.

101. Kamen G**.** Electromyographic Kinesiology. In: Robertson D, Caldwell GE, Hamill J, Kamen G, Whittlesey S, eds. Research Methods in Biomechanics. Champaign, IL: Human Kinetics; 2004.

102. Kapandji IA**.** The Kapandji-Sauve operation. Its techniques and indications in non rheumatoid diseases. Annales de chirurgie de la main : organe officiel des societes de chirurgie de la main 1986;5(3):181-193.

103. Kauer JM**.** Functional anatomy of the wrist. Clin Orthop Relat Res 1980(149):9-20.

104. Kauer JM**.** The distal radioulnar joint. Anatomic and functional considerations. Clinical orthopaedics and related research 1992(275):37-45.

105. Kelly BT, Cooper LW, Kirkendall DT, Speer KP**.** Technical considerations for electromyographic research on the shoulder. Clin Orthop Relat Res 1997(335):140-151.

106. Kendall FP**.** Muscles : testing and function with posture and pain. 5th ed. Baltimore, MD: Lippincott Williams & Wilkins; 2005.

107. Kihara H, Palmer AK, Werner FW, Short WH, Fortino MD**.** The effect of dorsally angulated distal radius fractures on distal radioulnar joint congruency and forearm rotation. The Journal of hand surgery 1996;21(1):40-47.

108. Kihara H, Short WH, Werner FW, Fortino MD, Palmer AK**.** The stabilizing mechanism of the distal radioulnar joint during pronation and supination. The Journal of hand surgery 1995;20(6):930-936.

109. Kilgore ML, Morrisey MA, Becker DJ, Gary LC, Curtis JR, Saag KG, et al. Health care expenditures associated with skeletal fractures among Medicare beneficiaries, 1999-2005. Journal of bone and mineral research : the official journal of the American Society for Bone and Mineral Research 2009;24(12):2050-2055.

110. King GJ, McMurtry RY, Rubenstein JD, Gertzbein SD**.** Kinematics of the distal radioulnar joint. The Journal of hand surgery 1986;11(6):798-804.

111. Kleinman WB**.** Stability of the distal radioulna joint: biomechanics, pathophysiology, physical diagnosis, and restoration of function what we have learned in 25 years. J Hand Surg Am 2007;32(7):1086-1106.

112. Kleinman WB, Graham TJ**.** Distal ulnar injury and dysfunction. Surgery of the Hand and Upper Extremity. New York: McGraw-Hill; 1996:667-709.

113. Kleinman WB, Graham TJ**.** The distal radioulnar joint capsule: clinical anatomy and role in posttraumatic limitation of forearm rotation. The Journal of hand surgery 1998;23(4):588-599.

114. Kopylov P, Tagil M**.** Distal radioulnar joint replacement. Techniques in hand & upper extremity surgery 2007;11(1):109-114.

115. Langenderfer J, Jerabek SA, Thangamani VB, Kuhn JE, Hughes RE**.** Musculoskeletal parameters of muscles crossing the shoulder and elbow and the effect of sarcomere length sample size on estimation of optimal muscle length. Clinical biomechanics 2004;19(7):664-670.

116. Langenderfer J, LaScalza S, Mell A, Carpenter JE, Kuhn JE, Hughes RE. An EMG-driven model of the upper extremity and estimation of long head biceps force. Comput Biol Med 2005;35(1):25-39.

117. Laurentin-Perez LA, Goodwin AN, Babb BA, Scheker LR. A study of functional outcomes following implantation of a total distal radioulnar joint prosthesis. The Journal of hand surgery, European volume 2008;33(1):18-28.

118. Laursen B, Jensen BR, Nemeth G, Sjogaard G. A model predicting individual shoulder muscle forces based on relationship between electromyographic and 3D external forces in static position. Journal of biomechanics 1998;31(8):731-739.

119. Leak RS, Rayan GM, Arthur RE. Longitudinal radiographic analysis of rheumatoid arthritis in the hand and wrist. The Journal of hand surgery 2003;28(3):427-434.

120. Lee SK, Hausman MR. Management of the distal radioulnar joint in rheumatoid arthritis. Hand clinics 2005;21(4):577-589.

121. Lemmen MH, Schreuders TA, Stam HJ, Hovius SE. Evaluation of restoration of extensor pollicis function by transfer of the extensor indicis. J Hand Surg Br 1999;24(1):46-49.

122. Lewiecki EM. Management of osteoporosis. Clinical and molecular allergy : CMA 2004;2(1):9.

123. Lidstrom A. Fractures of the distal end of the radius. A clinical and statistical study of end results. Acta orthopaedica Scandinavica. Supplementum 1959;41:1-118.

124. Lieber RL, Fazeli BM, Botte MJ. Architecture of selected wrist flexor and extensor muscles. The Journal of hand surgery 1990;15(2):244-250.

125. Lieber RL, Jacobson MD, Fazeli BM, Abrams RA, Botte MJ. Architecture of selected muscles of the arm and forearm: anatomy and implications for tendon transfer. The Journal of hand surgery 1992;17(5):787-798.

126. Lindau T, Adlercreutz C, Aspenberg P. Peripheral tears of the triangular fibrocartilage complex cause distal radioulnar joint instability after distal radial fractures. The Journal of hand surgery 2000;25(3):464-468.
127. Magnussen PA, Harvey FJ, Tonkin MA. Extensor indicis proprius transfer for rupture of the extensor pollicis longus tendon. J Bone Joint Surg Br 1990;72(5):881-883.
128. Markolf KL, Dunbar AM, Hannani K. Mechanisms of load transfer in the cadaver forearm: role of the interosseous membrane. The Journal of hand surgery 2000;25(4):674-682.
129. Markolf KL, Lamey D, Yang S, Meals R, Hotchkiss R. Radioulnar load-sharing in the forearm. A study in cadavera. The Journal of bone and joint surgery. American volume 1998;80(6):879-888.
130. McGinley JC, Kozin SH. Interosseous membrane anatomy and functional mechanics. Clinical orthopaedics and related research 2001(383):108-122.
131. McMurtry RY, Paley D, Marks P, Axelrod T. A critical analysis of Swanson ulnar head replacement arthroplasty: rheumatoid versus nonrheumatoid. The Journal of hand surgery 1990;15(2):224-231.
132. Mikic ZD. Galeazzi fracture-dislocations. The Journal of bone and joint surgery. American volume 1975;57(8):1071-1080.
133. Minami A, Iwasaki N, Ishikawa J, Suenaga N, Yasuda K, Kato H. Treatments of osteoarthritis of the distal radioulnar joint: long-term results of three procedures. Hand surgery : an international journal devoted to hand and upper limb surgery and related research : journal of the Asia-Pacific Federation of Societies for Surgery of the Hand 2005;10(2-3):243-248.
134. Miyake T, Hashizume H, Inoue H, Shi Q, Nagayama N. Malunited Colles' fracture. Analysis of stress distribution. Journal of hand surgery 1994;19(6):737-742.
135. Moore JC. Differences in electrical activity of the biceps brachii and brachioradialis muscles performing isometriclike supination and pronation exercises. Am J Occup Ther 1971;25(8):391-397.

136. Moore TM, Lester DK, Sarmiento A. The stabilizing effect of soft-tissue constraints in artificial Galeazzi fractures. Clinical orthopaedics and related research 1985(194):189-194.

137. Mukhopadhyay P, O'Sullivan LW, Gallwey TJ. Upper limb discomfort profile due to intermittent isometric pronation torque at different postural combinations of the shoulder-arm system. Ergonomics 2009;52(5):584-600.

138. Murdoch AH, Mathias KJ, Shepherd DE. Investigation into the material properties of beech wood and cortical bone. Bio-medical materials and engineering 2004;14(1):1-4.

139. Murray WM, Buchanan TS, Delp SL. The isometric functional capacity of muscles that cross the elbow. Journal of biomechanics 2000;33(8):943-952.

140. Naito A, Sun YJ, Yajima M, Fukamachi H, Ushikoshi K. Electromyographic study of the elbow flexors and extensors in a motion of forearm pronation/supination while maintaining elbow flexion in humans. Tohoku J Exp Med 1998;186(4):267-277.

141. Naito A, Yajima M, Fukamachi H, Ushikoshi K, Sun YJ, Shimizu Y. Electromyographic (EMG) study of the elbow flexors during supination and pronation of the forearm. Tohoku J Exp Med 1995;175(4):285-288.

142. Nakamura T, Yabe Y, Horiuchi Y, Yamazaki N. In vivo motion analysis of forearm rotation utilizing magnetic resonance imaging. Clinical biomechanics 1999;14(5):315-320.

143. Nathan RH. The isometric action of the forearm muscles. J Biomech Eng 1992;114(2):162-169.

144. Nishiwaki M, Nakamura T, Nagura T, Toyama Y, Ikegami H. Ulnar-shortening effect on distal radioulnar joint pressure: a biomechanical study. The Journal of hand surgery 2008;33(2):198-205.

145. Nishiwaki M, Nakamura T, Nakao Y, Nagura T, Toyama Y. Ulnar shortening effect on distal radioulnar joint stability: a biomechanical study. The Journal of hand surgery 2005;30(4):719-726.

146. O'Donovan TM, Ruby LK. The distal radioulnar joint in rheumatoid arthritis. Hand clinics 1989;5(2):249-256.

147. O'Sullivan LW, Gallwey TJ. Upper-limb surface electro-myography at maximum supination and pronation torques: the effect of elbow and forearm angle. J Electromyogr Kinesiol 2002;12(4):275-285.

148. O'Sullivan LW, Gallwey TJ. Forearm torque strengths and discomfort profiles in pronation and supination. Ergonomics 2005;48(6):703-721.

149. Oda M, Hashizume H, Miyake T, Inoue H, Nagayama N. A stress distribution analysis of a ceramic lunate replacement for Kienbock's disease. Journal of hand surgery 2000;25(5):492-498.

150. Ozer K, Scheker LR. Distal radioulnar joint problems and treatment options. Orthopedics 2006;29(1):38-49; quiz 50-31.

151. Palmer AK. The distal radioulnar joint. The Orthopedic clinics of North America 1984;15(2):321-335.

152. Palmer AK, Glisson RR, Werner FW. Ulnar variance determination. The Journal of hand surgery 1982;7(4):376-379.

153. Palmer AK, Werner FW. The triangular fibrocartilage complex of the wrist--anatomy and function. The Journal of hand surgery 1981;6(2):153-162.

154. Palmer AK, Werner FW. Biomechanics of the distal radioulnar joint. Clinical orthopaedics and related research 1984(187):26-35.

155. Perotto A, Delagi EF. Anatomical guide for the electromyographer : the limbs and trunk. 3rd ed. Springfield, Ill., USA: Charles C. Thomas; 1994.

156. Pfaeffle HJ, Fischer KJ, Manson TT, Tomaino MM, Herndon JH, Woo SL. A new methodology to measure load transfer through the forearm using multiple universal force sensors. Journal of biomechanics 1999;32(12):1331-1335.

157. Pfaeffle HJ, Fischer KJ, Manson TT, Tomaino MM, Woo SL, Herndon JH. Role of the forearm interosseous ligament: is it more than just longitudinal load transfer? The Journal of hand surgery 2000;25(4):683-688.

158. Pfaeffle HJ, Tomaino MM, Grewal R, Xu J, Boardman ND, Woo SL, et al. Tensile properties of the interosseous membrane of the human forearm. Journal of orthopaedic research : official publication of the Orthopaedic Research Society 1996;14(5):842-845.

159. Poitevin LA**.** Anatomy and biomechanics of the interosseous membrane: its importance in the longitudinal stability of the forearm. Hand clinics 2001;17(1):97-110, vii.

160. Powell PL, Roy RR, Kanim P, Bello MA, Edgerton VR**.** Predictability of skeletal muscle tension from architectural determinations in guinea pig hindlimbs. Journal of applied physiology: respiratory, environmental and exercise physiology 1984;57(6):1715-1721.

161. Rahimtoola ZO, Hubach P**.** Total modular wrist prosthesis: a new design. Scandinavian journal of plastic and reconstructive surgery and hand surgery / Nordisk plastikkirurgisk forening [and] Nordisk klubb for handkirurgi 2004;38(3):160-165.

162. Reckling FW, Peltier LF**.** Riccardo Galeazzi and Galeazzi's Fracture. Surgery 1965;58:453-459.

163. Rodriguez Merchan EC, de la Corte H**.** Injuries of the distal radioulnar joint. Contemporary orthopaedics 1994;29(3):193-200.

164. Ruby LK, Ferenz CC, Dell PC**.** The pronator quadratus interposition transfer: an adjunct to resection arthroplasty of the distal radioulnar joint. The Journal of hand surgery 1996;21(1):60-65.

165. Sanders RA, Frederick HA, Hontas RB**.** The Sauve-Kapandji procedure: a salvage operation for the distal radioulnar joint. The Journal of hand surgery 1991;16(6):1125-1129.

166. Sauerbier M, Fujita M, Hahn ME, Neale PG, An KN, Berger RA**.** [Radioulnar impingement after distal ulnar resection and ulnar head hemiresection interposition arthroplasty (Bowers procedure). An experimental biomechanical study]. Handchirurgie, Mikrochirurgie, plastische Chirurgie : Organ der

Deutschsprachigen Arbeitsgemeinschaft fur Handchirurgie : Organ der Deutschsprachigen Arbeitsgemeinschaft fur Mikrochirurgie der Peripheren Nerven und Gefasse : Organ der Vereinigung der Deutschen Plastischen Chirurgen 2003;35(3):138-146.

167. Sauerbier M, Fujita M, Hahn ME, Neale PG, Berger RA**.** The dynamic radioulnar convergence of the Darrach procedure and the ulnar head hemiresection interposition arthroplasty: a biomechanical study. Journal of hand surgery 2002;27(4):307-316.

168. Sauve L, Kapandji M**.** Nouvelle technique de traitement chirurgical des luxations recidivantes isolees de l'extremite inferieure de cubitus. Journal de Chirurgue 1936;47:589-594.

169. Savelberg HH, Kooloos JG, Huiskes R, Kauer JM**.** Stiffness of the ligaments of the human wrist joint. Journal of biomechanics 1992;25(4):369-376.

170. Scheker LR**.** Distal radioulnar joint prostheses to rescue the so-called salvage procedures. In: Simmen BR, Allieu Y, Lluch A, eds. Hand Arthroplasties. London: Martin Dunitz Ltd; 2000:151-158.

171. Scheker LR**.** Implant arthroplasty for the distal radioulnar joint. The Journal of hand surgery 2008;33(9):1639-1644.

172. Scheker LR, Babb BA, Killion PE**.** Distal ulnar prosthetic replacement. The Orthopedic clinics of North America 2001;32(2):365-376, x.

173. Scheker LR, Severo A**.** Ulnar shortening for the treatment of early post-traumatic osteoarthritis at the distal radioulnar joint. Journal of hand surgery 2001;26(1):41-44.

174. Schober F, van Schoonhoven J, Prommersberger KJ, Lanz U**.** [Bowers hemi-resection-interposition arthroplasty for treatment of post-traumatic arthrosis of the distal radio-ulnar joint after distal radius fractures]. Handchirurgie, Mikrochirurgie, plastische Chirurgie : Organ der Deutschsprachigen Arbeitsgemeinschaft fur Handchirurgie : Organ der Deutschsprachigen

Arbeitsgemeinschaft fur Mikrochirurgie der Peripheren Nerven und Gefasse : Organ der Vereinigung der Deutschen Plastischen Chirurgen 1999;31(6):378-382.

175. Schuind F, An KN, Berglund L, Rey R, Cooney WP, 3rd, Linscheid RL, et al. The distal radioulnar ligaments: a biomechanical study. The Journal of hand surgery 1991;16(6):1106-1114.

176. Schuurman AH, Teunis T**.** A new total distal radioulnar joint prosthesis: functional outcome. The Journal of hand surgery 2010;35(10):1614-1619.

177. Shaaban H, Giakas G, Bolton M, Williams R, Scheker LR, Lees VC**.** The distal radioulnar joint as a load-bearing mechanism--a biomechanical study. The Journal of hand surgery 2004;29(1):85-95.

178. Shaaban H, Giakas G, Bolton M, Williams R, Wicks P, Scheker LR, et al. The load-bearing characteristics of the forearm: pattern of axial and bending force transmitted through ulna and radius. Journal of hand surgery 2006;31(3):274-279.

179. Shipley NY, Dion GR, Bowers WH**.** Ulnar head implant arthroplasty: An intermediate term review of 1 surgeon's experience. Techniques in hand & upper extremity surgery 2009;13(3):160-164.

180. Stanley D, Herbert TJ**.** The Swanson ulnar head prosthesis for post-traumatic disorders of the distal radio-ulnar joint. Journal of hand surgery 1992;17(6):682-688.

181. Staudenmann D, Rudroff T, Enoka RM**.** Pronation-supination torque and associated electromyographic activity varies during a sustained elbow flexor contraction but does not influence the time to task failure. Muscle & nerve 2009;40(2):231-239.

182. Steindler A**.** Postgraduate Lectures in Orthopedics, Diagnosis, and Indications. Sprinfield, ILL: Charles C Thomas; 1950.

183. Stuart PR, Berger RA, Linscheid RL, An KN**.** The dorsopalmar stability of the distal radioulnar joint. The Journal of hand surgery 2000;25(4):689-699.

184. Swanson AB. Implant arthroplasty for disabilities of the distal radioulnar joint. Use of a silicone rubber capping implant following resection of the ulnar head. The Orthopedic clinics of North America 1973;4(2):373-382.

185. Taleisnik J. The Wrist. New York: Churchill Livingstone; 1985.

186. Tang P, Failla JM, Contesti LA. The radioulnar joints and forearm axis: surgeons' perspective. Journal of hand therapy : official journal of the American Society of Hand Therapists 1999;12(2):75-84.

187. Taniguchi R, Nakamura R, Kasai T. Influence of arm positions on EMG-reaction time of the biceps brachii for elbow flexion and forearm supination. Percept Mot Skills 1984;59(1):191-194.

188. Taylor JL, Gandevia SC. A comparison of central aspects of fatigue in submaximal and maximal voluntary contractions. J Appl Physiol 2008;104(2):542-550.

189. Teoh LC, Yam AK. Anatomic reconstruction of the distal radioulnar ligaments: long-term results. Journal of hand surgery 2005;30(2):185-193.

190. Thompson JC, Netter FH. Netter's concise atlas of orthopaedic anatomy. 1st ed. Teterboro, NJ: Icon Learning Systems; 2002.

191. Tolat AR, Stanley JK, Trail IA. A cadaveric study of the anatomy and stability of the distal radioulnar joint in the coronal and transverse planes. Journal of hand surgery 1996;21(5):587-594.

192. Trumble T, Glisson RR, Seaber AV, Urbaniak JR. Forearm force transmission after surgical treatment of distal radioulnar joint disorders. The Journal of hand surgery 1987;12(2):196-202.

193. Ulrich D, van Rietbergen B, Laib A, Ruegsegger P. Load transfer analysis of the distal radius from in-vivo high-resolution CT-imaging. Journal of biomechanics 1999;32(8):821-828.

194. Van der Heijden EP, Hillen B. A two-dimensional kinematic analysis of the distal radioulnar joint. J Hand Surg Br 1996;21(6):824-829.

195. van Hoecke J, Perot C, Goubel F. [Contribution of the biceps brachii and pronator teres muscles to the efforts of pronation or supination. II. dynamic work (author's transl)]. Eur J Appl Physiol Occup Physiol 1978;38(2):93-100.

196. van Schoonhoven J, Fernandez DL, Bowers WH, Herbert TJ. Salvage of failed resection arthroplasties of the distal radioulnar joint using a new ulnar head prosthesis. The Journal of hand surgery 2000;25(3):438-446.

197. van Zuylen EJ, Gielen CC, Denier van der Gon JJ. Coordination and inhomogeneous activation of human arm muscles during isometric torques. J Neurophysiol 1988;60(5):1523-1548.

198. Veeger HE, Yu B, An KN, Rozendal RH. Parameters for modeling the upper extremity. Journal of biomechanics 1997;30(6):647-652.

199. Vesely DG. The distal radio-ulnar joint. Clinical orthopaedics and related research 1967;51:75-91.

200. Viegas SF, Patterson RM, Werner FW. Joint contact area and pressure. In: an KN, Berger RA, Cooney WP, eds. Biomechanics of the wrist joint. New York: Springer-Verlag; 1991:99-126.

201. Viegas SF, Pogue DJ, Patterson RM, Peterson PD. Effects of radioulnar instability on the radiocarpal joint: a biomechanical study. The Journal of hand surgery 1990;15(5):728-732.

202. Waizenegger M, Schranz P, Barton NJ. The Kapandji procedure for post-traumatic problems. Injury 1993;24(10):662-666.

203. Walker SM, Schrodt GR. I segment lengths and thin filament periods in skeletal muscle fibers of the Rhesus monkey and the human. The Anatomical record 1974;178(1):63-81.

204. Wallace AL, Walsh WR, van Rooijen M, Hughes JS, Sonnabend DH. The interosseous membrane in radio-ulnar dissociation. The Journal of bone and joint surgery. British volume 1997;79(3):422-427.

205. Ward LD, Ambrose CG, Masson MV, Levaro F**.** The role of the distal radioulnar ligaments, interosseous membrane, and joint capsule in distal radioulnar joint stability. The Journal of hand surgery 2000;25(2):341-351.

206. Watanabe H, Berger RA, An KN, Berglund LJ, Zobitz ME**.** Stability of the distal radioulnar joint contributed by the joint capsule. The Journal of hand surgery 2004;29(6):1114-1120.

207. Watanabe H, Berger RA, Berglund LJ, Zobitz ME, An KN**.** Contribution of the interosseous membrane to distal radioulnar joint constraint. The Journal of hand surgery 2005;30(6):1164-1171.

208. Watson HK, Gabuzda GM**.** Matched distal ulna resection for posttraumatic disorders of the distal radioulnar joint. The Journal of hand surgery 1992;17(4):724-730.

209. Watson HK, Ryu JY, Burgess RC**.** Matched distal ulnar resection. The Journal of hand surgery 1986;11(6):812-817.

210. Werner FW, An KN**.** Biomechanics of the elbow and forearm. Hand Clin 1994;10(3):357-373.

211. Werner FW, Glisson RR, Murphy DJ, Palmer AK**.** Force transmission through the distal radioulnar carpal joint: effect of ulnar lengthening and shortening. Handchirurgie, Mikrochirurgie, plastische Chirurgie : Organ der Deutschsprachigen Arbeitsgemeinschaft fur Handchirurgie : Organ der Deutschsprachigen Arbeitsgemeinschaft fur Mikrochirurgie der Peripheren Nerven und Gefasse : Organ der Vereinigung der Deutschen Plastischen Chirurgen 1986;18(5):304-308.

212. Werner FW, Murphy DJ, Palmer AK**.** Pressures in the distal radioulnar joint: effect of surgical procedures used for Kienbock's disease. Journal of orthopaedic research : official publication of the Orthopaedic Research Society 1989;7(3):445-450.

213. Werner FW, Palmer AK, Somerset JH, Tong JJ, Gillison DB, Fortino MD, et al. Wrist joint motion simulator. J Orthop Res 1996;14(4):639-646.

214. Willis AA, Berger RA, Cooney WP, 3rd**.** Arthroplasty of the distal radioulnar joint using a new ulnar head endoprosthesis: preliminary report. The Journal of hand surgery 2007;32(2):177-189.

215. Winters JM, Kleweno DG**.** Effect of initial upper-limb alignment on muscle contributions to isometric strength curves. J Biomech 1993;26(2):143-153.

216. Yamaguchi G, Sawa A, Moran D, Fessler M, Winters J**.** A survey of human musculotendon acutator parameters. In: Winters JM, Woo SL, eds. Multiple Muscle Systems: Biomechanics and Movement Organization. New York: Springer-Verlag; 1990:715-773.

217. Zajac FE**.** How musculotendon architecture and joint geometry affect the capacity of muscles to move and exert force on objects: a review with application to arm and forearm tendon transfer design. The Journal of hand surgery 1992;17(5):799-804.

VITA

Joseph Scott Bader

Born June 8, 1979, Baton Rouge, LA

EDUCATION

Master of Science, Mechanical Engineering, University of Tennessee, August 2005.
Thesis: Clinical Significance of Hip Separation in Metal on Polyethylene, Metal on Metal, and Ceramic on Ceramic Total Hip Arthroplasty Due to Resonant and Energy Dispersion Effects

Bachelor of Science, Biomedical Engineering, University of Tennessee, May 2003.

PROFESSIONAL POSITIONS

1998–2001 **Researcher**, National Institute for Occupational Safety and Health, Morgantown, WV
2003-2005 **Research Assistant**, Center for Musculoskeletal Research, University of Tennessee, Knoxville, TN
2005-2009 **Research Assistant**, Center for Biomedical Engineering, University of Kentucky, Lexington, KY
2010-2011 **Senior Research Engineer I**, Zimmer Orthopedics, Warsaw, IN

HONORS

Won award for best poster in the hand and wrist category at the 75th Annual Meeting of the American Academy of Orthopedic Surgeons 2008

PEER-REVIEWED PUBLICATIONS

- **Bader JS,** Boland MR, Nitz A, Stone J, Uhl T, Pienkowski D. Forearm Muscle Activity During Isometric Pronation-Supination. Manuscript submitted to the Journal of Hand Surgery. May, 2011
- **Bader JS,** Boland MR, Nitz A, Uhl T, Royalty R, Pienkowski D. Determination of Distal Radioulnar Joint Reaction Forces Using Cadaver and EMG Data. Manuscript in preparation for submission to the Journal of Hand Surgery. October, 2011.
- **Bader JS,** Boland MR, Nitz A, Stone J, Uhl T, Pienkowski D. The Influence of Fifteen Muscles on Distal Radial-Ulnar Joint Loading. Manuscript in preparation for submission to the Journal of Hand Surgery, November, 2011.

CONFERENCE PRESENTATIONS

- **Bader JS**, Boland MR, Uhl T, Nitz A, Pienkowski D. Determination of the Distal-Radio-Ulnar Joint Reaction Forces Using Cadaver and EMG Data. Podium presentation at the 57th Annual Meeting of the Orthopaedic Research Society. Long Beach, CA. January, 2011.
- Nitz AJ, **Bader JS**, Boland M, Stone L, Uhl T, Pienkowski D. EMG Analysis of 15 Forearm Muscles and Their Influence on Distal Radioulnar Joint Loading During Pronation and Supination: A Biomechanical Model. Podium presentation at the 21st Annual ENMG Symposium. Provo, UT. July, 2010.
- Boland MR and **Bader JS**. The Role of the Abductor Pollicis Longus During Forearm Rotation. Podium presentation at the 11th Triennial Congress of the International Federation for Surgery of the Hand. Seoul, South Korea. October/November, 2010.
- Boland MR and **Bader JS**. Determination of Forces Occurring at the Distal Radioulnar Joint. Podium presentation at the 11th Triennial Congress of the International Federation for Surgery of the Hand. Seoul, South Korea. October/November, 2010.
- Boland MR and **Bader JS**. The Effect of Brachioradialis on the Distal Radioulna Joint. Poster presentation at the 11th Triennial Congress of the International Federation for Surgery of the Hand. Seoul, South Korea. October/November, 2010.
- Boland MR and **Bader JS**. The Function of Extensor Carpi Ulnaris During Forearm Rotation-It's Effect on the Distal Radioulna Joint. Poster presentation at the 11th Triennial Congress of the International Federation for Surgery of the Hand. Seoul, South Korea. October/November, 2010.
- **Bader JS**, Boland MR, Nitz A, Stone J, Uhl T, Pienkowski D. Forearm Muscle Activity During Isometric Pronation-Supination. Poster presentation at the 56th Annual Meeting of the Orthopaedic Research Society. New Orleans, LA. March, 2010.
- **Bader JS**, Boland MR, Rishmawi H, Uhl T, Pienkowski D. The Influence of Fifteen Muscles on Distal Radioulnar Joint Loading: A Biomechanical Model. Podium presentation at the 55th Annual Meeting of the Orthopaedic Research Society. Las Vegas, NV. February, 2009.
- **Bader JS**, Boland MR, Spigelman T, Uhl T, Pienkowski D. Brachioradialis Muscle Function During Forearm Rotation from EMG, Anatomy, and Biomechanical Modeling. Poster presentation at the 55th Annual Meeting of the Orthopaedic Research Society. Las Vegas, NV. February, 2009.
- Boland, MR, **Bader JS**, Spigelman T, Royalty R, Pienkowski D, Uhl T. The Protective Effect of Brachioradialis on the Distal Radioulnar Joint. Podium presentation at the 63rd Annual Meeting of the American Society for Surgery of the Hand. Chicago, IL. September, 2008.

- Boland MR, **Bader JS**, Royalty R, Uhl T, Pienkowski D. The Effect Extensor Carpi Ulnaris Has on the Distal Radioulnar Joint During Forearm Rotation. Poster presentation at the 63rd Annual Meeting of the American Society for Surgery of the Hand. Chicago, IL. September, 2008.
- Boland MR, **Bader JS**, Royalty R, Uhl T, Pienkowski D. Determination of Joint Reaction Forces in the Distal Radioulnar Joint Using Maximal Muscle Forces. Podium presentation at the 75th Annual Meeting of the American Academy of Orthopaedic Surgeons. San Francisco, CA. March, 2008.
- Boland MR, **Bader JS**, Royalty R, Uhl T, Pienkowski D. The Relationship Between Muscle Length and Function in the Forearm During Pronosupination. Poster presentation at the 75th Annual Meeting of the American Academy of Orthopaedic Surgeons. San Francisco, CA. March, 2008.
- **Bader JS**, Boland MR, Royalty R, Uhl T, Pienkowski D. Joint Reaction Forces in the Distal Radioulnar Joint Using Maximal Muscle Forces: A Biomechanical Model. Podium presentation at the Orthopaedic Research Society 6th Combined Meeting. Honolulu, HI. October, 2007.
- **Bader JS**, Boland MR, Royalty R, Uhl T, Pienkowski D. The Relationship Between Muscle Length and Function in the Forearm During Pronosupination. Poster presentation at the Orthopaedic Research Society 6th Combined Meeting. Honolulu, HI. October, 2007.
- **Bader JS**, Boland MR, Spigelman T, Royalty R, Uhl T, Pienkowski D. The Use of Length Data and Electromyography to Analyze Muscle Function. Poster presentation at the Orthopaedic Research Society 6th Combined Meeting. Honolulu, HI. October, 2007.
- Boland MR, **Bader JS**, Royalty R, Uhl T, Pienkowski D. Joint Reaction Forces in the Distal Radioulnar Joint During Pronosupination: A Biomechanical Study. Poster presentation at the 62nd Annual Meeting of the American Society for Surgery of the Hand. Seattle, WA. September, 2007.
- Boland MR, **Bader JS**, Royalty R, Uhl T, Pienkowski D. The Relationship Between Muscle Length and Function in the Forearm During Pronosupination. Poster presentation at the 62nd Annual Meeting of the American Society for Surgery of the Hand. Seattle, WA. September, 2007.
- Boland MR, **Bader JS**, Pienkowski D, Uhl T. Joint Reaction Forces in the Distal Radioulnar Joint – A Biomechanical Model. Poster presentation at the 61st Annual Meeting of the American Society for Surgery of the Hand. Washington D.C. September, 2006.
- **Bader JS**, Komistek RD, Wasserman JF, Haas BD. Clinical Significance of Hip Separation in Metal on Polyethylene, Metal on Metal and Ceramic on Ceramic THA Due to Resonant and Energy Dispersion Effects. Poster presentation at the 51st Annual Meeting of the Orthopaedic Research Society. Washington D.C. February, 2005.

- Dong RG, **Bader JS**, Welcome D, Rakheja S, Schopper AW. An Accurate Method for Measuring the Exposure Duration of Hand-Transmitted Vibration. Presented at the 36th UK Group Conference on Human Response to Vibration. Farnborough, UK. 2001.
- Dong RG, Rakheja S, Smutz PW, Schopper AW, Caporali SA, Stone S, **Bader JS**. Dynamic Characteristics of the Instrumented Handle and Adapter Recommended in the ISO 10819, 1996. Presented at the 9th International Conference on Hand-Arm Vibration. Nancy, France. 2001.